The Dual Roles of Reactive Oxygen Species during Erythropoiesis and the Effect of Salidroside on Erythropoiesis and Erythrocytes

QIAN, Wei

A Thesis Submitted in Partial Fulfillment

of the Requirements for the Degree of

Doctor of Philosophy

in

Biochemistry

The Chinese University of Hong Kong

July 2011

Thesis/Assessment Committee

Prof. **Tsui Kwok Wing Stephen** (Chair)

Prof. **Kong Siu Kai** (Thesis Supervisor)

Prof. **Kwan Yiu Wa** (Committee Member)

Prof. **Mak Nai Ki** (External Examiner)

I declare that the assignment here submitted is original except for source material explicitly acknowledged, and that the same or related material has not been previously submitted for another course. I also acknowledge that I am aware of University policy and regulations on honesty in academic work, and of the disciplinary guidelines and procedures applicable to breaches of such policy and regulations, as contained in the website.

Qian Wei	28/07/2011
Signature	Date
QIAN, Wei	1007056840
Name	Student ID
BCHE 8003	Thesis Research
Course code	Course title

Acknowledgements

I would like to express my sincere gratitude to my supervisor, Professor Kong Siu Kai, for his patient guidance, advice, and constant encouragement and care throughout the period of my PhD. study.

I would like to thank Dr. Y. K. Suen for his generous advice and help. I would like to thank my previous labmate Daniel Ge for his suggestion and support in my research work. Also, I would like to thank Ms. Irene Lau, Ms. Alice Yang, Ms. Erika Ngan, Ms. Rebecca Lee, Mr. Anthony Cheung and Ms. Jennifer Gao, and all my colleagues in BMSB 514, for their generous advice and support. Besides, I would like to extend my grateful thanks to all my friends in the department for their friendships and continuous encouragements.

Last but not least, I would like to thank my parents and my husband for their constant support, endless love and care in my life and study.

Abstract

Reactive oxygen species (ROS) have been considered to be deleterious to cells; however, increasing evidence demonstrates that they actually play dual roles. Unchecked high amounts of ROS can damage cellular components, whereas moderately well-regulated ROS play crucial roles as signaling messengers in the regulation of various biological processes. For example, ROS contribute significantly to the differentiation of hematopoietic cells, but the underlying mechanisms remain unresolved. Previous work of our laboratory has revealed that ROS was produced and contributed to the establishment of the antioxidant defense system during erythropoietin (EPO)-induced erythropoiesis in TF-1 cells. In the present study, the roles of ROS during erythroid maturation were further investigated and the effect of an antioxidant salidroside (SDS) on erythropoiesis or erythrocytes was examined.

Salidroside (SDS) is a widely used adaptogen and blood tonic supplement in traditional medicine for the treatment of high altitude sickness, anoxia and mountain malhypoxia. Here we show for the first time that SDS (100 μM) promoted erythroid differentiation and was able to protect erythroblasts against H_2O_2 to commit cell death through apoptosis. The protective effect of SDS was contributed by the up-regulation of anti-oxidative proteins. Furthermore, SDS was also found to be able to rescue human erythrocytes from apoptosis induced by oxidative stress. The rescue effect was

largely through the anti-oxidative effect, suppression of $[Ca^{2+}]_i$ rise and caspases-3 activation. These findings show the mechanism underlying the use of SDS and confirm the application of it as an antioxidant or blood tonic to enhance body's resistance to stress and fatigue.

Glucose-6-phosphate dehydrogenase (G6PD) is a key enzyme of anti-oxidative defense system of red blood cells (RBCs). G6PD deficiency affects more than 400 million people worldwide. Employing RNAi technology (miRNA), we developed a stable G6PD-knockdown TF-1 cell line. Using these G6PD-knockdown cells, we found that the efficacy of erythroid cells production during erythropoiesis was decreased, whereas the ROS production and apoptotic frequency were increased. Moreover, other important antioxidant enzymes such as glutathione peroxidase 1 (GPx1) and thioredoxin-1 (Trx1) were found to be down-regulated in the G6PD-knockdown cells, indicating G6PD plays a role in the regulation of these two antioxidant enzymes. Besides, SDS (100 μM) was shown to be able to protect G6PD-knockdown erythroblasts from the H_2O_2-induced oxidative stress.

Glucose transporter type 1 (Glut1) mediates the uptake of glucose that provides the major reducing equivalents in human erythrocytes. We found that Glut1 was up-regulated during erythropoiesis in TF-1 cells and reduction in ROS level resulted in a decrease in Glut1 level. Furthermore, elevated ROS up-regulated Glut1 and hypoxia-inducible factor-1α (HIF-1α), and inhibition of HIF-1α suppressed the

up-regulation of Glut1. Taken together, these observations indicate that ROS regulate Glut1 expression through the HIF-1α during erythropoiesis in TF-1 cells.

In conclusion, the findings of this study (1) provide support for therapeutic applications of SDS in preventing anemia after cancer chemotherapy and treating G6PD deficiency disease; (2) elucidate the role of G6PD during erythropoiesis, thereby contributing to the treatment of G6PD deficiency disease; and (3) further explore the role of ROS and its regulation on Glut1 via HIF-1α in erythropoiesis.

論文摘要

活性氧（ROS）被認為是有害於細胞。但是，越來越多的證據表明活性氧扮演雙重角色。不受抑制的高含量的活性氧會損傷細胞成分，而適度調節的活性氧可以作為信使，在各種生物過程中發揮關鍵作用。例如，活性氧能夠促進造血細胞的分化，但其作用機制仍不清楚。本實驗室以前的工作已經表明，活性氧在紅細胞生成素（EPO）誘導下的紅細胞分化過程中產生，並且幫助分化中的紅細胞建立抗氧化防禦系統。在本研究中，我們對紅細胞成熟過程中活性氧的作用作進一步的研究。另外，對抗氧化劑紅景天甙（Salidroside）在紅細胞分化或成熟紅細胞中的作用進行了檢測。

紅景天甙是一種廣泛使用的適應原和補血劑，在傳統醫學中用於治療缺氧等高海拔疾病。我們的研究首次表明紅景天甙能夠促進紅細胞的分化，並能保護分化中的紅細胞免受過氧化氫誘導的細胞凋亡。這種保護作用可能來自紅景天甙對抗氧化蛋白的增加。此外，我們還發現紅景天甙也能保護人類成熟紅細胞免受氧化劑誘導的細胞凋亡。這種保護作用主要是通過抗氧化效果，抑制細胞內鈣離子濃度的升高和遏制 Caspase-3 蛋白酶的活化來實現。這些發現闡明了紅景天甙作為一種抗氧化劑或補血劑來提高機體抗壓力和抗疲勞能力的內在機制。

葡萄糖-6-磷酸脫氫酶（Glucose-6-phosphate dehydrogenase, G6PD）是一個在紅細胞抗氧化防禦系統中發揮關鍵作用的酶。全世界有400多萬人患有G6PD缺乏症。利用RNA干擾技術（miRNA），我們構建了一個穩定的G6PD基因下調

的TF-1細胞系。在G6PD基因下調的紅細胞中，紅細胞分化效率顯著下降，而活性氧的產量和細胞凋亡顯著增加。並且，其他重要的抗氧化酶，如穀胱甘肽過氧化酶1 (glutathione peroxidase 1, GPx1)和硫氧還蛋白- 1 (thioredoxin-1, Trx1)的表達水平明顯下調，表明G6PD對这两种抗氧化酶起著調節作用。此外，我們的研究還表明在TF-1受誘導分化成紅細胞的過程中，紅景天甙能夠保護G6PD基因下調的細胞免受過氧化氫誘導的細胞凋亡。

在紅細胞中，葡萄糖提供主要的抗氧化所需的能量，而葡萄糖的攝取主要由葡萄糖轉運蛋白 1（GLUT1）介導。我們發現，在受紅細胞生成素誘導的 TF-1 細胞中，GLUT1 水平在紅細胞的成熟過程中逐漸升高，並且下降的活性氧水平會導致細胞內 GLUT1 的減少，而升高的活性氧水平會增加 GLUT1 和缺氧誘導因子 HIF-1a。另外，抑制 HIF-1a 的表達會導致 GLUT1 水平下降。這些研究結果說明，在 TF-1 細胞受誘導分化成紅細胞的過程中，活性氧能調節 GLUT1 的表達，並且這種調節作用通過 HIF-1a 來實現。

綜上所述，本研究的貢獻主要有以下三個方面：第一、為紅景天甙在預防癌症化療後貧血和治療 G6PD 缺乏症方面的應用提供了支持； 第二、闡明了 G6PD 在紅細胞分化過程中的作用，從而有助於 G6PD 缺乏症的治療；第三、進一步探討了活性氧在紅細胞生成過程中的作用，並揭示了活性氧在這過程中通過調節 HIF-1a 來調節 GLUT1 表達的機理。

List of Figures

List of Tables

Abbreviations

+	Positive
-	Negative
°C	Degree Celsius
µg	Microgram
µl	Microliter
µM	Micromolar
2-OG	2-oxoglutarate
APC	Allophycocyanin
ATCC	American Type Culture Collection
BCA	Bicinchoninic Acid
BFU-E	Burst-forming unit-erythroid
BSA	Bovine serum albumin
Caspase	Cysteinyl Aspartic Acid-Protease
CD	Cluster of Differentiation
CD71	Transferrin receptor
cDNA	Complimentary Deoxyribonucleic Acid
CFU-E	Colony-forming unit-erythroid
CLSM	Confocal Laser Scanning Microscopy
CM-H_2DCFDA	5-(and-6)-chloromethyl-2′,7′-dichlorodihydrofluorescein diacetate, acetyl ester
C_T	Threshold Cycle
ddH_2O	Double distilled water
DEPC	Diethyl Pyrocarbonate
DHA	L-dehydroascorbic acid
DHE	Dihydroethidium
DMSO	Dimethylsulphoxide
dNTP	Deoxynucleic Triphosphate

ds	Double-stranded
ECL	Enhanced Chemiluminescence
EPO	Erythropoietin
EPOR	Erythropoietin receptor
FACS	Flow Cytometry-Assisted Cell Sort
FBS	Fetal bovine serum
FITC	Fluorescein Isothiocyanate
G6P	Glucose 6-phosphate
G6PD	Glucose-6-phosphate dehydrogenase
GFP	Green fluorescent protein
Glut	Glucose transporter
Glut1	Glucose transporter type 1
GM-CSF	Granulocyte-Macrophage Colony Stimulating Factor
GPA	Glycophorin A/CD235a
GPx1	Glutathione peroxidase 1
GSH	Glutathione
GR	Glutathione reductase
GSSG	Glutathione disulfide
H_2O_2	Hydrogen peroxide
Hb	Hemoglobin
HEPES	N-[2-Hydroxyethl]piperazine-N'-[2-Ethanesulfonic Acid]
HIF	Hypoxia-inducible factor
HIF-1α	Hypoxia-inducible factor-1 α
hr	Hour
HSC	Hematopoietic stem cell
IgG	Immunoglobulin G
KDa	Kilo Dalton
LB	Lysogeny Broth
M	Molar
mg	Milligram

min	Minute
miRNA	Micro RNA
ml	Milliliter
mM	Millimolar
mRNA	Messenger Ribonucleic Acid
NAC	N-acetyl-l-cysteine
$NADP^+$	Nicotinamide adenine dinucleotide phosphate
NADPH	Reduced nicotinamide adenine dinucleotide phosphate
OD	Optical Density
$^{\bullet}O_2^-$	Superoxide anion
$^{\bullet}OH$	Hydroxyl radical
$ONOO^-$	Peroxynitrite anion
P	P Value
PBS	Phosphate buffered saline
PE	Phycoerythrin
PerCP	Peridinin Chlorophyll Protein Complex
PHD	Prolyl hydroxylase domain enzyme
PI	Propidium iodide
PMSF	Phenylmethyl-Sulfonyl Fluoride
PPP	Pentose phosphate pathway
pRPMI	Phenol red free RPMI
Prx	Peroxiredoxin
PS	Phosphatidyl-serine
PVDF	Polyvinylidene fluoride
PX-478	S-2-amino-3-[4-N, N,-bis (chloroethyl) amino] phenyl propionic acid N-oxide dihydrochloride
RBC	Red blood cell/erythrocyte
RNAi	RNA interference
ROOH	Peroxide
ROS	Reactive oxygen species

rpm	Revolution Per Minute
RPMI	Roswell Park Memorial Institute Tissue Culture Medium
RT	Room temperature
SD	Standard Deviation
SDS	Salidroside (*p*-hydroxyphenethyl-beta-d-glucoside)
SDS-PAGE	Sodium Dodecyl Sulfate-Polyacrylamide Gel Electrophoresis
sec	Second
SGLT	Sodium-Glucose Linked Transporter
siRNA	Small interfering RNA
SOD	Superoxide dismutase
STS	Staurosporine
TBE	Tris-Borate-EDTA
TBS	Tris Buffered Saline
TBST	Tris Buffered Saline with Tween-20
TE	Tris-EDTA
TGF–β	Transforming growth factor beta
TMRM	Tetramethylrhodamine, Methylester, Perchlorate
Trx1	Thioredoxin-1
TrxR	Thioredoxin reductase
U	Unit
VitC	Vitamin C
VEGF	Vascular endothelial growth factor
v/v	Volume by Volume
WHO	World Health Organization
w/v	Weight by Volume

Table of Content

Chapter 1

General Introduction

1.1 Erythropoiesis and the TF-1 erythropoiesis model

Erythropoiesis is the process by which red blood cells (RBCs / erythrocytes) are produced. In human adults, this usually takes place within the bone marrow. In the early fetus, erythropoiesis occurs in the mesodermal cells of the yolk sac. Then it transfers to the spleen and liver by the third or fourth month, and moves to bone marrow after seven months (Le *et al.*, 2010; Palis *et al.*, 1998; Sherwood *et al.*, 2005).

Erythropoiesis is an intricate multistep process in which hematopoietic stem cells (HSCs) differentiate into mature erythrocytes. The morphologically recognizable stages of the differentiation process comprise erythroid burst-forming units (BFU-E), erythroid colony-forming units (CFU-E), proerythroblasts, basophilic normoblasts, polychromatophilic normoblasts, orthochromatophilic normoblasts, reticulocytes and erythrocytes (Aispuru *et al.*, 2008; Koury *et al.*, 2002). The mature erythrocyte is the most specialized cell in the body. Since it loses its nucleus, ribosomes, and mitochondria, erythrocyte has no capacity for cell division, protein synthesis, and mitochondrial-based oxidative reactions (Cimen, 2008).

The regulation of erythropoiesis is complex and takes place at multiple levels. The renewal and proliferation of hematopoietic stem cells rely on the stimulation by stem cell factor (SCF), interleukin-3 (IL-3) and granulocyte/macrophage colony-stimulating factor (GM-CSF) at different stages (Koury *et al.*, 2002). Erythropoietin (EPO) is the principal regulator during erythropoiesis. Other cytokines or hormones also play a role in the process. Signaling from the EPO-receptor is able to activate numerous pathways,

including the JAK/STAT, ras/raf/MAP kinase and PI3 kinase/Akt cascades and thereby promotes cell survival, proliferation and differentiation. Transcription factors such as GATA-1, TAL-1 are crucial for erythropoiesis (Ingley *et al.*, 2004). Lineage specific antigens glycophorin A (GPA) and CD71 are important indications of the process (Nakahata and Okumura, 1994). Erythroid differention stages and erythroid markers are shown in Figure 1.1. In addition, during erythropoiesis, caspase-3 is activated as an important event required for human terminal erythroblast maturation. The definite function for caspase-3 in erythroid differentiation remains unclear (Ribeil *et al.*, 2005).

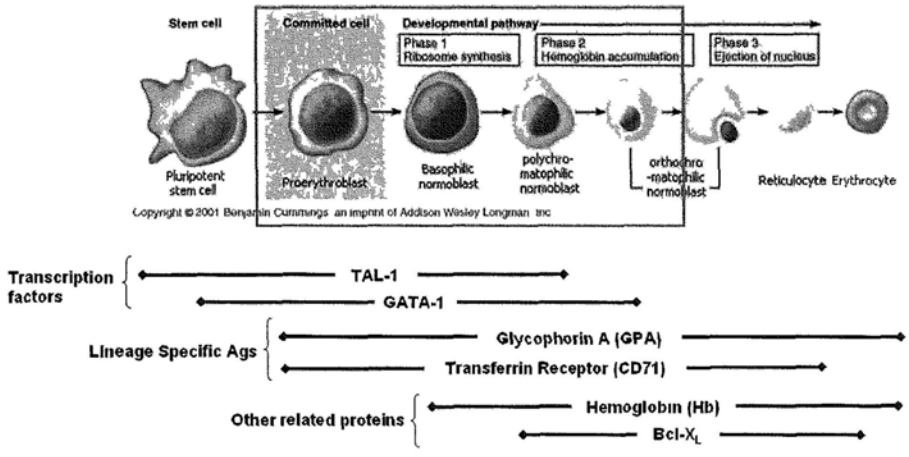

Figure 1.1 Erythroid differentiation and markers.

The stages of erythroid differentiation comprise pluripotent stem cells, proerythroblasts, basophilic normoblasts, polychromatophilic normoblasts, orthochromatophilic normoblasts, reticulocytes and erythrocytes. Erythroid transcription factors: basic helix-loop-helix factor (TAL1), zinc finger factor that bind GATA sequences (GATA-1); Proteins related to erythrocyte structure and function: glycophrin-A (GPA), transferrin receptor (CD71), hemoglobin (Hb) and Bcl-X_L (Modified from Koury MJ, Curr Opin Hematol, 2002).

Currently, the human erythroleukemia cell line TF-1 is one of the best *in vitro* erythropoiesis models. TF-1 was first established by Kitamura *et al.* (1989) and later adopted by a great many of other laboratories as the erythroid differentiation model (Akel *et al.*, 2007; Buck *et al.*, 2008; Jacobs-Helber and Sawyer, 2004; Lopez *et al.*, 2005; Uchida *et al.*, 2004). Over the last 15 years, the ready availability of recombinant human erythropoietin (r-HuEPO) has permitted the clinical investigation and application of this hormone to the treatment of anemia in various patient populations (Bieber, 2001). In TF-1 differentiation model, r-HuEPO was utilized to induce erythropoiesis. After r-HuEPO treatment, TF-1 becomes the polychromatophilic and orthochromatic normoblasts.

The expression of lineage specific antigen GPA (CD235a/GPA) and transferrin receptor (CD71) are widely accepted as the hallmarks of erythroid differentiation. In this study, the expression level of these two erythroid cell specific markers and a cytosolic protein hemoglobin (Hb) were evaluated. Each of the 3 proteins has their unique function in erythroid cells. GPA is a sialoglycoprotein and an essential component of the mature RBC membrane. Its expression increases throughout erythropoiesis. CD71 is the receptor of transferrin and is essential for delivery of iron required for cellular metabolism. Its expression peaks at the erythroblast stages and is absent in either hematopoietic stem cells or mature RBCs. Hb is the major cytosolic protein in RBCs to carry oxygen, its expression increases during erythroid maturation.

1.2 Salidroside (SDS)

The plant *Rhodiola rosea* L. (紅景天), belonging to the family Crassulaceae, is popularly used as an adaptogen to enhance body's resistance to stress and fatigue in Europe and China (Darbinyan *et al.*, 2000; Kelly, 2001; Ma *et al.*, 2009; Perfumi and Mattioli, 2007; Yu *et al.*, 2008; Zhang *et al.*, 2007; Zhu *et al.*, 2010). Previous studies indicate that *Rhodiola rosea* L. was able to enhance both the physical and mental performance (Panossian and Wikman, 2009; Panossian *et al.*, 2010; Shevtsov *et al.*, 2003; Spasov *et al.*, 2000). Its active component, salidroside (SDS) (*p*-hydroxyphenethyl-beta-d-glucoside ($C_{14}H_{20}O_7$), structure shown in Figure 1.2) (Panossian *et al.*, 2010), has been reported to have a broad spectrum of pharmacological properties such as anti-aging, (Hu *et al.*, 2010), anti-inflammatory (Skopinska-Rozewska *et al.*, 2008), anti-hypoxia (Ye *et al.*, 1993; Yu *et al.*, 2008) and anti-oxidative (Yu *et al.*, 2007; Kanupriya *et al.*, 2005) effects.

Rhodiola rosea L. or SDS has long been used as a blood tonic and adaptogen to prevent high altitude sickness, and to treat mountain malhypoxia and anoxia (Kelly, 2001; Wu *et al.*, 2008). Nowadays, *Rhodiola rosea* L. and its major active compound SDS are widely consumed as health food or dietary supplements. A commercial extract of *Rhodiola rosea* L. containing SDS, as high as 70%, extended the life span (24%) of *Drosophila melanogaster* by reducing the level of endogenous superoxide (Schriner *et al.*, 2009). Moreover, there are many studies showing that *Rhodiola rosea* L. and SDS can provide cardiovascular-protection against ischemic/reperfusion injuries (Wu *et al.*, 2009;

Zhang *et al.*, 2009). In human, it was found that chronic intake of *Rhodiola rosea* L. in trained male athletes reduced the lactate levels after exhaustive exercise and increased performance in physical activities (Parisi *et al.*, 2010). Also, Cifani *et al.* (2010) reported that SDS could reduce or abolish binge eating in a dose-dependent manner.

At the cellular level, SDS was demonstrated to protect the PC12 cells against the H_2O_2-induced apoptotic cell death (Yu *et al.*, 2010). Previous findings show that the aqueous extract of *Rhodiola rosea* L. was able to reduce the damages induced by hypochlorous acid in human erythrocytes (Battistelli *et al.*, 2005; De Sanctis *et al.*, 2004). Also, SDS was demonstrated to prevent the oxygen-glucose deprivation-induced apoptosis in rat neonatal cardiomyocytes (Zhong *et al.*, 2010).

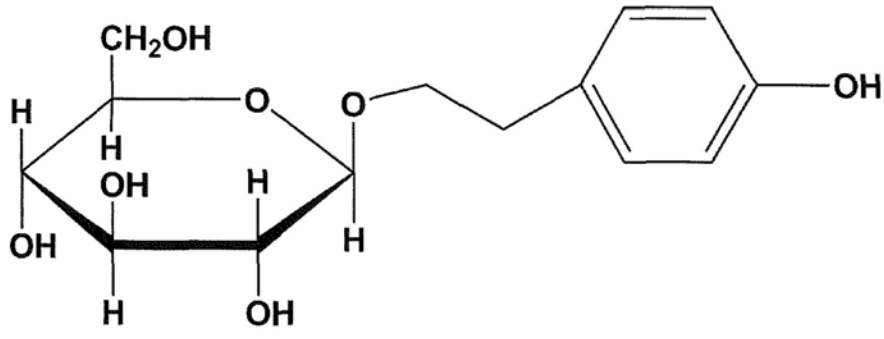

Figure 1.2 Chemical structure of salidroside (SDS).

1.3 Reactive Oxygen Species (ROS)

Reactive oxygen species (ROS) are oxygen-centered and chemically-reactive molecules with the presence of unpaired valence of electrons. Intracellular ROS consist of various chemical species including superoxide ($^{\bullet}O_2^-$), hydrogen peroxide (H_2O_2) and hydroxyl radicals ($^{\bullet}OH$). O_2 receives a single electron and is converted to superoxide ($^{\bullet}O_2^-$). The mitochondrial respiratory chain is a major source of superoxide. Because of its extremely unstable property, superoxide undergoes rapid dismutation spontaneously or by superoxide dismutase (SOD) and turns to H_2O_2 (Finkel and Holbrook, 2000; Ghaffari, 2008). H_2O_2 can be reduced by antioxidant enzymes such as catalase and two major hydrogen peroxide scavenging systems, the glutathione peroxidase (GPx) system and the thioredoxin (Trx) peroxidase system. Also, H_2O_2 can be removed by non-enzymatic antioxidants such as vitamins C and E, and carotenoids (Veal *et al.*, 2007). In addition, Fenton reaction ($H_2O_2 + Fe^{2+} \rightarrow Fe^{3+} + OH^- + {}^{\bullet}OH$) converts H_2O_2 to highly reactive hydroxyl radical ions ($^{\bullet}OH$) (Kietzmann and Gorlach, 2005).

ROS have been considered to be deleterious to cells (Finkel and Holbrook, 2000; Harman, 1956). However, several lines of recent evidence suggest that although unchecked high amounts of ROS can damage cellular components, moderately well-regulated ROS act as important primary or secondary messengers in signaling pathways involved in proliferation, differentiation and apoptosis (Dennery, 2007; Ghaffari, 2008; Kietzmann and Gorlach, 2005) (Figure 1.3). For example, ROS have been demonstrated to stimulate proliferation in cells such as fibroblasts, amnion cells, smooth muscle cells

and aortic endothelial cells, and to promote differentiation in neurons, osteoclasts, lens cells, and cardiomyocytes (Sauer *et al.*, 2001). Particularly, it was found that *Drosophila* multipotent hematopoietic progenitors display elevated levels of ROS under *in vivo* physiological conditions and removal of the ROS retards their differentiation into mature blood cells. Conversely, increasing the hematopoietic progenitor ROS above their basal level induces precocious differentiation into all mature blood cell types. In the mammalian hematopoietic system, the common myeloid progenitors (CMPs) produce significantly increased levels of ROS as well. These indicate a critical role for ROS in the regulation of hematopoietic cell fate (Owusu-Ansah and Banerjee, 2009). Furthermore, ROS have been reported to be involved in the chemical-triggered erythroid differentiation of K562 human leukemia cells (Chenais *et al.*, 2000). However, the exact role of ROS during erythropoiesis remains unclear.

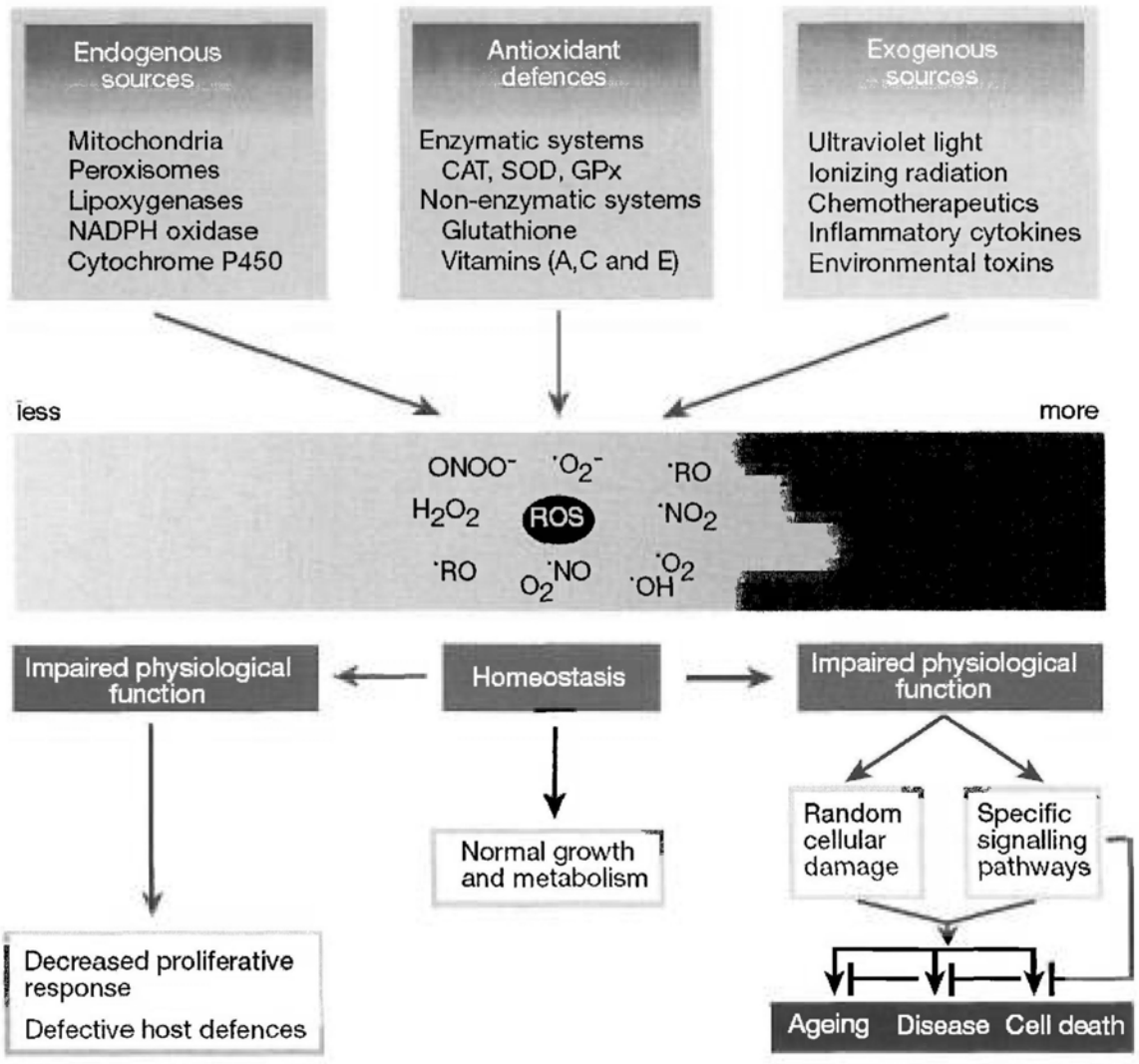

Figure 1.3 The sources and cellular responses to Reactive Oxygen Species (ROS).

Abbreviations: CAT, catalase; SOD, superoxide dismutase; GPx, glutathione peroxidase; NADPH, reduced nicotinamide adenine dinucleotide phosphate (Adapted from Finkel and Holbrook, 2000).

1.4 Regulation of oxidative stress in human red blood cells and precursors

Regulation of oxidative stress is particularly important to erythropoiesis (Socolovsky, 2007) (Figure 1.4). Oxidative stress is due to the effects of ROS. As erythroid precursors express and accumulate Hb as they mature, iron inserted into heme in mitochondria of erythroid precursors are capable of producing high amounts of ROS by the Fenton reaction. Circulating erythrocytes carry oxygen bound to Hb and thus are extraordinarily prone to oxidative damage (Winterbourn, 1990). As a result, erythrocytes are exposed to one of the highest levels of oxidative-stress conditions in the body (Ghaffari, 2008).

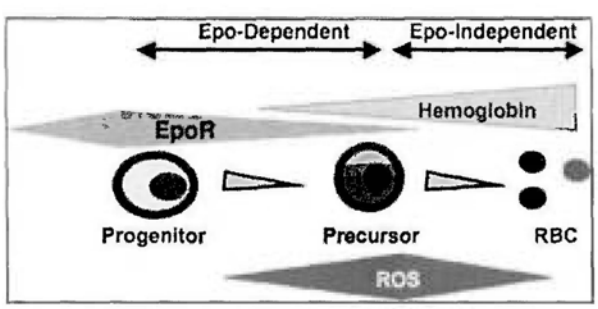

Figure 1.4 Schematic of erythroid cell differentiation.
Abbreviations: EPO, erythropoietin; EPOR, erythropoietin receptor; RBC, red blood cell/erythrocyte; ROS, reactive oxygen species (Adapted from Ghaffari, 2008).

Not surprisingly, erythroid cells in healthy individuals develop a strong antioxidant system that can counterbalance the oxygen stress *in vivo* and thus protects the cells (Ghaffari, 2008; Johnson *et al.*, 2005). These include SOD, catalase and GPx, and nonenzymatic scavengers such as glutathione, Trx, peroxiredoxin and ascorbic acid.

Deficiencies in several ROS scavengers lead to insufficient protection from ROS and result in either anemia that is severe or even lethal and/or malignancies of hematopoietic tissues (Friedman *et al.*, 2001; Kong *et al.*, 2004; Lee *et al.*, 2004; Neumann *et al.*, 2003).

Glucose is the only fuel used in mature RBCs. After transported into cells, glucose is rapidly converted into glucose-6 phosphate. Generally 80-90% of glucose is turned to lactate through the glycolytic pathway, which provides the only source of energy for RBCs. The unexpended 10% glucose goes into the pentose phosphate pathway (PPP, Figure 1.5) and produces NADPH, which serves as the principle intracellular reductant that enables cells to counterbalance oxidative stress (Cappellini and Fiorelli, 2008; Cimen, 2008) (Figure1.6).

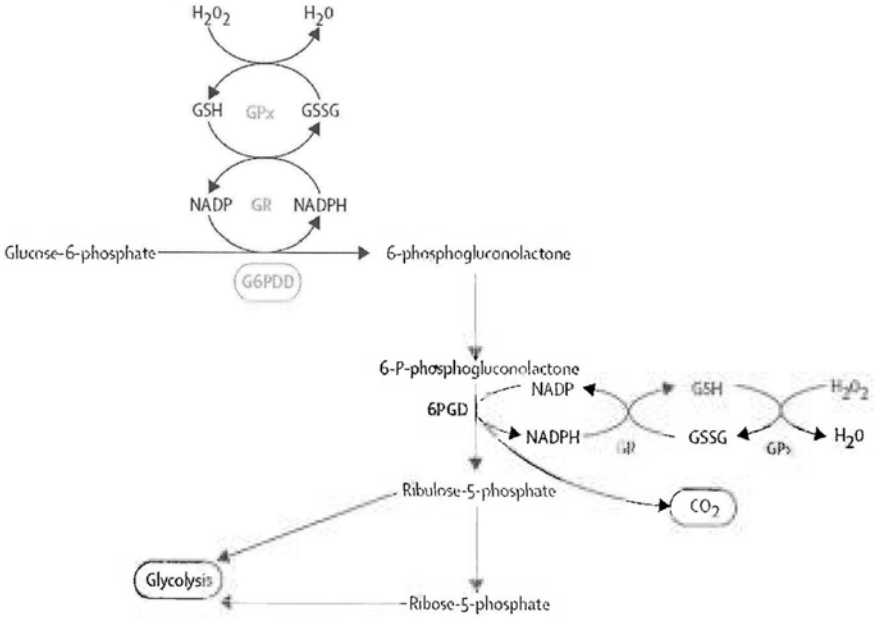

Figure 1.5 Pentose phosphate pathway (PPP).

Abbreviations: G6PDD, glucose - 6 phosphate dehydrogenase; 6PGD, 6-phosphogluconate dehydrogenase; GPx, glutathione peroxidase; GR, glutathione reductase; GSH, reduced glutathione; GSSG, oxidised glutathione. (Modified from Cappellini and Fiorelli, 2008).

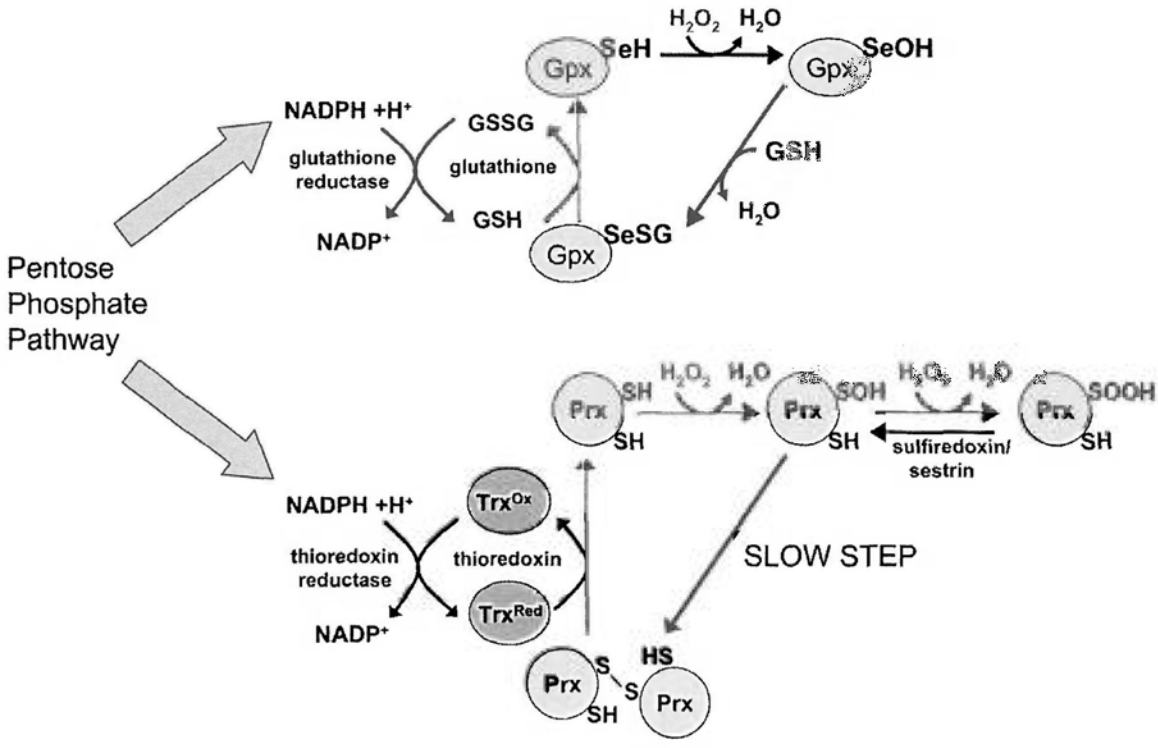

Figure 1.6 Scavenging of hydrogen peroxide by the glutathione peroxidase (Gpx) and thioredoxin (Trx) peroxidase systems.

Abbreviations: NADPH, reduced nicotinamide adenine dinucleotide phosphate; $NADP^+$, nicotinamide adenine dinucleotide phosphate; Gpx, glutathione peroxidase; GSH, reduced glutathione; GSSG, oxidised glutathione; Trx, thioredoxin; Prx, peroxiredoxin; SeH, selenocysteine; SH, cysteine; SOH, sulfenic acid; SOOH, sulfinic acid (SOOH) derivative (Adapted from Veal *et al.*, 2007).

1.5 Glucose-6-phosphate Dehydrogenase (G6PD)

The *glucose-6-phosphate dehydrogenase (G6PD)* gene is an X-linked housekeeping gene that encodes the first and rate-limiting enzyme of the pentose phosphate pathway (Jain *et al.*, 2003; Leopold *et al.*, 2001; Paglialunga *et al.*, 2004). It catalyzes the synthesis of riboses and serves as the principal source of the major intracellular reductant NADPH (reduced form of nicotinamide adenine dinucleotide phosphate) (Zhang *et al.*, 2010). NADPH enables cells to counterbalance oxidative stress that can be triggered by several oxidant agents, and to preserve the reduced form of glutathione. Since RBCs do not contain mitochondria, the pentose phosphate pathway is their only source of NADPH; therefore, defense against oxidative damage is dependent on G6PD (Cappellini and Fiorelli, 2008).

G6PD deficiency is the most common human enzyme defect, present in more than 400 million people worldwide (Cappellini and Fiorelli, 2008; Elyassi and Rowshan, 2009; Mason, 1996). G6PD deficiency is a hereditary genetic defect caused by mutations in the G6PD gene, resulting in protein variants with different levels of enzyme activity (Cappellini and Fiorelli, 2008). As RBCs do not have the "other NADPH producers", G6PD deficiency becomes especially lethal in RBCs, where any oxidative stress will result in hemolytic anemia. Oxidative stresses can arise from numerous things, such as consumption of fava beans, certain drugs, infections, and certain metabolic conditions like diabetic ketoacidosis. Hence, G6PD deficiency disease is also called favism (Elyassi and Rowshan, 2009; Manganelli *et al.*, 2010) (Figure 1.7).

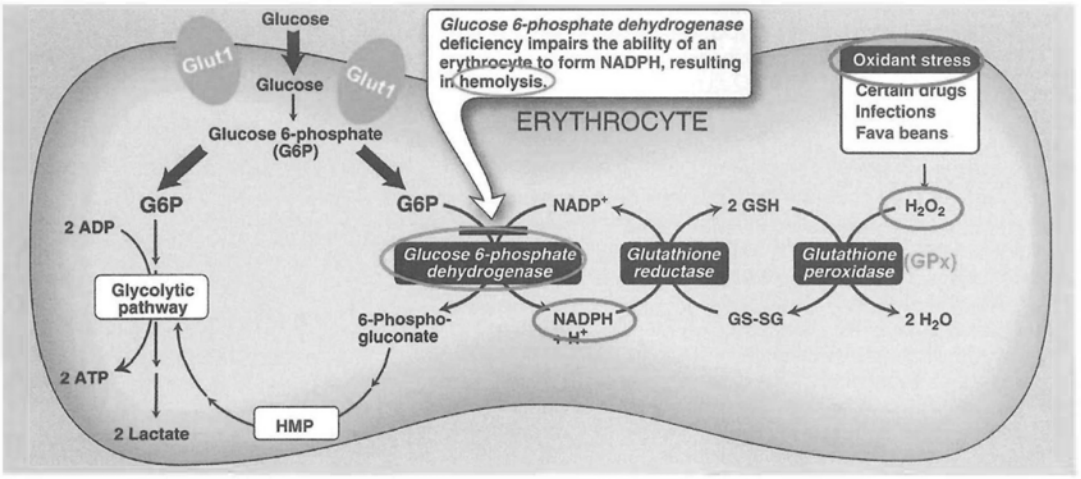

Figure 1.7 Schematic of G6PD (Glucose 6-phosphate dehydrogenase) deficiency disease.

Abbreviations: Glut1, glucose transporter type 1; G6P, Glucose 6-phosphate; HMP, hexose monophosphate; NADPH, reduced nicotinamide adenine dinucleotide phosphate; $NADP^+$, nicotinamide adenine dinucleotide phosphate; GSH, reduced glutathione; GSSG, oxidised glutathione (Modified from Pamela C. Champe, Lippincott's Illustrated Reviews: Biochemistry, 3rd edition, 149-151).

WHO classification of G6PD deficiency

Class I
Severely deficient (< 1%), associated with chronic non-spherocytic hemolytic anaemia

Class II
Severely deficient (1 - 10% residual activity), associated with acute hemolytic anaemia

Class III
Moderately deficient (10 - 60% residual activity)

Class IV
Normal activity (60 - 150%)

Class V
Increased activity (>150%)

(Adapted from Cappellini and Fiorelli, 2008)

1.6 Glucose transporter type 1 (Glut1)

Glucose enters eukaryotic cells via two different types of membrane associated carrier proteins, glucose transporter facilitators (GLUT) and the Na^+-coupled glucose transporters (SGLT) (Scheepers *et al.*, 2004). The human GLUT family consists of fourteen members but Glut1, the first identified protein, is the main functional transporter of glucose in most transformed cells as well as in various hematopoietic cell lineages and brain (Montel-Hagen *et al.*, 2008; Mueckler, 1994; Mueckler *et al.*, 1985; Seidner *et al.*, 1998). Glut1 is a type 2 integral membrane protein composed of 12 transmembrane domains that delineate six extracellular loops (Mueckler *et al.*, 1985).

Of all cell lineages, the human erythrocyte expresses the highest level of the Glut1 transporter, possessing greater than 200,000 molecules per cell. Moreover, Glut1 is the sole glucose transporter in human erythrocytes and in the context of the red cell membrane, Glut1 accounts for 10% of the total protein mass (Devaskar and Mueckler, 1992; Helgerson and Carruthers, 1987; Montel-Hagen *et al.*, 2008; Mueckler, 1994). In addition, erythrocyte Glut1 also transports L-dehydroascorbic acid (DHA), an oxidized intermediate of ascorbic acid (AA) into cells, which is a unique trait of humans and the few other mammals that have lost the ability to synthesize AA from glucose (Montel-Hagen *et al.*, 2008).

ROS has been increasingly recognized as intracellular messengers in signal transduction. Recent research indicates that ROS are also involved in the regulation of

Glut1 in several human megakaryocytic cell lines (Fiorentini *et al.*, 2004; Maraldi *et al.*, 2004; Prata *et al.*, 2004). Nevertheless, the underlying mechanisms by which ROS regulate Glut1 remain unresolved.

1.7 Hypoxia-inducible factor-1 (HIF-1)

Hypoxia-inducible transcription factors (HIFs) are key players in the cellular response to changes in oxygen tension (Kietzmann and Gorlach, 2005). HIFs are composed of one oxygen-regulated α-subunit and one stable β-subunit (Wenger, 2002). Hypoxia-inducible factor-1 (HIF-1) was originally identified as an EPO enhancer induced by hypoxia during mammalian erythrocytes production, and the following studies found it is a master regulator of oxygen homeostasis, playing critical roles in physiological and pathological processes (Semenza and Wang, 1992; Smith *et al.*, 2008). HIF-1 is a crucial transcription factor for erythropoiesis. In HIF-1-deficient embryos, the committed erythroid progenitors are reduced, together with decreased Hb content and EPOR mRNA levels (Dennery, 2007).

Normally, the formation and transcriptional activity of HIF-1 depend on the amount of HIF-1α, and the expression of HIF-1α is tightly controlled by the cellular oxygen tension, specifically, by hypoxia (Chun *et al.*, 2002). However, there is now accumulating evidence showing that HIF-1α is also regulated by non-hypoxia stimuli. Recent reports indicate that ROS regulate HIF stability and transcriptional activity in well-oxygenated cells, as well as under hypoxic conditions (Pouyssegur and Mechta-Grigoriou, 2006).

HIF-1 is considered to be the major regulator of about 100 physiologically important genes and was found to be conserved from *Caenorhabditis elegans* via *Drosophila melanogaster* to Homo sapiens, suggesting that the HIF-1 system plays an

essential role during evolution (Bacon *et al.*, 1998; Jiang *et al.*, 2001; Kietzmann and Gorlach, 2005; Nagao *et al.*, 1996; Wang *et al.*, 1995). *Glut1*, which encodes glucose transporter 1, is one of these genes that are regulated by HIF-1 (Chen *et al.*, 2001). The stability of HIF-1α is regulated by PHD (prolyl hydroxylase domain) enzymes (Bruick and McKnight, 2001; Epstein *et al.*, 2001; Ivan *et al.*, 2002). PHD enzymes catalyze hydroxylation of critical proline residues within the oxygen-dependent degradation domain of HIF-1α and lead to degradation of HIF-1α (Bruick and McKnight, 2001; Ivan *et al.*, 2002; Jaakkola *et al.*, 2001; Yu *et al.*, 2001). The activity of PHD enzymes is dependent on O_2, 2-oxoglutarate (2-OG) and ferrous iron [Fe(II)] (Schofield and Ratcliffe, 2004; Schofield and Zhang, 1999). Lack any of these co-factors leads to inactivation of PHD enzymes and stabilization of HIF-1α. Under hypoxia condition, lower intracellular O_2 levels decrease PHD activity, thus promoting accumulation of HIF-1α in cells. ROS regulates PHD activity through modulation of iron availability, promoting the oxidation of Fe(II) to Fe(III), thereby activating the HIF-1α response (Gerald *et al.*, 2004; Pouyssegur and Mechta-Grigoriou, 2006) (Figure 1.8).

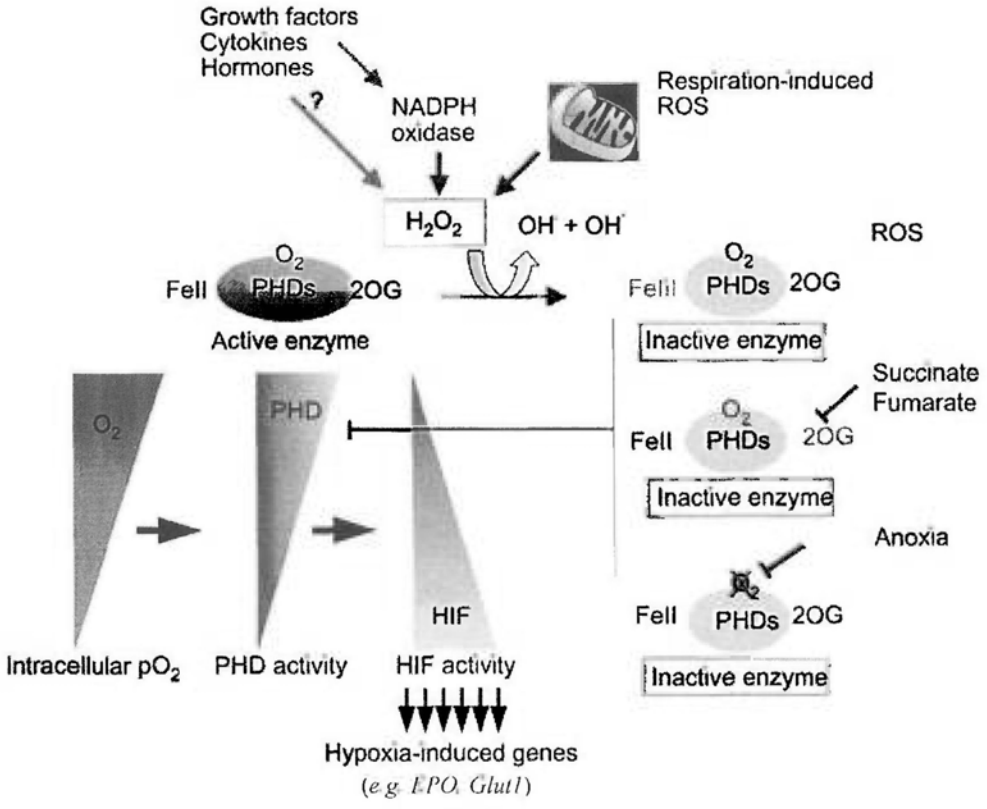

Figure 1.8 Regulation of HIF-α via PHD enzymes.

HIF-α protein is regulated by PHD (prolyl hydroxylase domain) enzymes. In the presences of three necessary co-factors, which are O_2, 2-oxoglutarate (2-OG) and Fe(II), the PHD enzymes catalyze hydroxylation of HIF-α and thus lead to its degradation. Lack any of these three co-factors leads to inactivation of PHD enzymes and stabilization of HIF-α, thereby activating HIF target genes (Adapted from Pouyssegur and Mechta-Grigoriou, 2006).

1.8 Erythrocytes programmed cell death

An adult human harbors over 30 trillion erythrocytes, and the life span of them is about 120 days, that is, approximately 200 billion erythrocytes need to be replaced each day. Erythrocytes are considered to experience senescence eventually resulting in the clearance of aged erythrocytes (Föller *et al.*, 2008; Lang *et al.*, 2008). Apart from that, it has been known for a while that mature enucleated erythrocytes also share the programme for self-destruction through apoptosis, similar to the programmed cell death or apoptosis in nucleated cells. Although the mechanism is poorly understood, mature erythrocytes can undergo a special type of apoptosis known as eryptosis or erythroptosis without the involvement of mitochondria and nucleus (Lang *et al.*, 2006).

Similar to apoptosis, eryptosis/erythroptosis is characterized by membrane blebbing, cell shrinkage, activation of proteases, loss of membrane integrity and the externalization of phosphatidylserine (PS) at the cell surface. Exposed phosphatidylserine is recognized by macrophages that engulf and degrade the affected cells in spleen and liver. After phagocytosis, PS-exposing erythrocytes are degraded intracellularly inside the phagocytes and Hb is not released into the blood stream. In some occasions, erythrocytes are destroyed inside the blood vessels and Hb is released into the blood, which is known as hemolysis. Under this situation, haptoglobin in the blood binds the free Hb tightly to inhibit its oxidative activities and the damages to the vascular endothelium. Unbound Hb is filtrated into urine and causes devastations in the cells of

proximal tubule. Because of this, hemolysis in the blood vessels is high risk leading to renal failure (Jeney *et al.,* 2002, Lang *et al.,* 2005). Therefore, eryptosis/erythroptosis allows clearance of defective erythrocytes without hemolysis. On the other hand, excessive eryptosis/erythroptosis leads to the development of anemia. Diseases associated with accelerated eryptosis/erythroptosis include malaria, β-thalassemia, G6PD-deficiency, iron deficiency, phosphate depletion and so on. Hence, a delicate balance between pro-eryptotic and anti-eryptotic mechanisms is required to achieve homeostasis (Föller *et al.,* 2008; Lang *et al.,* 2008).

Eryptosis/erythroptosis is triggered by erythrocyte injury after several stressors, including oxidative stress. Besides caspase activation under oxidative stress, activation of Ca^{2+}-permeable cation channels is one of the main factors to trigger apoptosis in erythrocytes (Föller *et al.,* 2008; Lang *et al.*, 2006).

1.9 Research objectives and long-term significance

This study primarily concerns the ROS in erythropoiesis or erythrocytes, consisting of two major parts. The first part mainly focuses on the effect of salidroside (SDS) on erythropoiesis or erythrocytes, and the second part focuses on the ROS and anti-oxidant systems during erythropoiesis.

SDS is an antioxidant and adaptogen, which is widely used in traditional medicine for the treatment of high altitude sickness, anoxia and mountain malhypoxia. With this information in mind, we formulated a hypothesis that SDS plays a positive role in erythropoiesis and mature RBCs. The aims of our investigation in this part are therefore (a) to examine the effect of SDS, if any, on erythropoiesis and its possible protective effect against oxidative stress; (b) to find out whether SDS could protect mature erythrocytes from eryptosis triggered by oxidative stress and if any, to elucidate the possible mechanisms.

During erythropoiesis, it is likely that a strong antioxidant system is established and proteins like G6PD, GPx1, Trx1 and Glut1 all play important roles in this system. The aims of our study to evaluate this hypothesis are (a) to develop well controlled G6PD-knockdown TF-1 cells and to determine the possible role of G6PD in erythropoiesis; (b) to investigate the mechanism by which Glut1 is regulated and its possible relationship with ROS during erythropoiesis in TF-1 cells.

The long term significance of this study is therefore to (1) provide support for therapeutic applications of SDS in preventing anemia after cancer chemotherapy and treating G6PD deficiency disease; (2) clearly elucidate the role of G6PD during erythropoiesis, thereby contributing to the treatment of G6PD deficiency disease; and (3) further explore the role of ROS and the underlying mechanisms in erythropoiesis; (4) find out the pathway by which Glut1 is regulated during erythropoiesis, thereby contributing to the treatment of Glut1-related diseases such as Glut1 deficiency syndrome and diabetic complications.

Chapter 2

Materials and Methods

2.1 Materials

2.1.1 Human Erythrocytes

Fresh human RBCs were obtained from healthy donors following informed consent. Heparinized RBCs were washed with PBS, pH 7.4.

2.1.2 Culture of Cells

2.1.2.1 Human Erythroleukemia Cell Line, TF-1

TF-1 cells were purchased from American Type Culture Collection (ATCC, Rockville, MD, USA). It was a GM-CSF / IL-3 dependent human erythroleukemia cell line established by Kitamura *et al.* in October 1987 from the bone marrow of a Japanese patient suffering from severe pancytopenia. Cells were cultured in RPMI 1640 medium (Gibco) supplemented with 10% (v/v) fetal bovine serum, 1% (v/v) penicillin-streptomycin, 1 mM sodium pyruvate, 2.5 g/L glucose (Gibco) and 2 ng/ml GM-CSF (Sigma G5035) (complete medium), according to ATCC instructions. Cells were kept at 37°C, 5% CO_2 incubator (SHEL LAB) with humidified atmosphere.

In general, cells were cultured in a 25 or 75 cm^2 culture flask (IWAKI) and were passaged every 2 to 3 days when 70-90% confluence is reached. In each passage, cells were collected by centrifugation at 1,500 rpm (Eppendorf Centrifuge 5810R) for 3 min. The used medium was discarded, and the cell pellet was then resuspended in complete medium and passaged to a new flask. For the induction of differentiation, cells were kept in a GM-CSF free medium overnight. On the next day, cells were

centrifuged at 1,500 rpm for 3 min and resuspended in GM-CSF free medium supplemented with EPO (10 ng/ml) (Calbiochem 329871), which is considered as day 0 throughout the experiments.

2.1.2.2 Preservation of Cells

Frozen stock of cells were kept in freezing medium and stored in liquid nitrogen. The freezing medium was composed of 95% complete medium (v/v) and 5% DMSO (v/v).

To prepare the stock, cells were first collected by centrifugation at 1,500 rpm (Eppendorf Centrifuge 5810R) for 3 min. Each 2 millions of cells were resuspended in 1 ml of freezing medium and transferred to freezing vials (Nalgene, USA). Cells were first cooled briefly at 4°C for 5 min, and then kept at –20°C until frozen for subsequent storage at –80°C for overnight. Cells can then be stored in liquid nitrogen until use.

To thaw cells, the frozen stock was warm quickly in a 37°C water bath and suspended in 30 ml pre-warmed complete medium for 5 min. Afterwards, cells were collected by centrifugation at 1,500 rpm for 3 min and resuspended with 15 ml of complete medium. The cells were then ready for use after passage of at about 1 week.

2.1.3 Culture Medium

RPMI 1640 medium (Invitrogen 23400-021) was used for culturing TF-1 cells.

Each pack of RPMI 1640 powder with phenol red, L-glutamine and 0.5 mM HEPES was dissolved in 1 L distilled water and 2 g of sodium bicarbonate and 2.5 g of D-glucose (Gibco) were added and the pH was adjusted to 7.2. The medium was then sterilized by filtration with 0.22 μm bottle-top filter (Millipore). Complete medium was obtained by adding 10% (v/v) fetal bovine serum, 1% (v/v) penicillin-streptomycin, 1 mM sodium pyruvate and 2 ng/ml GM-CSF to the sterilized RPMI medium. Differentiation medium was prepared by adding just the same set of supplements to the RPMI medium but excluding GM-CSF, and EPO (10 ng/ml) is added to the medium every time when differentiation is induced. Simply, different media were named as follows:

M

The RPMI medium 1640 was supplemented with 2.5 g/L glucose and 2 g/L sodium bicarbonate (pH 7.2). The medium was filtered by passing through a Steritop-GP Filter (Millipore) and was stored at 4 °C for up to three months.

M2(–)

The M medium was supplemented with 1 mM sodium pyruvate, 10% (v/v) FBS and 1% (v/v) penicillin-streptomycin (all sterile) and was stored at 4 °C for up to one month.

M1

The M2(–) medium was supplemented with 2 ng/ml GM-CSF (Sigma G5035) and stored at 4 °C before use.

M2

The M2(–) medium was supplemented with 10 ng/ml EPO (Calbiochem 329871) immediately before use.

In some experiments, phenol red free RPMI (pRPMI) medium was used. It was prepared by dissolving one pack of phenol red free RPMI powder with L-glutamine in 1 L distilled water and 2 g of sodium bicarbonate was added. The pH was adjusted to 7.2 and was sterilized by filtration as described above.

Unless otherwise specified, human RBCs (1 x 10^7/ml) were incubated in physiological HEPES buffer (PHB) (as described in section 2.1.5) during treatments.

2.1.4 Chemicals and Drugs

Salidroside (SDS), an active component of the medicinal plant *Rhodiola rosea* L., was purchased from International Laboratory (San Bruno, CA, USA). Fluo-4/AM, calcein/AM, were purchased from Molecular Probes. H_2DCFDA and DHE dyes, and blastidin were purchased from Invitrogen. Calcium ionomycin, NAC and vitamin E were obtained from Sigma. EUK-134 was purchased from Cayman. PX-478 was provided by ProlX Pharmaceuticals, AZ. SYBR Green PCR master mix was purchased from Applied Biosystems.

2.1.5 Buffers and Reagents

Unless otherwise specified, buffers were prepared by dissolving chemicals in double distilled water (ddH_2O) and adjusted to suitable pH either with HCl or NaOH.

2.1.5.1 Buffers and Reagents for Common Uses

Phosphate buffered saline (PBS) was composed of 136 mM NaCl, 2.7 mM KCl, 1.5 mM KH_2PO_4 and 8 mM Na_2HPO_4. PBS was titrated to pH 7.4, sterilized by autoclave and stored at room temperature.

Physiological HEPES buffer (PHB) was composed of 140 mM NaCl, 5 mM KCl, 10 mM HEPES, 2.5 mM $CaCl_2$, 10 mM Glucose and 0.1% (w/v) BSA. pH was adjusted to 7.4. Sterilized by filtration and stored at 4°C.

2.1.5.2 Buffers and Reagents for Work of Molecular Biology

Lysis buffer for DNA extraction was composed of 5 mM Tris, 100 mM EDTA and 1% (w/v) SDS. pH was adjusted to 8.0 and stored at 4°C.

6X loading dye for DNA was composed of 0.25% (w/v) bromophenol blue, 0.25% (w/v) xylene cyanol FF and 40% (w/v) sucrose.

50X TAE buffer was composed of 2 M Tris base and 50 mM EDTA and 5.71% (v/v) glacial acetic acid. The 50X buffer is stored at room temperature and diluted 50-fold to 1X TAE buffer when used.

TE buffer was composed of 10 mM Tris and 1 mM EDTA. Buffer was adjusted to pH 7.4 and sterilized by autoclave. TE buffer was stored at room temperature

DEPC-ddH_2O was prepared by mixing 0.1% (v/v) of DEPC (diethyl pyrocarbonate) with ddH_2O and incubated at 37°C with stirring for at least 1 hour

followed by autoclave. It was stored at room temperature.

2.1.5.3 Buffers and Reagents for Bacterial Culture

LB medium was purchased in pre-mixed powder form from USB. It was composed of 1% (w/v) casein peptone, 0.5% (w/v) yeast extract and 0.5% (w/v) sodium chloride. LB broth solution was autoclaved and stored at 4°C. Suitable antibiotic can be added before use when necessary.

LB agar plate was purchased in pre-mixed powder form from USB. It was composed of 1.5% agar, 1% (w/v) casein peptone, 0.5% (w/v) yeast extract and 0.5% (w/v) sodium chloride. LB agar solution was autoclaved and cooled to 55°C. Suitable antibiotic can then be added if necessary. The LB agar solution was then mixed well and poured to Sterilin plates (Bibby Sterilin Ltd) and allowed to solidify at room temperature. The LB agar plates are stored at room temperature.

2.1.5.4 Buffers and Reagents for Annexin-V/Propidium Iodide (PI) Assay

Annexin-V-Fluos labeling solution (Annexin-V) was purchased from Roche. It was stored as aliquots at –20°C and thaw prior to use.

Propidium Iodide (PI) was purchased from Sigma (Sigma Chemical Co., St. Louis, MO, USA). It was stored at 4°C at concentration of 2 mg/ml.

Incubation buffer was composed of 10 mM HEPES, 140 mM NaCl and 5 mM $CaCl_2$. It was adjusted to pH 7.4 and stored at 4°C after preparation.

2.1.5.5 Buffers and Reagents for APOLOGIX Carboxyfluorescein Caspase Detection Kit

The APOLOGIX carboxyfluorescein caspase detection kit was purchased from Cell Technology. Lyophilized FAM-DEVD-FMK (carboxyfluorescein caspase-3 substrate was provided by the kit and was reconstituted in 50 μl of DMSO as the 150X stock solution. The stock was stored as aliquots at -20°C (Cell Technology manual). Repeated freezing and thawing should be avoided. Prior to use, 30X working dilution was made by mixing the 150X stock solution with PBS at volume ration of 1:4. The resultant reagent should be kept in dark and used immediately to obtain best results.

1X washing buffer was obtained by 10-fold dilution of the pre-warmed 10X wash buffer provided by the detection kit with ddH_2O.

10X fixative solution and **propidium iodide** were also provided by the detection kit and stored at room temperature and 4°C, respectively.

2.1.5.6 Buffers and Reagents for Western Blotting

Lysis buffer for total protein extraction was composed of 1% (w/v) SDS, 1 mM Na_3VO_4, 10 mM Tris, and titrated to pH 7.4. The buffer was stored at room temperature. When used, it was supplemented with 21 μg/ml aprotinin, 5 μg/ml leupeptin, 1 mM PMSF and 5 mM $MgCl_2$.

4X lower gel buffer was composed of 1.5 M Tris base and 14 mM SDS. The pH was adjusted to 8.8 and stored at 4°C.

4X upper gel buffer was composed of 0.5 M Tris base and 14 mM SDS. The

pH was adjusted to 6.8 and stored at 4°C.

Separating gel buffer was composed of 40% (for 12% gel) to 60% (for 18% gel) (v/v) acrylamide/bis-acrylamide (30%) solution, 25% (v/v) 4X lower gel buffer, 0.05% (w/v) ammonium persulfate and 0.012% (v/v) TEMED. The buffer was prepared freshly for each experiment.

4.5% stacking gel buffer was composed of 15% (v/v) acrylamide/bis-acrylamide (30%) solution, 25% (v/v) 4X upper gel buffer, 0.07% (w/v) ammonium persulfate and 0.13% (v/v) TEMED. The buffer was also prepared freshly for each experiment.

SDS running buffer was prepared in 10X stock composed of 250 mM Tris base, 1.92 mM glycine and 0.1% (w/v) SDS and stored at room temperature, when used, it was freshly diluted in ddH_2O to 1X concentration.

2X SDS loading dye was composed of 62.5 mM Tris base, 10% (w/v) sucrose, 2% (w/v) SDS, 0.01% (w/v) bromophenol blue and 5% (v/v) 2-mercaptoethanol. Load dye was titrated to pH 6.8 and stored at 4°C.

Electroblotting buffer (E-Blot Buffer) was composed of 48 mM Tris base, 29 mM glycine, 0.0375% (w/v) SDS and 20 % (v/v) methanol. Its pH was adjusted to 9.2 to 9.4 and freshly prepared prior to use.

10X Tris-buffered saline solution (10X TBS) was composed of 0.1 M Tris base and 1.5 M NaCl, its pH was adjusted to 7.4 and was autoclaved and stored at room temperature.

Tris-buffered saline-Tween-20 (TBS-T) was prepared by diluting the 10X TBS for 10-fold with ddH_2O and subsequent addition of 0.1% (v/v) Tween-20. The solution was stored at room temperature.

2.1.6 Antibodies and Kits

Table 2.1 A list of primary antibodies used in this study.

Antibody	Species	Storage temperature	Dilution used	Source
Anti-Catalase	Rabbit	-20°C	1:6000	Calbiochem
Anti-GPx	Rabbit	-20°C	1:250	Cell Signalling
Anti-Trx1	Rabbit	-20°C	1:250	Cell Signalling
Anti-G6PD	Rabbit	4°C	1:1000	Bethyl
Anti-Glut1	Rabbit	4°C	1:1000	Chemicon
Anti-HIF-1α	Mouse	4°C	1:1000	Chemicon
Anti-Hemoglobin	Mouse	-20°C	1:500	Abcam
Anti-CD71	Mouse	4°C	1:2000	Pharmingen
Anti-GlycophorinA -PE	Mouse	4°C	1:500	Pharmingen
Anti-GlycophorinA -APC	Mouse	4°C	1:500	BioLegend
Anti-β-actin	Mouse	4°C	1:2000	Santa Cruz Biotechnology, Inc.
EGFP-Glut1 ligand	—	-20°C	1:25	AbCys SA

Table 2.2 A list of secondary antibodies used in this study.

Antibody	Species	Storage temperature	Dilution used	Source
Anti-mouse-HRP	Rabbit	4°C	1:2000	ZYMED
Anti-mouse-FITC	Goat	-20°C	1:2000	Calbiochem, CA, USA
Anti-rabbit-HRP	Goat	4°C	1:2000	Santa Cruz Biotechnology, Inc.
Anti-rabbit-FITC	Goat	4°C	1:2000	ZYMED

Table 2.3 Table of the name, components included and source of assay kits used in this study.

Name of Kit	Components	Manufacturer
SuperScript First-Strand Synthesis System for RT-PCR	Oligo(dT)$_{12-18}$ (0.5 μg/μl) Random nexamers (50n g/μl) 10X RT buffer (200mM Tris-HCl pH 8.4, 500 mM KCl) 25 mM $MgCl_2$ 0.1 M DTT 10 mM dNTP mix (10 mM each dATP, dCTP, dGTP, dTTP) SuperScript II RT (50 units/μl) RNaseOUT Recombinant RNase Inhibitor (40 units/μl) DEPC-treated water Control RNA (50 ng/μl) Control Primer A (10 μM) Control Primer B (10 μM) *E. coli* RNase H (2 units/μl)	Invitrogen Corporation, USA
Apologix Carboxyfluorescein Caspase Detection Kit (caspase-3)	FAM-DEVD-FMK (lyophilized powder) 10X Washing Buffer Fixative Solution Propidium Iodide	Cell Technology Inc, MN, USA
NADP+/NADPH Quantification Kit	NADP/NADPH Extraction Buffer NADP Cycling Buffer NADP Cycling Enzyme Mix NADPH Developer Stop Solution NADPH Standard (MW:833.36)	BioVision, USA

2.2 Methods

2.2.1 MTT Assay

3-(4,5-dimethylthiazol-2-yl)-2,5-diphenyl-tetrazolium bromide (MTT) assay was used to measure cell viability. Briefly, 20 μl MTT (0.5 mg/ml) solution was added to TF-1 cells (1 x 10^5/ml) after treatments and incubation was continued for 3 h at 37°C, 5% CO_2. Subsequently, 200 μl DMSO was added and absorbance was measured at 540 nm.

2.2.2 Hemolysis Assay

Freshly isolated human RBCs (1 x 10^7/ml) were treated with different agents at 37°C, 5% CO_2 in physiological HEPES buffer. After treatment, absorbance of supernatant was measured at 415 nm with an ELISA plate reader (Bio-Rad) for the leakage of hemoglobin.

2.2.3 Fluorescence Emission Spectrum Measurement

Emission spectrum of 100 μM salidroside in PBS was detected by luminescence spectrometer LS 50B (Perkin Elmer). FITC dye in PBS was served as control.

2.2.4 Confocal Laser Scanning Microscopy

Confocal laser scanning microscopy (CLSM) was first developed by Marvin Minsky in 1953, and after subsequent modifications and improvements, it became a

valuable tool for gaining high resolution blur-free and/or 3-dimentional images from cells in the end of 1980s. In this study, confocal images of cells were acquired on a system of CLSM (Leica Microsystems, SP5) that fitted with an argon laser (488 nm for excitation).

TF-1 cells used in this study are suspension cells and need to be adhered onto a glass slide before observation by CLSM. Therefore glass bottom dishes (35 mm dish with 20 mm bottom well, In Vitro Scientific, China) were pre-coated with 0.1% (v/v) poly-L-lysine for 15 min, then washed twice with PBS and air-dried. 5 x 10^5 cells were then coated onto the center of each dish at 37°C, 5% CO_2 for 15 min. The cell-coated dishes was then washed twice with PBS to remove unbound cells and filled in 300 μl PBS and observed under CLSM.

2.2.5 Flow Cytometry

2.2.5.1 Introduction

Flow cytometry is a technology simultaneously measures and analyses multiple physical or optical characteristics of single particles when they flow through a beam of light in a fluid system. When a single particle (or usually cell) is met by the incident light (argon laser), its properties including size, relative complexity (or granularity if it refers to cell), and fluorescence signals can be recorded based on the way it reflects or scatters the light beam and emits fluorescence. The setup of a typical flow cytometry was illustrated in Figure 2.1.

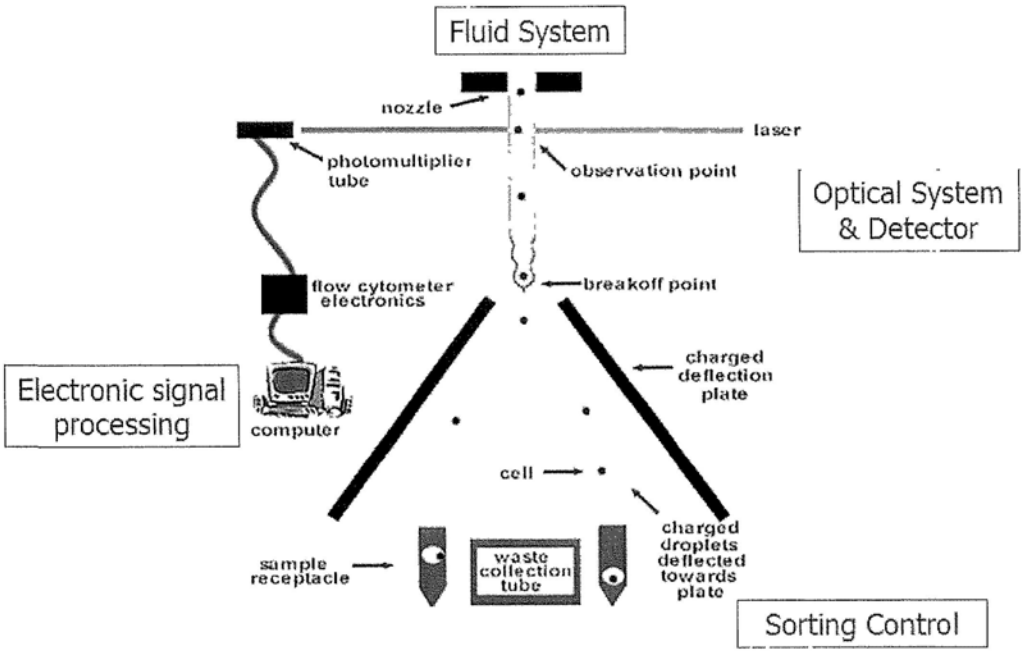

Figure 2.1 Principle of flow cytometry. A flow cytometer is composed of four main systems: fluidics, optics, electronics and sorting control. The fluidics system transports particles to the laser beam for examination. The mechanism which allows it to deliver particles to the center of the laser beam is called hydrodynamic focusing, which is done by injecting the particle in the center of shealth fluid at a different velocity and pressure. The optics system consists of one or more lasers to generate light beams to hit on the particle, as well as optical filters to direct the resultant signals to suitable detectors. The electronics system translates the light signals into comprehensible electronic signals to the computer for data interpretation. The sorting control system separates cells with different signals.

(Source: nanobio.snu.ac.kr/eng/research_2/research_2_microFACS.htm)

2.2.5.2 Detection of Cellular Characteristics by FCM

Flow cytometric analysis was used to study different cellular properties of TF-1 cells during its differentiation. Cells were acquired on a system of FACSort FCM (Becton Dickinson), and the acquisition of cells was performed by CellQuest program (Becton Dickinson). Excitation filter with 488 nm (argon laser) was used and the population of cells was located by signals collected from the forward scatter (FSC) and the side scatter (SSC), which determines the size and granularity of a cell, respectively. A suitable region was selected to restrict the subsequent fluorescence analysis and thus guaranteed the data collected should be highly representing the properties of the cells. Unless otherwise specified, every single FCM analysis contains the fluorescence data of 10,000 events (or 10,000 cells) being measured. The sample flow rate was adjusted in all experiments not to exceed 300 cells/sec if possible.

2.2.5.3 Estimation of Erythroid Maturation by FCM

Study of expression of different lineage specific markers, usually concerning the cluster of differentiation (CD), is a very popular method in evaluation of differentiation in various cell types (Clarke, 2005; Stetler-Stevenson and Braylan, 2001). In this study, the expression level of two erythroid cell specific markers, glycophorin A (CD235a/GPA) and transferrin receptor (CD71) and a cytosolic protein Hb was evaluated by FCM.

For surface marker **GPA** staining, approximately 5 x 10^5 cells were collected and washed twice with PBS. The cells were then resuspended in PBS containing 1% (w/v) BSA, 0.5 μg/μl mouse IgG and 0.5 μg/μl rat IgG for blocking of non-specific binding. After 15 min of incubation on ice, phycoerthrin (PE)-conjugated mouse anti-GPA monoclonal antibody (Pharmingen) was added and further incubated on ice for 30 min. Cells were subsequently washed in PBS for 3 times and analyzed using FCM by collection of fluorescence of PE at channel FL-2H at logarithm (log) scale.

For surface marker **CD71** staining, approximately 5 x 10^5 cells were collected and washed twice with PBS. The cells were then resuspended in buffer containing 1% (w/v) BSA, 0.5 μg/μl goat IgG and 0.5 μg/μl rat IgG for blocking of non-specific binding and incubated on ice for 15 min. Thereafter, mouse anti-CD71 monoclonal antibody (Pharmingen) was added and further incubated on ice for 30 min. Cells were then washed in PBS for 3 times and FITC-conjugated goat anti-mouse secondary antibody (Calbiochem) was added for incubation on ice for another 30 min. After washing the cells for 3 times, analysis was performed by FCM for fluorescence of FITC at channel FL-1H at log scale.

For **Hb** staining, approximately 1 x 10^6 cells were collected and washed twice with PBS. The cells were fixed with 1% (v/v) paraformaldehyde at 4°C for 1 hr and permeabilized with 0.1% (v/v) triton X-100 in PBS at 4°C for 30 min. Cells were then incubated on ice in PBS containing 1% (w/v) BSA, 0.5 μg/μl goat IgG and 0.5 μg/μl rat IgG for blocking of non-specific binding for 15 min. Thereafter, mouse anti-Hb monoclonal antibody (Abcam) was added and further incubated on ice for 30 min.

Cells were then washed in PBS for 3 times and FITC-conjugated goat anti-mouse secondary antibody (Calbiochem) was added for incubation on ice for another 30 min. After washing the cells for 3 times, analysis was performed by FCM for fluorescence of FITC at channel FL-1H at log scale.

2.2.5.4 Detection of Cell Surface Glut1 by FCM

It has been difficult to raise antibodies against the extracellular part of GLUT1, thus hampering detection of this receptor at the cell surface, its main function location. The recent identification of the receptor binding domain of the human T cell leukemia virus (HTLV) envelope glycoprotein (HRBD) that is necessary and sufficient to bind GLUT1 (Kim *et al.*, 2004; Manel *et al.*, 2003a) has allowed the development of an HRBD-derived peptide coupled with EGFP (EGFP-GLUT1 ligand).

EGFP-GLUT1 ligand has been shown to bind the carboxy terminal extracellular loop of GLUT1 (Manel *et al.*, 2005a). EGFP-GLUT1 ligand allows GLUT1 expression to be monitored at the plasma membrane of all mammalian cell lines by FACS analysis or fluorescence staining (Manel *et al.*, 2005b). EGFP-GLUT1 ligand can provide insights, as a qualitative and quantitative marker, into the molecular bases of both normal and disordered glucose homeostasis.

Assessment of GLUT1 expression via binding of the ligand correlates with increased glucose uptake, as observed in malignant cancer cells or metabolically active cells. EGFP-GLUT1 ligand has facilitated studies of GLUT1 expression during T cell activation (Manel *et al.*, 2003b) and has been critical for the successful

identification of an immature $CD4^+CD8^+$ human thymocyte population with high metabolic activity (Swainson *et al.*, 2005).

For binding assay of **Glut1**, 1:25 dilution of EGFP-Glut1 ligand is generally appropriate for 10^5 cells. The procedures are as follows:

1. Dilute EGFP-Glut1 ligand 25X in PBA (PBS containing 2% FCS [FBS] and 0.01% sodium azide). Pellet 10^5 cells for each binding assay.
2. Resuspend the cell pellet in 100 µl of diluted EGFP-Glut1 ligand.
3. Incubate at 37°C for 30 min.
4. Centrifuge at 3200 rpm for 3min at 4°C and gently aspirate the supernatant.
5. Wash the pellet with 1 ml of cold PBA.
6. Cells can be further stained with conjugated antibodies at 4°C.
7. Acquisition and analysis by flow cytometry.

2.2.5.5 Detection of Caspase Activity by FCM

In this study, the APOLOGIX FAM caspase detection kit was employed. This kit is based on the use of carboxyfluorescein labeled fluoromethyl ketone (FMK)-peptide inhibitors of caspases, which are cell permeable and non-cytotoxic. The inhibitor forms a covalent bond with the cysteine residues in the active site of activated caspases once inside the cell, and thus its fluorescence signal can be measured by FCM.

3 x 10^5 cells were collected and washed once in PBS. Cells were then

resuspended in 300 μl complete medium with 10 μl of 30X cell permeable fluorogenic caspase-3 inhibitor FAM-DEVD-FMK (Cell Technology Inc, MN, USA) and incubated in dark for 1 hr at 37°C and 5% CO_2. The cells were then washed with 1X washing solution twice and then analyzed by FCM for collection of fluorescence from intracellular FAM-DEVD-FMK at FL-1H (log scale).

2.2.5.6 Detection of Apoptotic and Necrotic/late Apoptotic Cells by FCM

Phosphatidylserine (PS) is one of the components of the plasma membrane of human cells. In healthy cells, PS was asymmetrically predominated on the inner cytosolic membrane. This could be due to the active transport of PS on the outer membrane back to the inner membrane by flippase. In apoptotic cells, such membrane asymmetry is lost and PS can be found on both side of the lipid bilayer. In the presence of calcium, the specific binding of annexin-V to PS can be used to label externalized PS, and thus serves as a method to detect apoptosis if the annexin-V is conjugated to a fluorescent dye like FITC. PI is another dye with red fluorescence that cannot penetrate the cytosolic membrane so can be used to detect dead cells.

To detect apoptosis in cells, cells 5 x 10^5 cells were first collected and washed twice with PBS. The following steps should be done in dark environment. Cells were resuspended in 100 μl incubation buffer containing 2% (v/v) annexin-V-FITC and incubated for 20 min at room temperature. Cells were then loaded with 400 μl incubation buffer that contained 2.5 μg/ml PI. Cells were further incubated at room

temperature for 5 min and analysed by FCM. Signals of annexin-V-FITC and PI were collected at channels of FL-1H and FL-3H respectively, and both channels were set at log scale.

To evaluate apoptosis in RBCs, flow cytometric analysis using annexin-V and calcein/AM, similar to the annexin-V/propidium iodide assay for nucleated cells, was employed (Bratosin *et al.*, 2005; Vermes *et al.*, 1995). After treatments, erythrocytes were loaded with PE-annexin-V and calcein/AM (1 μg/ml) for 20 min at room temperature. PE-annexin-V is able to label the PS externalized on the outer leaflet of plasma membrane. Calcein/AM is a non-fluorescent dye. After diffusing into the cytoplasm across the plasma membrane, the ester linkage between calcein and the AM group is cleaved by cytosolic esterases and the hydrophilic calcein cannot diffuse out. However, in cells with damaged membrane, calcein is leaked out and a reduction in fluorescence will be detected.

Increase in $[Ca^{2+}]_i$ is an important factor of apoptosis in RBCs (Föller *et al.*, 2008). For the determination of $[Ca^{2+}]_i$, RBCs were loaded with fluo-4/AM (10 μM) for 20 min at room temperature and changes in the $[Ca^{2+}]_i$ after various treatments were measured semi-quantitatively by flow cytometry with an excitation at 488 nm.

2.2.5.7 Analysis of Intracellular ROS by FCM

Intracellular ROS levels were measured by using the fluorescent dyes CM-H_2DCFDA (Invitrogen C6827) and DHE (Invitrogen D1168). CM-H_2DCFDA detects hydrogen peroxide (H_2O_2), hydroxyl radicals (HO·), peroxyl radicals (ROO·)

and peroxynitrite anions (ONOO–). DHE detects superoxide anions (·O2–). For each sample, 5 x 10^5 cells were washed twice with ice-cold PBS and pelleted by centrifugation at 4300 rpm for 3 min at 4 °C (Eppendorf Centrifuge 5417R). The cells were then resuspended in 0.5 ml PBS containing 5% FBS (v/v) and either CM-H_2DCFDA (10 μM) or DHE (10 μM). The samples were incubated for 30 min at 37 °C in dark. Subsequently, the cells were washed and subjected to flow cytometric analysis. Signals for CM-H_2DCFDA (FITC), DHE (PE) were collected from the respective channels as indicated in the brackets.

2.2.5.8 FACS Cell Sorting

Differentiating erythroblasts were separated from undifferentiated cells by FACS cell sorting. For each sample, 5 x 10^6 cells were washed twice with ice-cold PBS and pelleted by centrifugation at 3000 rpm for 3 min at 4°C (Eppendorf Centrifuge 5810R). The cells were then resuspended in 5 ml PBS containing 100 μg/ml mouse IgG and 5 mg/ml BSA and incubated for 30 min on ice. Anti-GPA-PE antibody was then added into the samples at a dilution of 1:500. The cells were further incubated for 30 min on ice in dark. Subsequently, the cells were washed with ice-cold PBS for three times and subjected to FACS cell sorting on the PE channel according to the intensity of PE labeling. GPA^+ cells were regarded as differentiating cells whereas GPA^- cells were undifferentiated cells. The GPA levels of sorted samples were confirmed by another flow cytometer FACSCanto.

2.2.5.9 Analysis of FCM Data

All data from FCM were analysed using the FlowJo version 5.7.2 software. Files with one fluorescence parameter were analysed with histogram, whereas those with two different fluorescence signals were analysed either with dot plot or contour plot.

2.2.6 NADPH / $NADP^+$ Ratio Quantification

1. Sample Preparation: wash cells with cold PBS. Pellet 10^5 cells for each assay in a microcentrifuge tube (2000 rpm for 5 min). Extract the cells with 200 µl of NADP/NADPH Extraction Buffer by freeze/thaw two cycles (20 min on dry-ice, then 10 min at room temperature), or homogenization. Vertex the extraction for 10 sec. Spin the sample at 14000 rpm for 5 min. Transfer the extracted NADP/NADPH solution into a new labeled tube.
2. Standard Curve: Dilute 10 µl of the 1 nmol/µl NADPH standard with 990 µl NADP/NADPH Extraction Buffer to generate 10 pmol/µl standard NADPH. Diluted NADPH solution is unstable, must be used within 4 hours. Add 0, 2, 4, 6, 8, 10 µl of the diluted NADPH standard into labeled 96-well plate in duplicate to generate 0, 20, 40, 60, 80, 100 pmol/well standard. Set blank control in duplicate. Make the final volume to 50 µl with NADP/NADPH extraction buffer.
3. Samples: To detect total NADP/NADPH (NADPt), transfer 50 µl of extracted samples into labeled 96-well plate in duplicates. Several sample dilutions should be performed to ensure the reading can be within the standard curve range.
4. Decompose of NADP from extraction: To detect NADPH only, aliquot 200 µl

samples into eppendorf tubes. Heat samples to 60 °C for 30 min in a water bath or a heating block. Under the conditions, all NADP will be decomposed while NADPH will still be intact. Cool samples on ice. Quick spin samples if precipitates occur. Transfer 50 µl of NADPH samples into labeled 96-well plate in duplicates. Several sample dilutions should be performed to ensure the reading can be within the standard curve range.

5. Prepare a NADP Cycling Mix for each reaction:

   NADP Cycling Buffer Mix: 98 µl

   NADP Cycling Enzyme Mix: 2 µl

   Mix well and add 100 µl of the mix into each well, mix well.

6. Incubate the plate at room temperature for 5 min to convert NADP to NADPH.

7. Add 10 µl NADPH developer into each well. Let the reaction develop for 1 to 4 hours. Read the plate at OD 450 nm. The signal increases as the reaction time. The plate can be read multiple times while the color is in developing. The reaction can be stopped by addition of 10 µl Stop Solution each well and mix well. The color should be stable within 48 hours in a sealed plate, after the reactions are stopped.

8. Calculation: Apply the sample OD 450nm reading to standard curve. The background reading is very significant in the enzyme cycling reaction. Therefore the reading of blank control should be subtracted from standard and samples. The amount of NADPt or NADPH can be expressed in pmol/10^6 cells or ng/mg protein (NADPH molecular weight 833.36). NADPH / $NADP^+$ ratio is calculated as: NADPH / (NADPt – NADPH)

2.2.7 Real-Time PCR

Real-time PCR is a quantitative PCR method allowing simultaneous DNA amplification and quantification through polymerase chain reaction. By means of gene specific probes (modified oligonucleotides that emit fluorescence when forming double strand with a gene specific sequence), DNA content in a PCR can be determined after or during each cycle of amplification, and thus the number of mRNA or cDNA copies of a particular gene in a sample can be quantified.

2.2.7.1 Extraction of mRNA

RNA was first extracted from cells that acted as a template for the subsequent first stranded cDNA construction. During RNA extraction, all the materials used should be cleaned with DEPC water and autoclaved if possible, the lab bench and equipment used should also be cleaned with RNase Away (Molecular BioProducts Inc., San Diego, CA, U.S.A.) to ensure a RNase-free working area.

About 2 x 10^6 of TF-1 cells were collected and washed twice with PBS. Cells pellet were then lysed with 1 ml of Trizol reagent and transferred to a microcentrifuge tube. Pipetting up and down for several times will improve the yield of extraction. All the subsequent steps should be kept at 4°C in order to prevent the degradation of RNA. Cells were first lysed at 4°C for 5 min, then 200 μl of chloroform was added and vortexed for 15 sec to mix well. Samples were then incubated at 4°C for an additional 3 min and then centrifuged at 12,000 rpm (Eppendorf Centrifuge, 5417R) for 10 min at 4°C. After centrifugation, 3 layers were formed, a lower phase with red colour

(protein), an interphase (DNA) and an upper transparent phase (RNA). The upper phase was transferred to a new tube and 500 μl of isopropanol was added for RNA precipitation. Samples were mixed and incubated at 4°C for 10 min followed by centrifuged at 12,000 rpm (Eppendorf Centrifuge, 5417R) for 10 min at 4°C. Supernatant was discarded and the pellet was washed once with 1 μl of ice-cool 75% ethanol. The RNA samples can be stored in this format at –70°C. When used, the pellet was again centrifuged at 9,000 rpm (Eppendorf Centrifuge, 5417R) for 5 min at 4°C. The ethanol was discarded and the RNA was air-dried at room temperature. 25 μl of DEPC-dH2O was added to dissolve the RNA pellet. Samples were incubated at 60°C for 10 min and their quantities and integrities were determined before reverse transcription can be carried out.

Optical density at 260 and 280 nm were examined under UV-visible spectrophotometer (Shimadzu, model UV-1601). Two μl of RNA sample was added up to 500 μl in DEPC-dH_2O for optical density determination. The ratio of absorbance at OD 260/280 should be greater than 2.0, and the quantity of RNA in samples was calculated by the equation: RNA (μg/μl) = OD 260 x 40 (μg/ml) x 250 (dilution factor). The integrity of RNA was then confirmed by running RNA samples under 1.5% agarose gel electrophoresis in TBE buffer. The presence of 18S and 28S ribosomal RNA (rRNA) and neglectable smear in the gel indicated successful RNA extraction.

2.2.7.2 First-Strand cDNA Synthesis by Reverse Transcription

Reverse transcription was carried out using SuperScript First-Strand Synthesis System for RT-PCR from Invitrogen according to the manufacturer's manual. Incubations at different temperature were performed in PCR tubes placed in a thermalcycler.

First of all, 5 μg total RNA was mixed with 1 μl dNTP mix (10 mM) and 0.5 μg oligo$(dT)_{12-18}$ and add up to 10 μl with DEPC-treated water. The RNA/primer mixture was incubated at 65°C for 5 min and then cooled down to 4°C for 1 min. Then 9 μl of reaction mixture composed of 2 μl of 10X RT buffer, 4 μl of 25 mM $MgCl_2$, 2 μl of 0.1 M DTT and 1 μl of RNaseOUT recombinant RNase inhibitor was added to the RNA/primer mixture, mixed gently and incubated at 42°C for 2min. One μl of SuperScript II reverse transcriptase (50 U/μl) was added to the mixture and further incubated at 42°C for 50 min. The reaction was terminated at 70°C for 15 min and chilled on ice. At last, 1 μl of RNase H was added to each reaction and incubated for 20 min at 37°C to remove the RNA remained and the resultant cDNA pool can be stored at –70°C.

Parallel positive and negative controls can be setup respectively by using a control RNA (50 ng/μl) or DEPC-treated water in place of the total RNA when preparing the RNA/primer mixture. A pair of known primers provided by the kit was then employed in the subsequent PCR of the positive and negative controls, and a band with correct size in the positive, but not in the negative control, indicate

successful RT reaction.

2.2.7.3 Polymerase Chain Reaction (PCR)

Primers used in real-time PCR are as follows:

For HIF-1α

Forward: 5' TGGCTGCATCTCGAGACTTT 3'

Reverse: 5' GAAGACATCGCGGGGAC 3'

For Glut1

Forward: 5' ATGGAGCCCAGCAGCAA 3'

Reverse: 5' GGCATTGATGACTCCAGTGTT 3'

For β- actin (ACTB)

Forward: 5' AGCACAGAGCCTCGCCTTT 3'

Reverse: 5' GTTGTCGACGACGAGCG 3'

(Designed from http://primerdepot.nci.nih.gov/)

cDNA prepared was 10-fold diluted in ddH2O and 1 μl of the diluted cDNA was used in each reaction in real-time PCR. SYBR Green PCR master mix was employed. Reaction mixture was prepared as follows:

SYBR Green PCR master mix	10 μl
Forward primer (10 μM)	0.5 μl
Reverse primer (10 μM)	0.5 μl
Diluted cDNA	1.0 μl
Autoclaved ddH_2O	8 μl
Total	20 μl

Each set of experiments was done in triplicates to ensure reproducibility. Real-time PCR were performed by Fast 7500 Real Time-PCR machine (Applied Biosystems) according to manufacturer's instruction and the PCR conditions were as follows with adding dissociation analysis:

1. 50 °C 2 min
2. 95 °C 10 min
3. 95 °C 15 s
4. 60 °C 1 min
5. Repeat step 3 for 39 cycles.

The basis of gene quantification in real-time PCR relies on the comparison of the threshold cycle (C_T), the number of cycle for fluorescence emission in a sample to exceed a fixed intensity. The threshold cycle is theoretically inversely proportional to the initial mRNA copy number of a particular gene. The C_T was determined by using "Sequence Detection Systems, Version 1.9" (Applied Biosystems). The expression level of the target gene is thus calculated as the "Mean fold change" according to manufacturer's protocol (Livak, *et al.*, 2001) as follows:

Mean fold change = $2^{-\Delta\Delta C_T}$

Where $-\Delta\Delta C_T = \Delta C_T$ of target gene of sample - ΔC_T of target gene of control

$\Delta C_T = C_T$ of target gene – C_T of control gene

The mean fold changes of target gene from different samples were calculated using β-actin (ACTB) as the control gene.

2.2.8 Western Blot Analysis

2.2.8.1 Protein Extraction

SDS lysis method was used to completely lyse cells for total protein extraction. Cells were collected by centrifugation at 2,800 rpm (Eppendorf Centrifuge, 5417R) and washed twice with PBS. Each million of cell pellet was then resuspended with 100 μl of SDS lysis buffer (1% (w/v) SDS, 1 mM Na_3VO_4, 10 mM Tris, 5 mM $MgCl_2$, 21 μg/ml aprotinin, 5 μg/ml leupeptin, 1 mM PMSF and pH 7.4) and incubated at room temperature for 1 hr. The lysate was then boiled for 10 min and centrifuged at 14,000 rpm (Eppendorf Centrifuge, 5417R) at 4°C for 7 min. After centrifugation, the supernatant was collected and stored at –20°C.

2.2.8.2 Protein Quantification by BCA assay

The concentration of protein extracted should be more or less similar, but to ensure a fair comparison between different samples, an equal amount of protein should be used for SDS-PAGE, thus BCA method was used to determine the concentration of each protein sample. 96-well plate was used in the assay, a set of protein standards were prepared by adding different amount (0, 2, 4, 6, 8 and 10 μg) of bovine serum albumin (BSA) into each well. Each 2 μl of protein sample was mixed with 8 μl of PBS and added into a well. Both protein samples and BSA standard were done in triplicate. BCA reagent was then prepared freshly by mixing bicinchoninic acid (BCA) solution with $CuSO_4$-$5H_2O$ by the volume ratio 50:1. 150

μl BCA reagent was added to each well and incubated at 37°C for 30 min. Absorbance at OD 540 nm was then determined, with BCA reagent used as blank. A standard curve was constructed according to the results of the BSA protein standard (Figure 2.7). The resultant linear equation of the standard curve was then used to calculate the concentration of different protein samples.

2.2.8.3 SDS-PAGE

The apparatus of Mini-Protean II Cell (BIO-RAD Laboratories) was set up according to the steps in manual. Generally, 12% separating gel was used and 25 μg of protein was loaded into each well. In other cases, if the protein being determined is relatively small in size (below 20 kDa), 18% separating gel can be used to improve the resolving effect, and if the expression level of the protein in cell is relatively trace, the amount of protein loaded can be increased to 50 μg. Protein sample was mixed with equal amount of 2X SDS loading buffer and boiled for 10 min. Benchmark protein marker and samples were added to each well and the SDS gel was run at 150 V for 1 hr (12% gel) or 1.5 hrs (18% gel).

2.2.8.4 Electroblotting of Protein

Mini Trans-Blot Cell (tank transfer system, BIO-RAD Laboratories) was set up according to the steps in the manufacturer's manual. 0.22 μm PVDF (polyvinylidene fluoride) membrane (Immobilon, Millipore) was used for electroblotting. Preparation

of E-blot buffer has been described in section 2.1.3.10 and was freshly prepared in each experiment. The dry PVDF membrane was soaked briefly in absolute methanol for rehydration and then in E-blot buffer for 5 min. One mm filter paper (Whatman) was also used and was soaked in E-blot buffer for 15 min. The sequence of setting up an electroblotting was: cathode, fiber pad, 3 X filter paper, gel, membrane, 3 X filter paper, fiber pad, and anode. Electroblotting was carried out at constant current (400 mA) for 1 hr.

2.2.8.5 Probing of Protein with Antibodies

Non-specific binding of the membrane was blocked with 10% (w/v) non-fat milk in TBS-T at room temperature for 2 hr. The membrane was then probed with primary antibody in 10% (w/v) non-fat milk in TBS-T at 4°C for overnight. The membrane was then washed for 3 times with TBS-T each for 15 min. Membrane was then probed with secondary antibody in 10% (w/v) non-fat milk in TBS-T for 1 hr. At last, the membrane was again washed 3 times with TBS-T each for 15 min.

2.2.8.6 Enhanced Chemiluminescence (ECL)

Membrane was probed with ECL reagent mixture (ECL reagent 1 and ECL reagent 2, volume ratio 1:1) (Amersham Pharmacia Biotech) for 1 min at room temperature. ECL reagent mixture was then dipped off the edge of the membrane and the membrane was wrapped in saran wrap. Signal was develop on Fuji Medical x-ray film (super Rx, Fuji) for various time points. Films were processed in a film processor

(M35 X-OMAT, Kodak).

2.2.9 Construction of Stable G6PD-knockdown TF-1 Cells

2.2.9.1 Introduction

MicroRNAs (miRNAs) are endogenously expressed small ssRNA sequences of ~22 nucleotides in length which naturally direct gene silencing through components shared with the RNAi pathway (Bartel, 2004). The mature miRNAs regulate gene expression by mRNA cleavage (mRNA is nearly complementary to the miRNA) or translational repression (mRNA is not sufficiently complementary to the miRNA). Target cleavage can be induced artificially by altering the target or the miRNA sequence to obtain complete hybridization (Zeng *et al.*, 2002). In animals, most miRNAs imperfectly complement their targets and interfere with protein production without directly inducing mRNA degradation (Ambros, 2004). The engineered miRNAs produced by the BLOCK-iT™ Pol II miR RNAi Expression Vector Kits (Invitrogen, K493600) fully complement their target site and cleave the target mRNA. In this project, we employed this kit and ordered BLOCK-iT™ miR RNAi Select oligos targeting G6PD gene (Invitrogen, 1299003MIR) for construction of G6PD-knockdown TF-1 cells.

2.2.9.2 Procedures

Using the reagents supplied in the BLOCK-iT™ Pol II miR RNAi Expression

Vector Kit and according to its instructions, perform the following steps to generate an expression clone in pcDNA™6.2-GW-EmGFP-miR:

1. Anneal the single-stranded oligonucleotides targeting G6PD to generate a double-stranded oligo (ds oligo).
2. Clone the ds oligo into the linearized pcDNA™6.2-GW-EmGFP-miR vector.
3. Transform the ligation reaction into One Shot TOP10 chemically competent *E. coli* and select for spectinomycin-resistant transformants (50 μg/ml spectinomycin in LB agar plates).
4. Sequence the vectors of the transformants using the primers as follows:

Primer	Sequence
miRNA forward sequencing primer **or** EmGFP forward sequencing primer	5′ - TCCCAAGCTGGCTAGTTAAG -3′ **or** 5′ - GGCATGGACGAGCTGTACAA -3′
miRNA reverse sequencing primer	5′ - CTCTAGATCAACCACTTTGT -3′

5. Transfect the well-targeted G6PD pcDNA™6.2-GW-EmGFP-miR expression construct to TF-1 cells by electroporation as follows: (i) Resuspend 2 x 10^6 TF-1 cells in 400 μl sterile PBS containing 16 μg of DNA of the construct; (ii) Shock the cell suspension in a BTX T820 electroporator for 700 volts, 900 μs, 5 pluses; (iii) Incubate cells in 3 ml complete medium at 37°C, 5% CO_2 overnight and renew medium the next day.
6. Isolate stable TF-1 cell line expressing the miRNA target G6PD by culture selection using blasticidin (10 μg/ml in culture medium).

2.2.10 Statistical Anaylsis

Results of all experiments were expressed as mean ± SD of triplicate determinations. Data were compared using the Student's *t*-test. *P*-values less than 0.05 were considered statistically significant.

Chapter 3

Salidroside Promotes Erythropoiesis and Protects Erythroblasts against Oxidative Stress

3.1 Introduction

In the 19th century, medicinal plant *Rhodiola rosea* L. was used as a folk medicine in France, Germany and many European countries to fight fatigue. Salindroside (SDS) is an active constituent of *Rhodiola rosea* L.. It has been reported to have a broad spectrum of pharmacological properties including anti-oxidative effect. In China and Tibet, SDS has long been used as a blood tonic and adaptogen. However, the mechanism underlying the SDS use remains unclear. Employing commonly used erythropoiesis model TF-1 cells, the effect of SDS on erythropoiesis and its possible protective effect against oxidative stress was examined.

3.2 Fluorescence Emission Spectrum of Salidroside

In flow cytometric assay, 488 nm laser line was employed and in order to exclude the possibility that SDS emits fluorescence when excited by a 488 nm laser which could affect the result, we detected the emission spectra of SDS. As shown in Figure 3.1, 100 μM SDS hardly emitted any fluorescence (blue line) as compared to the positive control FITC (red curve) under 488 nm laser excitation, suggesting that SDS did not emit any fluorescence that affects flow cytometric results.

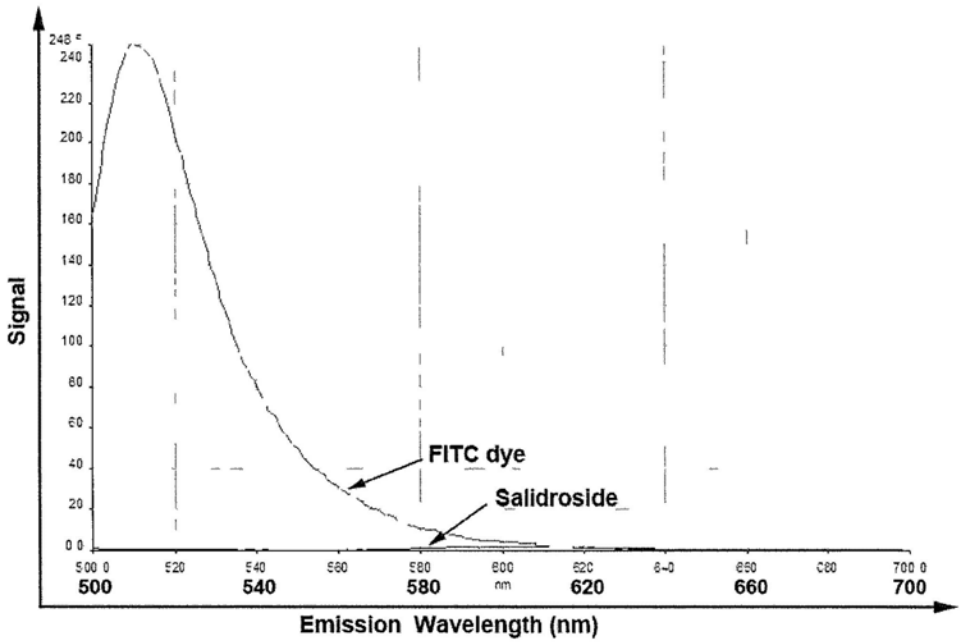

Figure 3.1 Detection of fluorescence emission spectrum of salidroside. Emission spectrum of salidroside (100 μM) was obtained in PBS as excited with a 488nm laser line from a luminescence spectrometer. FITC dye (25 nM) in PBS was served as control.

3.3 Effects of Salidroside on TF-1 Erythropoiesis

3.3.1 Salidroside promotes cell growth in the EPO-treated TF-1 cells

The potential cytotoxic effect of SDS on the EPO-treated TF-1 cell was determined by MTT assay. As shown in Figure 3.2a, the number of viable cells (indicated by mitochondrial dehydrogenase activity) increased in a time- and dose-dependent manner when cells were treated with SDS in the range from 0-100 μM for 4 to 8 days. In fact, concentration of SDS up to 200 μM could still promote TF-1 cell growth but the effect was not as significant as 100 μM. Therefore, 100 μM was chosen as an optimal concentration for further studies.

The effect of SDS on the cell growth of TF-1 cells in terms of cell number was subsequently measured by flow cytometry. EPO alone was able to induce cell growth in TF-1 cells and after incubation for 4 days, the cell number was almost double (Figure 3.2b). In the groups co-cultured with EPO and SDS (100 μM), more cells were obtained and the effect was more obvious at day 6 and day 8. However, in the absence of EPO, SDS alone could not maintain the survival of cells and the cell number decreased in a time-dependent manner. Taken together, our results show that SDS (100 μM) is able to promote cell growth in TF-1 cells in the presence of EPO.

(a)

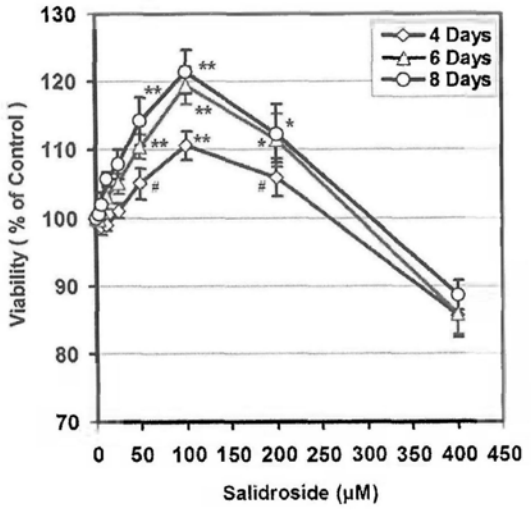

(b)

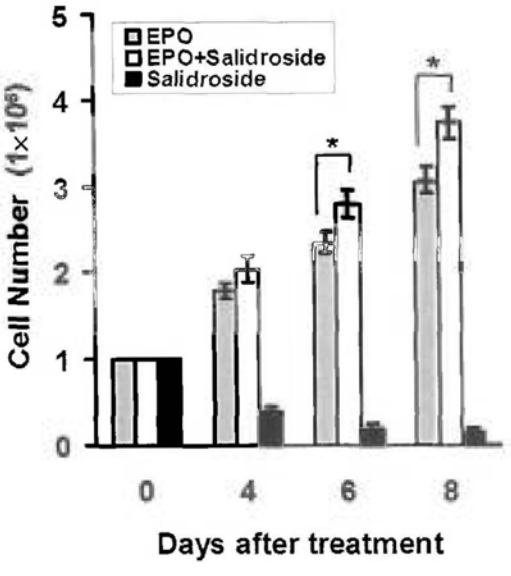

Figure 3.2 Effect of salidroside on the viability and cell growth in the EPO-treated TF-1 cells. TF-1 cells were cultured with EPO (10 ng/ml) with various concentrations of salidroside at 37 °C, 5% CO_2. Viability (% of control) was measured by MTT assay. Mean ± SD, n=3, $*P < 0.05$, $**P < 0.005$, # p>0.05 (**a**). TF-1 cells (1×10^5/ml) were treated with EPO (10 ng/ml) alone, salidroside (100 μM) alone or EPO (10 ng/ml) with salidroside (100 μM) at 37 °C, 5% CO_2 for 2 to 8 days. Total cell number was determined by flow cytometry and results are mean ± SD, n=5 (bar-chart), * $P < 0.05$ (**b**).

3.3.2 Salidroside promotes erythroid differentiation in EPO-treated TF-1 cells

Next, we examined whether SDS promotes the expression of erythroid markers in TF-1 cells in the EPO-induced development. Expressions of lineage specific antigen GPA, CD71 and Hb are widely accepted as the hallmarks of erythroid differentiation. To examine the effect of SDS on erythroid differentiation, the expression level of these markers were determined by flow cytometry. Again, SDS alone could not induce the expression of GPA. Less than 1% of the total cell population showed the GPA signals even after 8 days treatment (Figure 3.3a). On the other hand, the GPA-positive population increased significantly when EPO was added. These results indicate that SDS could not substitute EPO to induce erythropoiesis in TF-1 cells. At day 8 of treatment, ~44% of the cell population in the group incubated with both EPO and SDS were GPA-positive while only 38% were found in the group treated with EPO alone (Figure 3.3a). These observations suggest that SDS promotes the EPO-mediated erythropoiesis. Experiments were repeated and results were depicted in the bar chart of Figure 3.3a. As can be seen, SDS significantly enhanced the expression of GPA in the EPO-treated cells. Likewise, similar enhancements from SDS were obtained when erythroid markers CD71 (Figure 3.3b) and Hb (Figure 3.3c) were determined.

(a)

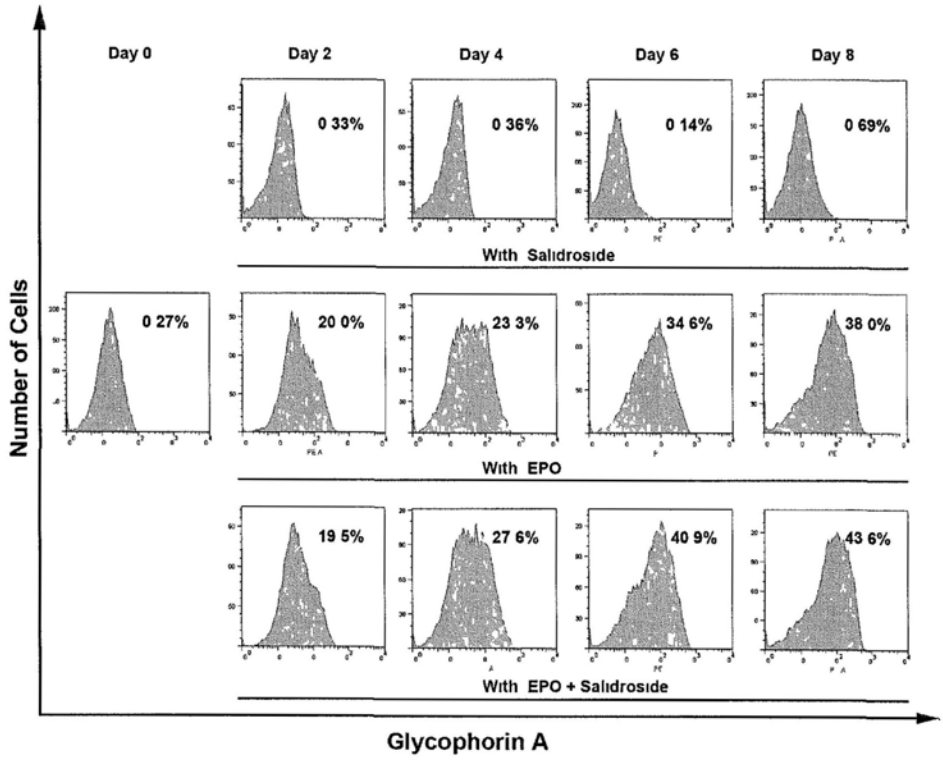
Day 0
Day 2
Day 4
Day 6
Day 8
0 33%
0 36%
0 14%
0 69%
With Salidroside
0 27%
20 0%
23 3%
34 6%
38 0%
With EPO
19 5%
27 6%
40 9%
43 6%
With EPO + Salidroside
Number of Cells
Glycophorin A

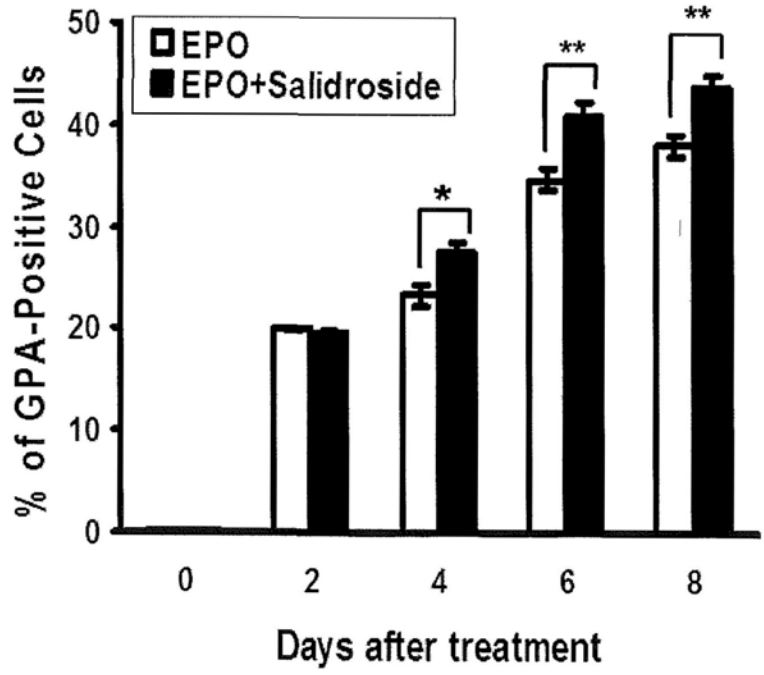
EPO
EPO+Salidroside
% of GPA-Positive Cells
50
40
30
20
10
0
*
**
**
0
2
4
6
8
Days after treatment

(b)

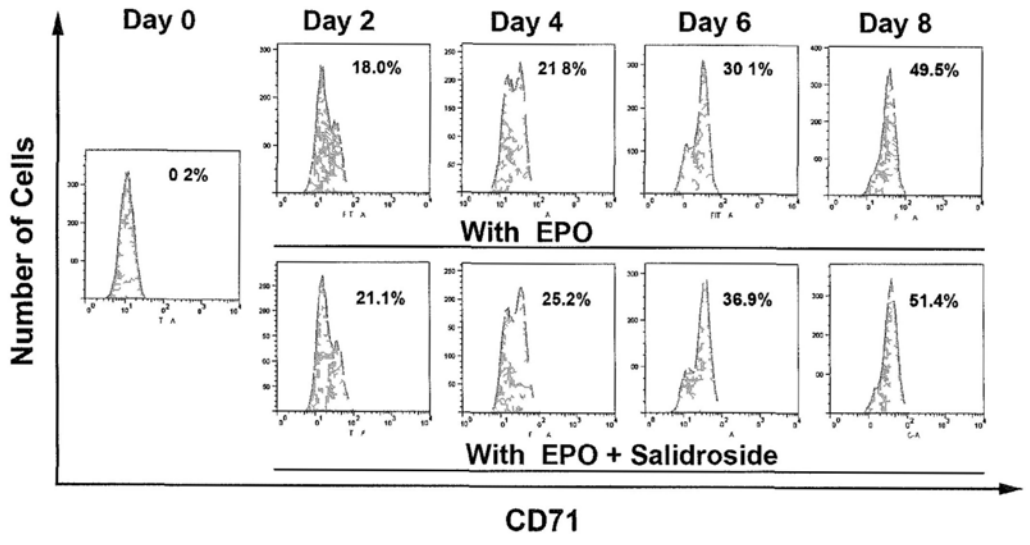
Day 0
Day 2
Day 4
Day 6
Day 8
0 2%
18.0%
21 8%
30 1%
49.5%
With EPO
21.1%
25.2%
36.9%
51.4%
With EPO + Salidroside
Number of Cells
CD71

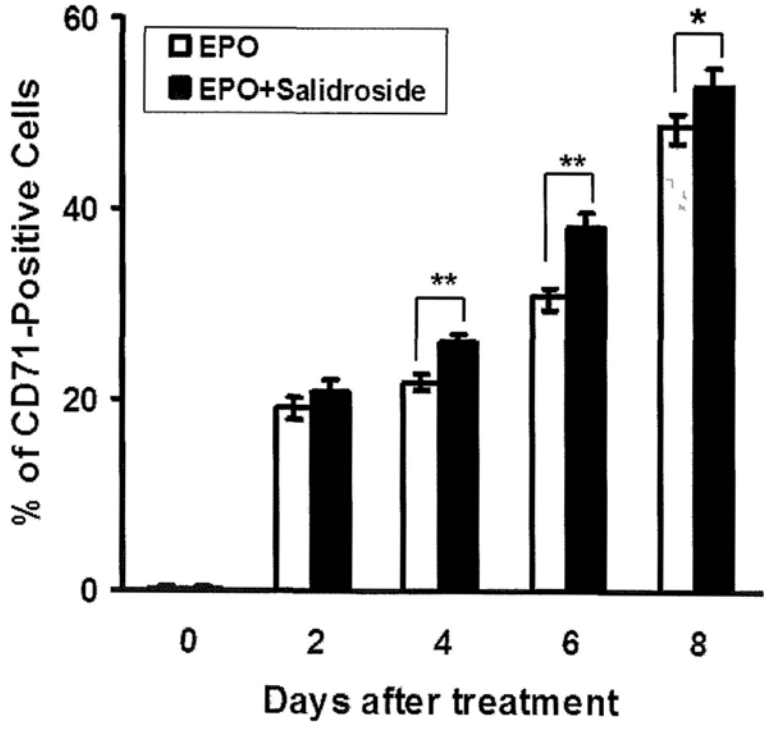
EPO
EPO+Salidroside
% of CD71-Positive Cells
60
40
20
0
0
2
4
6
8
Days after treatment
*
**
**

(c)

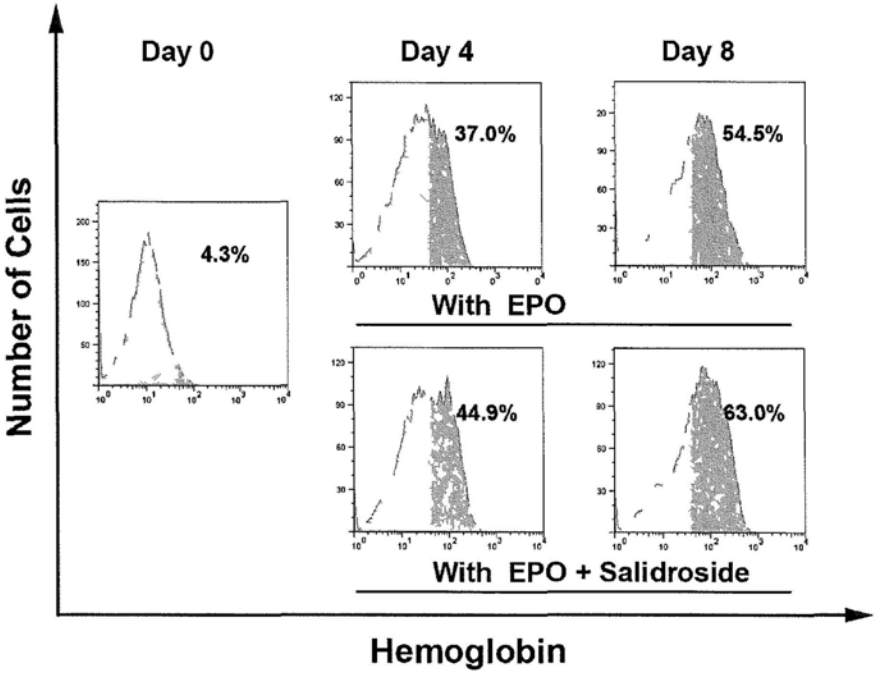
Day 0
Day 4
Day 8
4.3%
37.0%
54.5%
With EPO
44.9%
63.0%
With EPO + Salidroside
Number of Cells
Hemoglobin

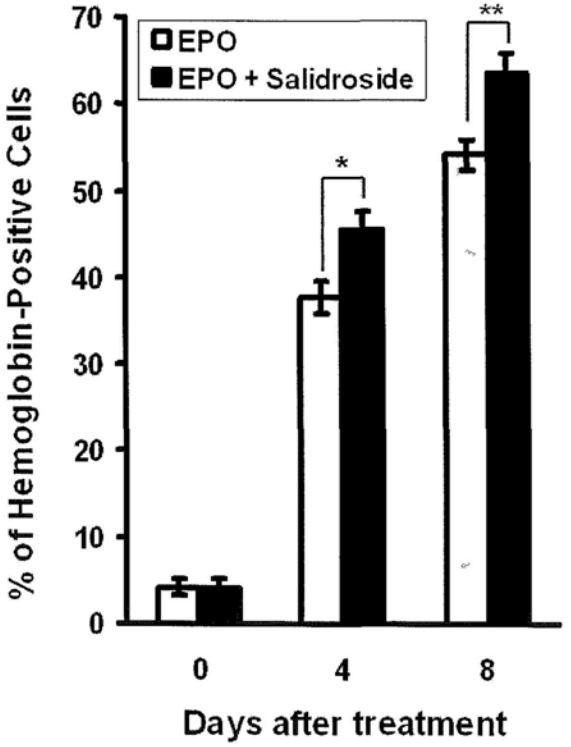
EPO
EPO + Salidroside
*
**
% of Hemoglobin-Positive Cells
0
10
20
30
40
50
60
70
0
4
8
Days after treatment

Figure 3.3 Effect of salidroside on the expression of erythroid markers in the EPO-treated TF-1 cells. TF-1 cells (4×10^5/ml) were treated with salidroside (100 μM) alone, EPO (10 ng/ml) alone, or EPO (10 ng/ml) with salidroside (100 μM) at 37 °C, 5% CO_2. Erythroid marker GPA (**a**), CD-71 (**b**) or Hb (**c**) were determined by flow cytometry. Figure represents the % of cells expressing erythroid marker in the selected region. Mean ± SD, n=3 (bar-chart). $*P < 0.05$, $**P < 0.005$.

3.3.3 Salidroside reduces the ROS level in TF-1 cells during erythroid differentiation

ROS has been reported to be a mediator of erythroid differentiation in K562 human cells (Chenais *et al.*, 2000; Nagy *et al.*, 1995). With this background information, we tested whether ROS were produced in TF-1 cells during the EPO-induced erythropoiesis by staining the cells with CM-H_2DCFDA, a ROS probe that is converted to a fluorescent product upon oxidation. As can be seen, two sub-populations were observed in each of the flow histogram and the shadowed population represents the cells with elevated ROS level (Figure 3.4). When the percentage of this ROS-positive sub-population was determined, we can see a time-dependent change in ROS production with a peak at day 4 during EPO treatment. Experiments were repeated and this notion is clearly demonstrated in the bar chart of Figure 3.4. Interestingly, less ROS-positive cells were found on all days of differentiation when cells were co-treated with both SDS and EPO (Figure 3.4). This suggests that SDS reduced the ROS level in TF-1 cells during erythroid differentiation.

(a)

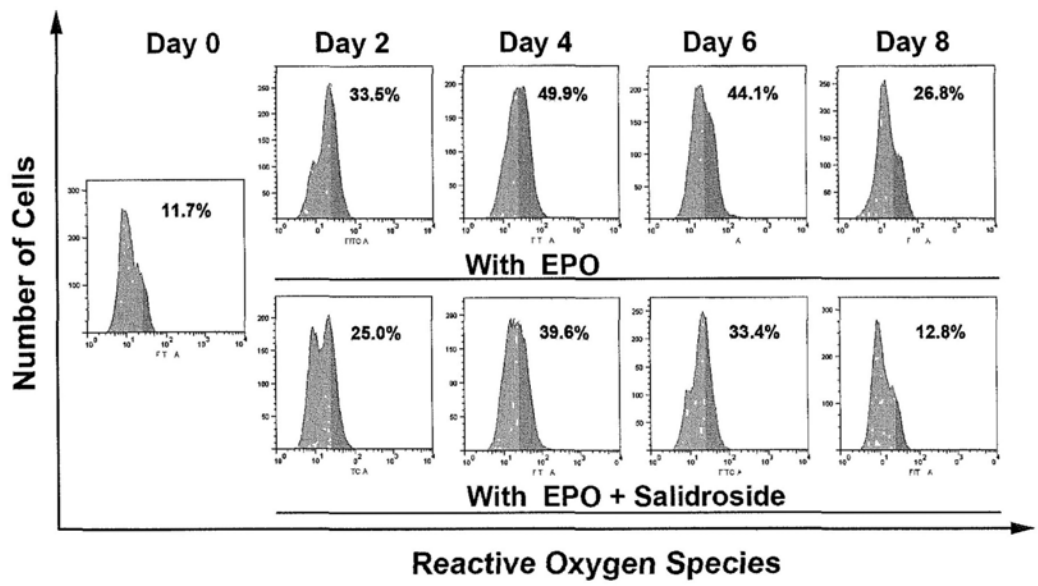

(b)

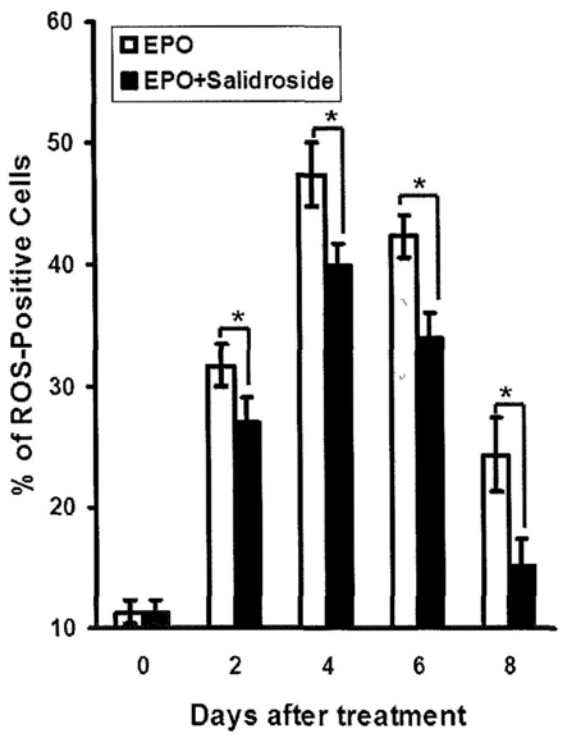

Figure 3.4 Effect of salidroside on the production of ROS in TF-1 cells. TF-1 cells (4×10^5/ml) were treated with EPO (10 ng/ml) alone or EPO (10 ng/ml) together with salidroside (100 μM) at 37 °C, 5% CO_2. ROS level was determined by CM-H_2DCFDA dye and flow cytometry. Figure represents the % of ROS producers in the selected region (**a**). Mean ± SD, n=3 (bar-chart). * $P < 0.05$ (**b**).

3.3.4 Salidroside increases the expression of antioxidant enzymes in EPO-treated TF-1 cells

Antioxidant enzymes such as GPx1, Trx1 and catalase play a crucial role in reducing intracellular ROS therefore protecting the cells from oxidative stress (Ghaffari, 2008). In searching for the mechanism of the reduction of ROS production mediated by SDS, we examined the levels of a number of antioxidant enzymes such as catalase, GPx1 and Trx1 in TF-1 cells during erythropoiesis in the absence or presence of SDS. As shown in Figure 3.5, SDS (100 μM) increased the expression of GPx1 and Trx1 during TF-1 differentiation, as their levels in the SDS-treated group were higher than that of their corresponding controls at day 4 and day 8 of differentiation. On the other hand, no significant change was observed in catalase and β-actin in the SDS-treated and control groups. These results showed that the up-regulation of antioxidant enzymes Trx1 and GPx1 may contribute to the ROS-reducing effect of SDS in TF-1 cells.

(a)

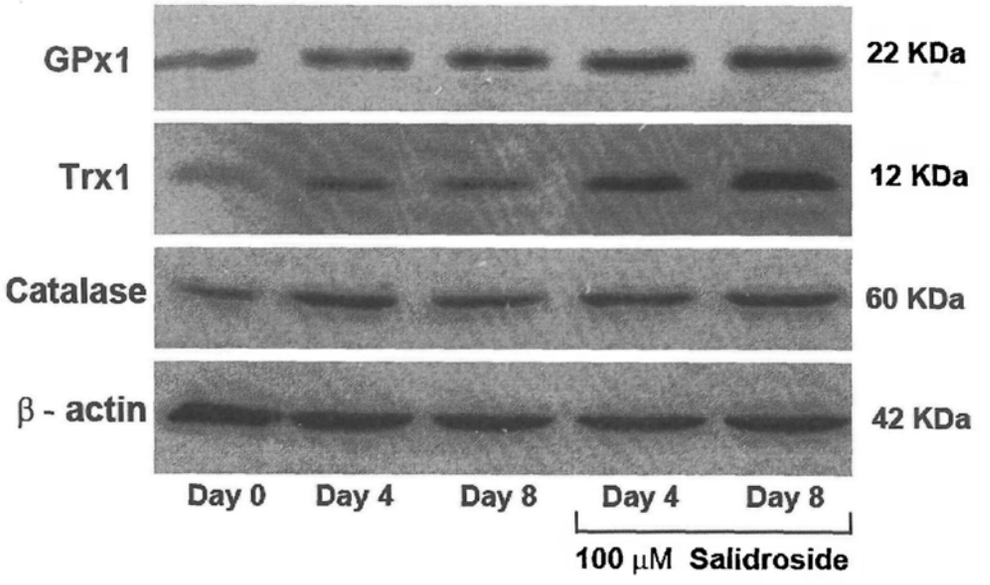
GPx1
22 KDa
Trx1
12 KDa
Catalase
60 KDa
β - actin
42 KDa
Day 0
Day 4
Day 8
Day 4
Day 8
100 μM Salidroside

(b)

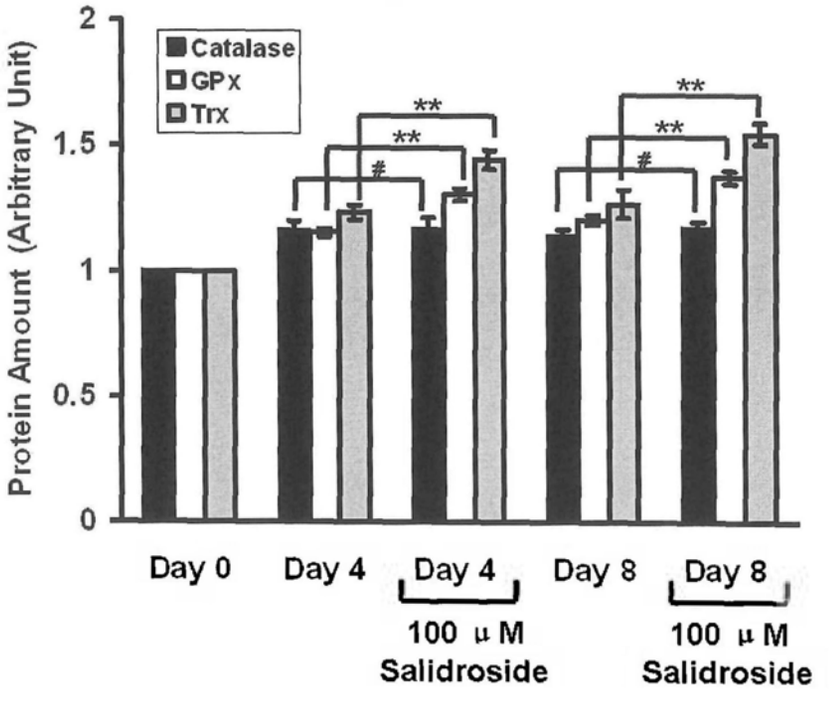
Protein Amount (Arbitrary Unit)
2
1.5
1
0.5
0
Catalase
GPx
Trx
**
**
#
**
**
#
Day 0
Day 4
Day 4
Day 8
Day 8
100 μ M Salidroside
100 μ M Salidroside

Figure 3.5 Effects of salidroside on the level of catalase, GPx1 and Trx1 during erythroid differentiation. TF-1 cells (4×10^5/ml) were treated with EPO (10 ng/ml) alone or EPO (10 ng/ml) together with salidroside (100 μM) at 37 °C, 5% CO_2 as indicated. After cell lysis, lysates were subject to standard SDS-PAGE and Western analysis for catalase, GPx1, Trx1 and β-actin (**a**). Results, normalized by corresponding day 0 control, are Mean ± SD, n=3 (bar-chart). $^{**}P < 0.005$, $\#P > 0.1$ (**b**).

3.3.5 Salidroside protects oxidative stress in EPO-treated TF-1 cells

Results from our previous study indicate that no significant change was found in the early and late apoptotic cells during EPO treatment when compared to the undifferentiated control in the standard annexin-V/PI assay (Lui and Kong, 2006). This suggests that apoptosis was not obvious in the EPO-treated TF-1 cells during erythroid differentiation. To investigate whether SDS provided protection against oxidative challenge, we cultured TF-1 cells with EPO alone or in combination with vitamin E or SDS and challenged the cells with exogenous H_2O_2 (2 mM) for 9 hours before conducting the annexin-V/PI flow cytometric analysis. As shown in Figure 3.6a, more and more viable cells (cells in the lower left quadrant, annexin-V^-/PI^-) were found in the EPO-treated group along the course of differentiation, indicating that cells developed stronger anti-oxidative strength to cope with the stress from H_2O_2. When compared to the corresponding EPO control groups, vitamin E provided more protections in the combined treatment as more viable cells were obtained. For the combined treatment of cells with EPO and SDS, the protective effect against oxidative stress was more obvious (Figure 3.6a). The first major finding in Figure 3.6 is that the number of PS-positive cells, including the early and late apoptotic cells, reduced during the EPO-mediated erythroid differentiation under the same H_2O_2 treatment. This indicates that TF-1 cells developed endogenous defense mechanism against oxidative stress during erythropoiesis. The second finding is that the presence of vitamin E or SDS enhanced such protection, and the latter had a stronger effect. Obviously, this protection is not a result of the direct interaction between H_2O_2 and

SDS or vitamin E as they had been washed away before the 9-hour H_2O_2 treatment. Taken together, our findings show that SDS exerted protective effect on TF-1 erythroblasts against oxidative stress possibly by up-regulating antioxidant enzymes.

(a)

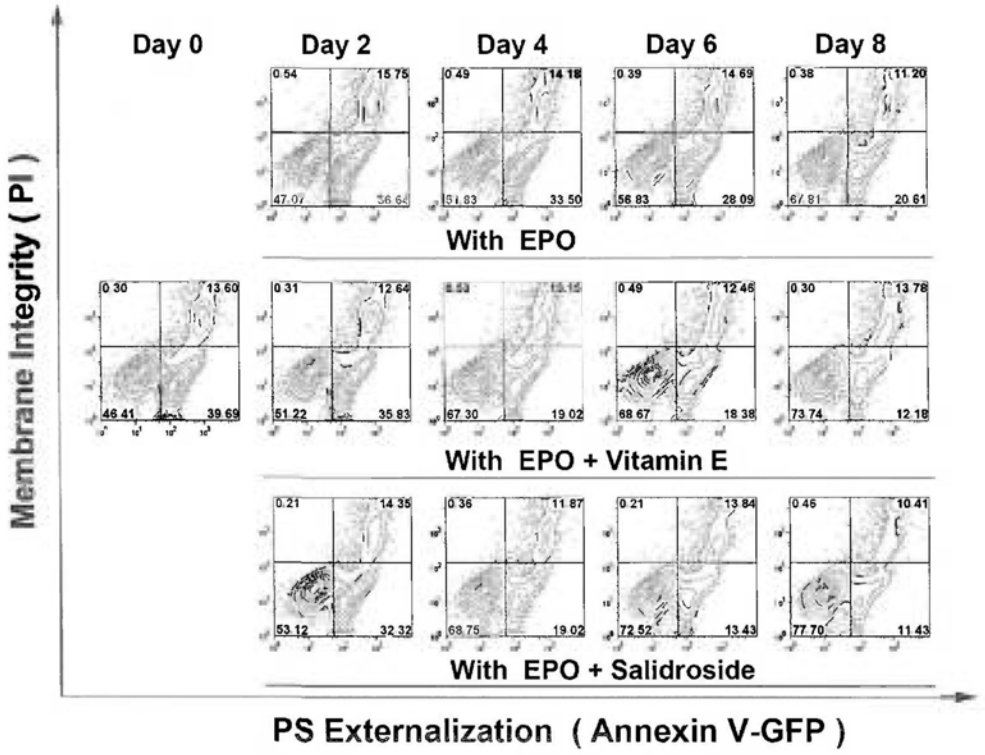

(b)

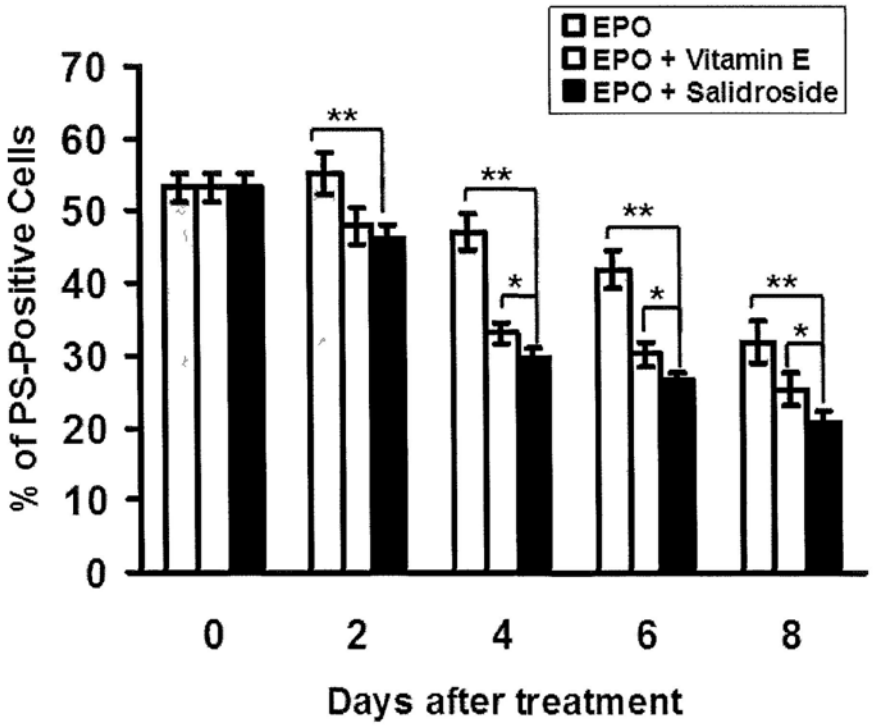

Figure 3.6 Effects of salidroside on the H_2O_2-mediated apoptosis. TF-1 cells (4×10^5/ml) were treated with EPO (10 ng/ml) alone, EPO (10 ng/ml) with vitamin E (100 μM) or EPO (10 ng/ml) together with salidroside (100 μM) at 37 °C, 5% CO_2. At the day as indicated, the cells were incubated with H_2O_2 (2 mM) for 9 h at 37 °C, 5% CO_2 before the annexin V-GFP/PI flow cytometric assay. Number at the corner represents the % of cells found in the corresponding quadrant (**a**). Percentage of PS-positive cells (% sum in the upper- and lower-right quadrants) was shown in the bar-chart, Mean ± SD, n=3, $*P < 0.05$, $**P < 0.005$ (**b**).

3.4 Discussion

Production and detoxification of ROS are of major importance in the regulation of erythropoiesis (Ghaffari, 2008). It has been known for a while that when erythroid precursors express and accumulate Hb during erythropoiesis, Fe (II) ions inserted into hemes in the mitochondria of erythroid precursors are capable of generating highly reactive hydroxyl radicals (·OH) through Fenton reaction. Erythroblasts carrying Hb are therefore highly prone to oxidative damage (Cimen, 2008; Ghaffari, 2008; Winterbourn, 1990). To combat these threats, highly regulated mechanisms are developed during normal erythropoiesis to balance the production of ROS (Ghaffari, 2008).

To dissect these mechnisms in erythropoiesis, a human erythroleukemia cell line TF-1, established in 1989 (Kitamura *et al.*, 1989), was employed in this study. TF-1 has also been utilized as an *in vitro* erythroid model by many laboratories (Jacobs-Helber and Sawyer, 2004; Uchida *et al.*, 2004; Zhang *et al.*, 1998; Kitamura *et al.*,1989) and it remains to be one of the best *in vitro* models in studying human erythropoiesis. By using this model, our lab previously indentified the role of caspase-3 and heat shock protein 70 (Hsp-70) in erythropoiesis (Lui and Kong, 2006, 2007). Similar results were found in normal human erythroblasts (Ribeil *et al.*, 2007). As an erythroid model, EPO increased the expression of erythroid markers such as GPA, CD71 and Hb in TF-1 cells (Figure 3.3) with a peak of ROS production at day 4

during erythroid differentiation (Figure 3.4). The subsequent decrease in ROS production at day 6 and day 8 in the EPO treatment suggests that endogenously protective anti-oxidative mechanism might be activated during the erythroid development. In fact, the level of antioxidant defense proteins Trx1 and GPx1 were up-regulated during the EPO-elicited erythropoiesis and the TF-1 erythroblasts had a stronger resistance against the oxidative stress mediated by the exogenous H_2O_2 (Figure 3.6).

SDS extracted from *Rhodiola rosea* L. has long been used as blood tonic and adaptogen in traditional Chinese and Tibetan medicine. Using TF-1 cells, we provided evidence that SDS, in conjunction with EPO, was able to promote cell growth and to enhance the expression of erythroid markers (Figure 3.2 and 3.3). Also, TF-1 cells treated with both EPO and SDS reduced more the level of ROS (Figure 3.4) and produced more Trx1 and GPx1 (Figure 3.5). Yet, the amount of catalase remains unchanged on later days of differentiation even in the presence of SDS. This observation is consistent with the results from animal study that mice lacking catalase develop normally (Ho *et al*, 2004). GPx1 is one of the major anti-ROS defense enzymes in erythroid cells. This enzyme employs NADPH, generated from the hexose monophosphate shunt through G6PD (glucose 6-phosphate dehydrogenase), as the electron donor and glutathione as the ROS scavenger (Ghaffari, 2008). Also, Trx1 is able to eliminate the H_2O_2 produced intracellularly (Kang *et al.*, 1998). Its action is similar to the GPx system, which also utilizes NADPH as the reducing power. With

the up-regulation of GPx1 and Trx1, it is not surprising why TF-1 erythroblasts had a stronger capability to ameliorate the H_2O_2-induced oxidative stress (Figure 3.6).

Another important finding of this study is that SDS on one hand promotes erythropoiesis and on the other hand reduces the ROS production. A logical conclusion from these observations is that reduction in the ROS level promotes erythroid differentiation. This conclusion is in contrast to the observations in cardiomyocytes, lens cells, neurons and hematopoietic cells that ROS promotes differentiation (Sauer *et al.*, 2001). More work is needed in this regard to define the role of ROS in erythropoiesis.

In summary, our study provides direct evidence for the first time that SDS promotes erythroid differentiation and it can protect erythroblasts against H_2O_2 to commit cell death through apoptosis. The protective effect of SDS may be contributed by the up-regulation of anti-oxidative proteins. Therefore, our work showed the mechanism underlying the use of SDS as blood tonic supplement and adaptogen in the folk medicine. Since SDS needs EPO to exert its erythropoiesis stimulating effect, SDS can be used as an adjuvant for EPO or other erythropoiesis-stimulating agent to help the patients with anemia and mountain malhypoxia.

Chapter 4

Salidroside Protects Human Erythrocytes against the H_2O_2-induced Eryptosis

4.1 Introduction

It has been known for a while that programmed cell death or apoptosis is not only limited to nucleated cells, mature enucleated erythrocytes also share the programme for self-destruction through apoptosis. Although mechanism is poorly understood, mature RBCs can undergo a special type of apoptosis known as eryptosis or erythroptosis without the involvement of mitochondria and nucleus (Lang *et al.*, 2006). Similar to apoptosis, eryptosis/erythroptosis is characterized by membrane blebbing, cell shrinkage, and the externalization of phosphatidylserine (PS) at the cell surface. As an antioxidant and blood tonic, SDS was found to be able to protect erythroblasts against H_2O_2 to commit cell death through apoptosis in TF-1 cells as described in chapter 1. Here the possible protective effect of SDS against oxidative stress-triggered eryptosis in human mature RBCs was examined.

4.2 SDS protects human erythrocytes against the H_2O_2-induced hemolysis

The potential cytotoxic effect of SDS on the freshly isolated human erythrocytes was determined by hemolysis assay. As shown in Figure 4.1a, SDS did not exhibit any observable hemolytic effect at concentration up to 800 μM in a 2-hour incubation or 400 μM in a 24-hour treatment. These indicate that the erythrotoxicity of SDS in human cells is minimal.

Next, we examined whether SDS exerts any protective effect against hemolysis elicited by H_2O_2. When RBCs were incubated with H_2O_2 (1 mM) alone in the absence of SDS, ~50% and 20% of total hemolysis were obtained in the 24- and 2-hour incubation respectively (Figure 4.1b). When the RBCs were treated with H_2O_2 together with SDS, a dose-dependent rescue of H_2O_2-induced hemolysis was observed. The higher the dose of SDS, the stronger the protection obtained. Although the toxic effect from H_2O_2 could not be totally neutralized, our results indicate that SDS could, at least in part, protect the RBCs from the acute and long-term oxidative stress from H_2O_2.

(a)

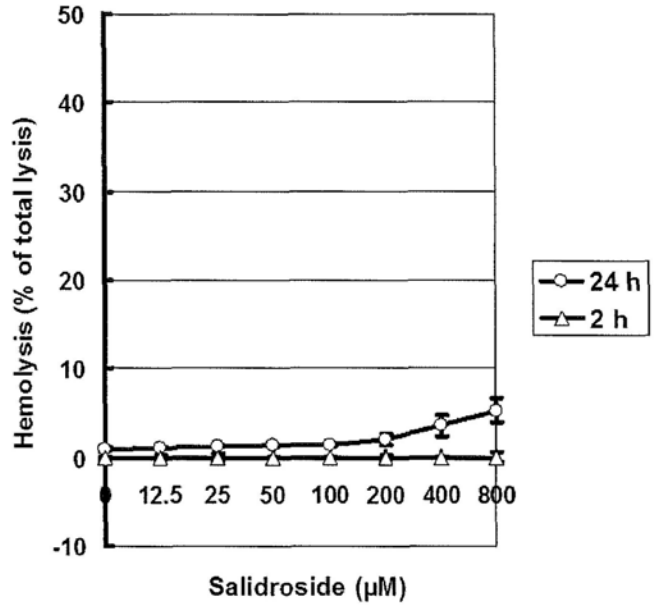

(b)

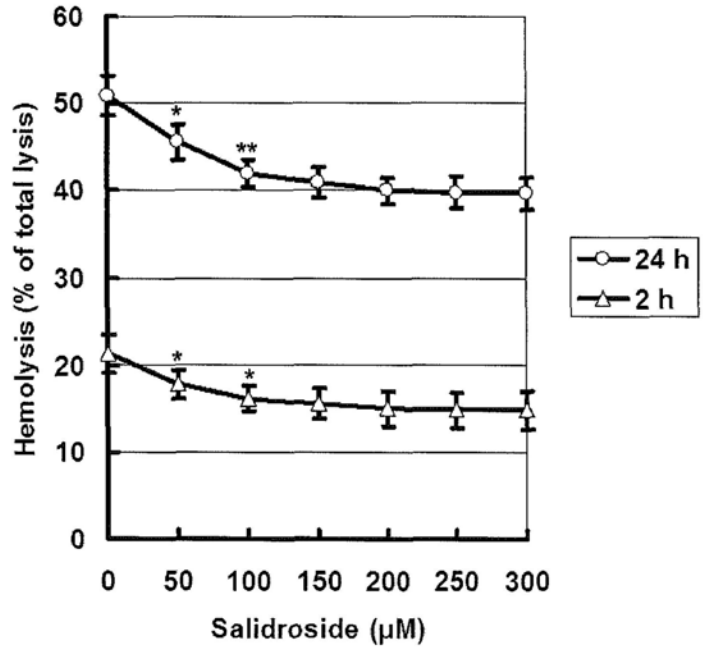

Figure 4.1 Effect of salidroside on the hemolysis in human erythrocytes. Erythrocytes were cultured with various concentrations of salidroside in the absence (**a**) or presence (**b**) of H_2O_2 (1 mM) for 2 and 24 hours at 37 °C, 5% CO_2. Hemolysis was then measured. Mean ± SD, n=5, $*P < 0.05$, $**P < 0.001$.

4.3 SDS protects human erythrocytes against the H_2O_2-induced eryptosis

To determine the effect of SDS on the H_2O_2-mediated eryptosis/erythroptosis, we employed the flow cytometric PE-annexin-V/calcein assay to examine the possible protection. As can be seen in Figure 4.2a, most of the cells in the control group were found in the lower right quadrant (97.20%). They were the healthy cells with normal membrane integrity and PS asymmetry (calcein$^+$ and annexin-V$^-$). To confirm the assay validity, we employed Ca^{2+} ionomycin that elicits eryptosis/erythroptosis in erythrocytes as a positive control (Bratosin *et al.*, 2001). In the positive control group, Ca^{2+} ionomycin (1 μM) significantly increased the number of early eryptotic cells (calcein$^+$ and annexin-V$^+$) in the upper right quadrant (68.5% vs 2.6% in control) with a concomitant decrease in the number of healthy cells (0% vs 97% in control). Also, the number of late eryptotic (calcein$^-$ and annexin-V$^+$) in the upper left quadrant of the ionomycin-treated group also slightly increased (25.2% vs 0% in control).

When cells were treated with H_2O_2 (1 mM) alone, not too many erythrocytes were found in the late eryptotic quadrant (<1%), ~9% showed the early eryptotic features, and 27.2% were found in the lower left quadrant (calcein$^-$ and annexin-V$^-$) (Figure 4.2a). Findings from Bratosin *et al.* (2005) indicate that the death of enzyme esterase occurs earlier than that of the PS externalization during eryptosis. As a consequence of the death of esterase, the calcein/AM could not be converted into

calcein to generate fluorescence. Therefore, cells in the lower left quadrant are the very early eryptotic cells. However, in the presence of SDS, the % of viable cells increased from 63% (SDS 0 μM) to 70% (SDS 100 μM) and 75% (SDS 300 μM) while the very early eryptotic cells in the lower left quadrant decreased correspondingly from 27% to 17% and 14%. Experiments were repeated and similar response is demonstrated in Figure 4.2b.

(a)

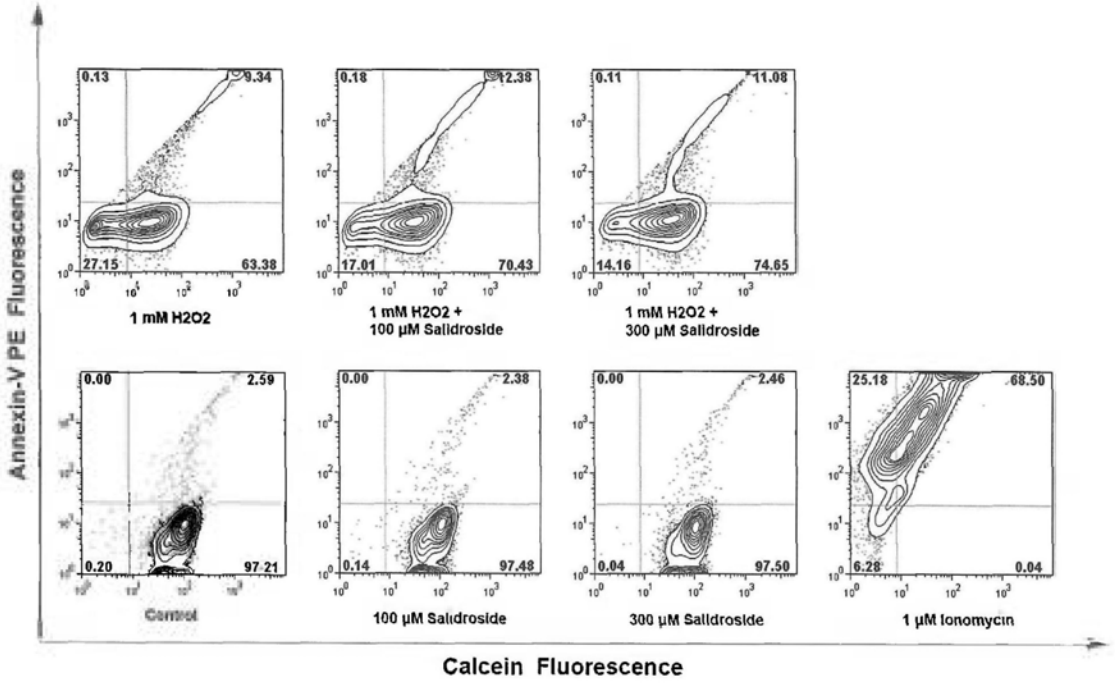

(b)

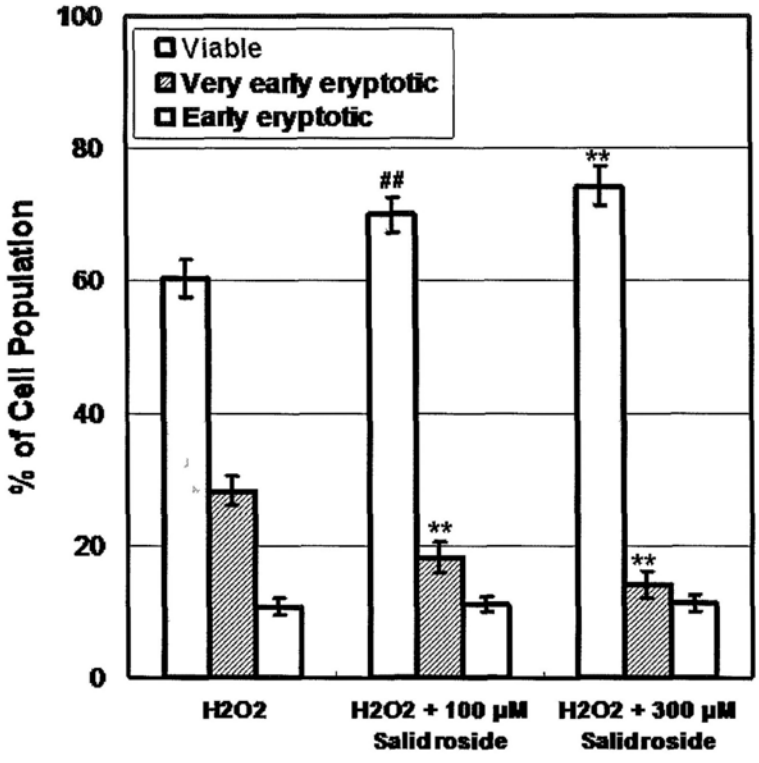

Figure 4.2 Effect of salidroside on the induction of eryptosis. Erythrocytes were treated with medium alone, salidroside (100 or 300 µM), ionomycin (1 µM) in the absence or presence of H_2O_2 (1 mM) as indicated at 37 °C, 5% CO_2 for 24 hours. Externalization of PS and loss of membrane integrity were determined by flow cytometry. Figure represents the % of cell population in the quadrant (**a**). Mean ± SD, n=4 (bar-chart). $^{\#\#}P < 0.005$, $^{**}P < 0.001$, compared to the H_2O_2-treated group (**b**).

4.4 Determination of intracellular calcium ($[Ca^{2+}]_i$) in RBCs

Increase in $[Ca^{2+}]_i$ is an important mediator in eryptosis (Dekkers *et al.,* 2002). We therefore measured the change in the $[Ca^{2+}]_i$ in RBCs using Fluo-4/AM. Without Ca^{2+} binding, fluo-4 is non-fluorescent but the fluorescence increases in a concentration dependent manner when bound with free Ca^{2+} ions. True to our expectation, the calcium ionomycin increased the $[Ca^{2+}]_i$ and at the same time promoted the PS externalization (Figure 4.3a). This finding agreed well with the previous observations that ionomycin is an apoptotic agent in erythrocytes (Dekkers *et al.,* 2002). When RBCs were challenged with H_2O_2 (1 mM) alone, the fluorescence signals from single cells moved to the upper right corner in the PE-annexin-V/Fluo-4 two-variant plot, indicating an increase in $[Ca^{2+}]_i$ and PS externalization. On the contrary, cells treated with SDS alone (100 μM and 300 μM) did not alter much the positioning of the fluorescence in the two-variant plot when compared to control. When cells were co-treated with H_2O_2 (1 mM) and SDS (100 μM or 300 μM), more signals moved, in a dose-dependent manner, back to the lower left corner (Figure 4.3a). Experiments were repeated and results were summarized in Figure 4.3b. As can be seen, the higher the dose of SDS, the stronger was the protection. This observation again indicates that SDS protects the erythrocytes from the H_2O_2-induced apoptosis through the inhibition of $[Ca^{2+}]_i$ rise.

(a)

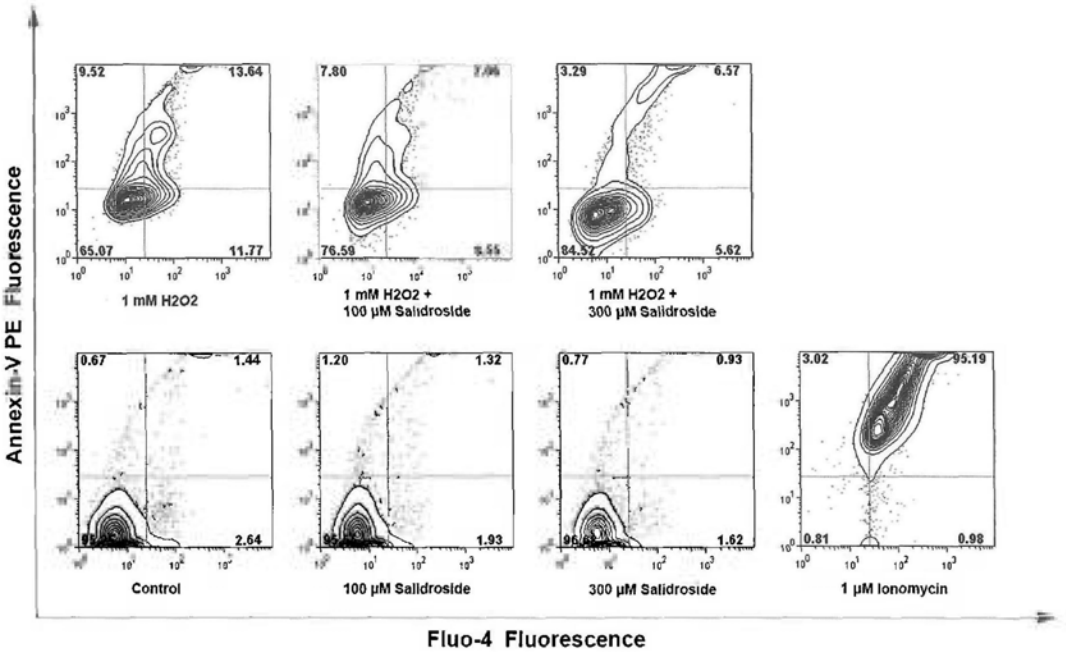
Annexin-V PE Fluorescence
9.52
13.64
65.07
11.77
1 mM H2O2
7.80
76.59
1 mM H2O2 +
100 μM Salidroside
3.29
6.57
84.57
5.62
1 mM H2O2 +
300 μM Salidroside
0.67
1.44
2.64
Control
1.20
1.32
1.93
100 μM Salidroside
0.77
0.93
1.62
300 μM Salidroside
3.02
95.19
0.81
0.98
1 μM Ionomycin
Fluo-4 Fluorescence

(b)

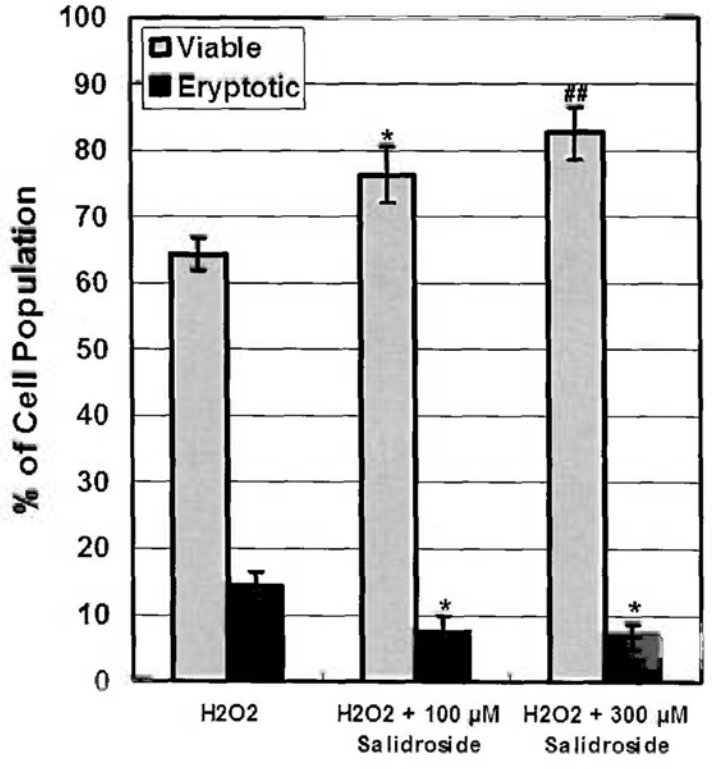
Viable
Eryptotic
% of Cell Population
100
90
80
70
60
50
40
30
20
10
0
*
*
*
##
H2O2
H2O2 + 100 μM Salidroside
H2O2 + 300 μM Salidroside

(c)

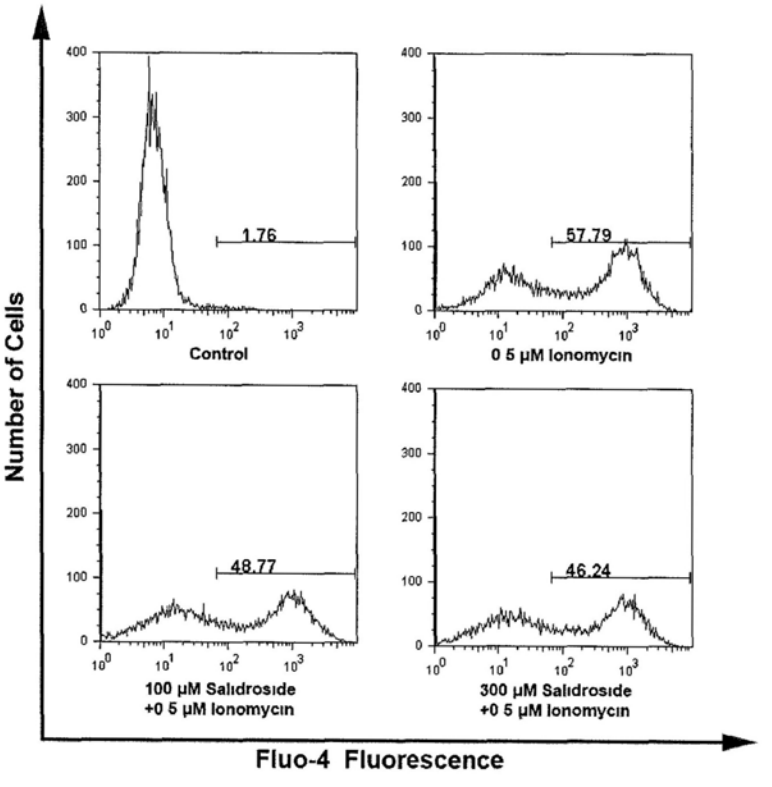
Number of Cells
Fluo-4 Fluorescence
1.76
Control
57.79
0 5 μM Ionomycin
48.77
100 μM Salidroside
+0 5 μM Ionomycin
46.24
300 μM Salidroside
+0 5 μM Ionomycin

(d)

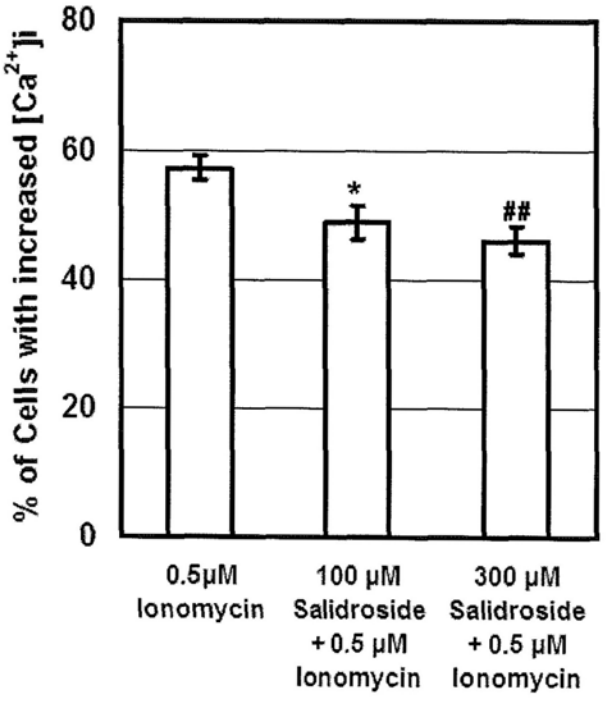
% of Cells with increased [Ca2+]i
80
60
40
20
0
*
##
0.5μM Ionomycin
100 μM Salidroside +0.5 μM Ionomycin
300 μM Salidroside + 0.5 μM Ionomycin

Figure 4.3 Effect of salidroside on the $[Ca^{2+}]_i$ in erythrocytes after H_2O_2 treatment. Erythrocytes were treated with medium alone, salidroside (100 or 300 μM), ionomycin (1 or 0.5 μM) in the absence or presence of H_2O_2 (1 mM) as indicated at 37 °C, 5% CO_2 for 24 hours. Level of PS externalization and increase in $[Ca^{2+}]_i$ were then determined. Figure represents the % of cell population in the quadrant. Mean ± SD (bar-chart). $^{*}P < 0.05$, $^{\#\#}P < 0.005$, compared to the H_2O_2- (**a, b,** n=4) or ionomycin- (**c, d,** n=3) treated group.

4.5 Determination of Caspase-3 activity in RBCs

Activation of caspase-3 is an important step in apoptosis (Green and Kroemer, 2004). We therefore asked if caspase-3 was involved in the H_2O_2-mediated eryptosis and whether SDS provided any protection in this aspect. To address these questions, the caspase-3 activity was studied by using a fluorogenic caspase-3 assay. For the positive controls, erythrocytes were treated with a potent apoptotic agent staurosporine (STS). As can be seen in Figure 4.4a, STS increased the caspase-3 activity (94.5% in the selected region) significantly when compared to that of control (0.3%) or SDS (300 μM) (0.2%). When RBCs were treated only with H_2O_2 (1 mM), the cell population moved to the right hand side indicating an activation of caspase-3 enzyme. However, the degree of activation was less than that of the STS-treated group (51.2% vs 94.5%). When cells were incubated with H_2O_2 (1 mM) together with SDS, the degree of caspase-3 activity was partially suppressed.

(a)

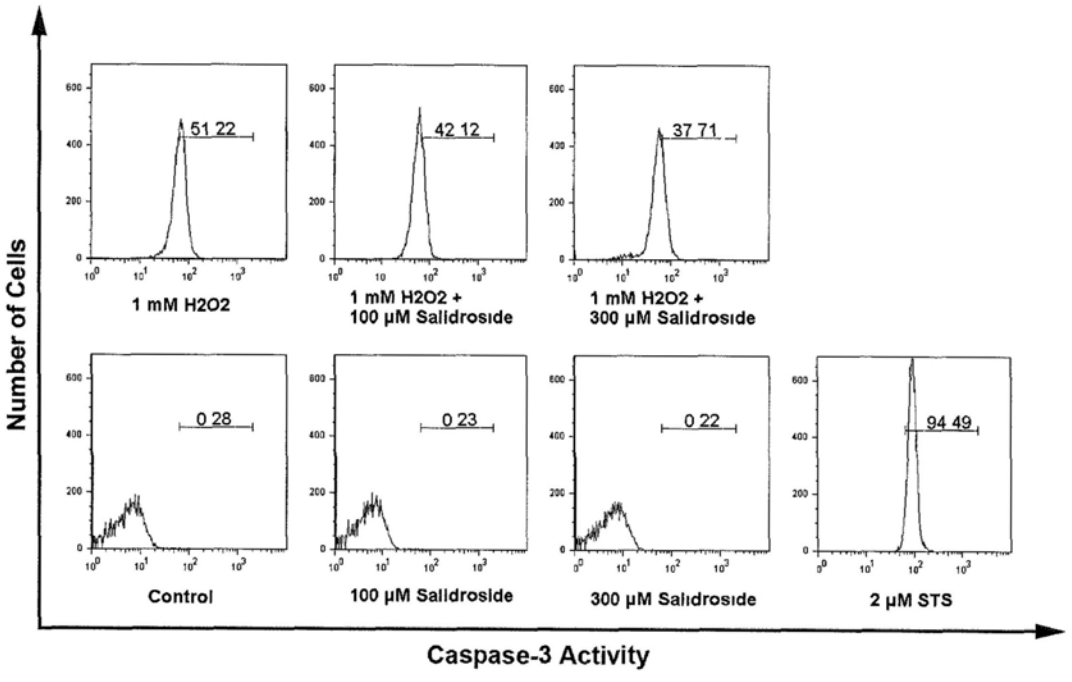
Number of Cells
51 22
42 12
37 71
1 mM H2O2
1 mM H2O2 +
100 μM Salidroside
1 mM H2O2 +
300 μM Salidroside
0 28
0 23
0 22
94 49
Control
100 μM Salidroside
300 μM Salidroside
2 μM STS
Caspase-3 Activity

(b)

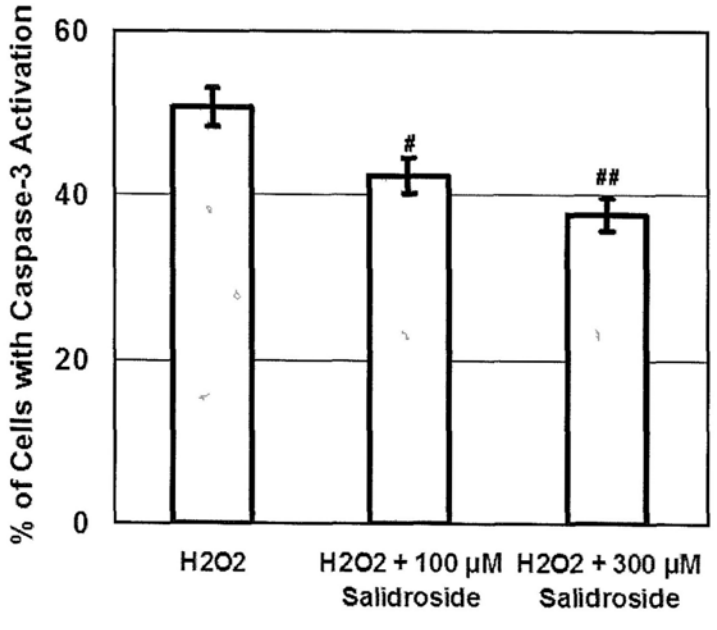
% of Cells with Caspase-3 Activation
60
40
20
0
#
##
H2O2
H2O2 + 100 μM
Salidroside
H2O2 + 300 μM
Salidroside

(c)

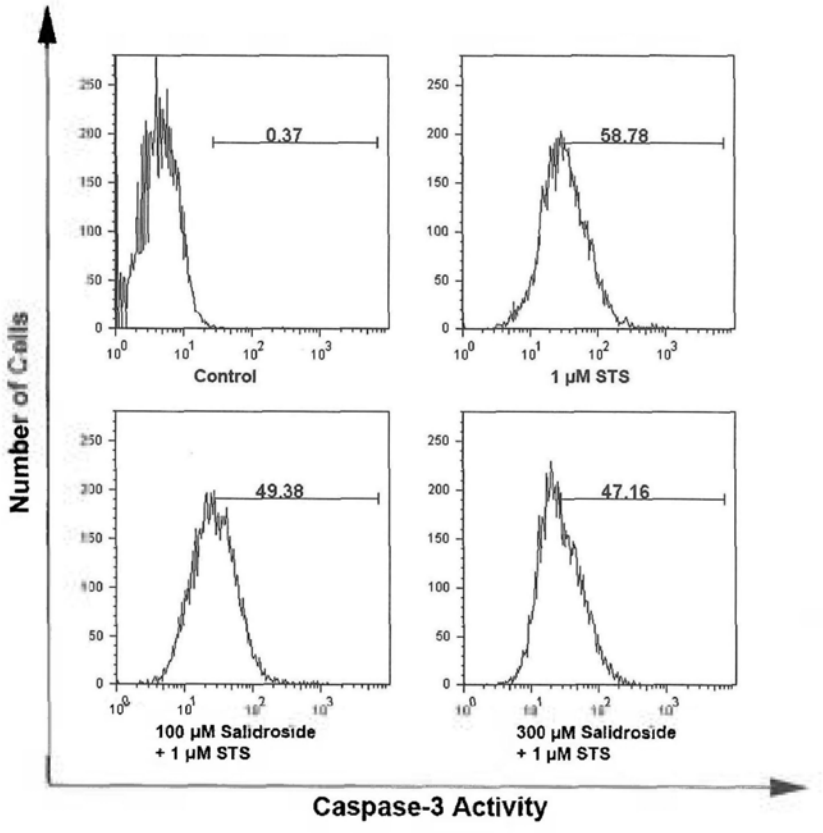
Number of Cells
0.37
Control
58.78
1 μM STS
49.38
100 μM Salidroside
+ 1 μM STS
47.16
300 μM Salidroside
+ 1 μM STS
Caspase-3 Activity

(d)

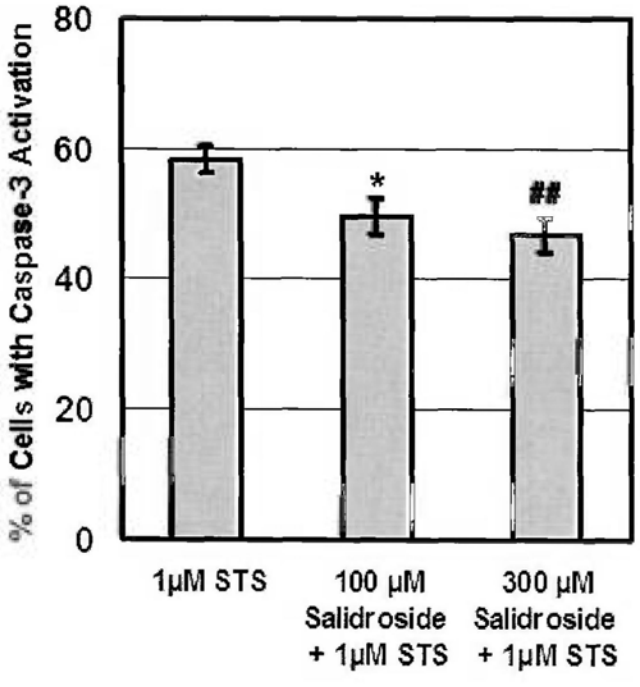
% of Cells with Caspase-3 Activation
80
60
40
20
0
*
##
1μM STS
100 μM Salidroside + 1μM STS
300 μM Salidroside + 1μM STS

Figure 4.4 Effects of salidroside on the level of caspase-3 activation in erythrocytes after H_2O_2 treatment. Erythrocytes were treated with medium alone, salidroside (100 or 300 μM), staurosporine (STS) (1 or 2 μM) in the absence or presence of H_2O_2 (1 mM) as indicated at 37 °C, 5% CO_2 for 24 hours. Level of caspase-3 activation was then determined. Figure represents the % of cell population in the selected region. Mean ± SD (bar-chart), n=3. $^{\#}P < 0.01$, $^{*}P < 0.05$, $^{\#\#}P < 0.005$, compared to the H_2O_2- (**a, b**) or STS- (**c, d**) treated group.

4.6 Mechanism study

In Figure 4.3a, it seems likely that SDS suppressed the H_2O_2-mediated increase in the $[Ca^{2+}]_i$. As cellular Ca^{2+} ion is a crucial trigger for the induction of eryptosis, we asked whether SDS directly blocked the $[Ca^{2+}]_i$ rise elicited by ionomycin. As shown in Figures 4.3c & d, SDS partially blocked the ionomycin-induced $[Ca^{2+}]_i$ rise indicating that the protective effect is due, at least in part, to the Ca^{2+} influx on the membrane in the RBCs in which RBC are devoid of organelles to uptake the Ca^{2+} ions into internal stores. Likewise, SDS partially blocked the STS-mediated activation of caspase-3 (Figures 4.4c & d). Previous studies have shown that SDS is an anti-oxidant (Yu *et al.,* 2007; Kanupriya *et al.,* 2005), we therefore evaluated the potential protection from the SDS against the oxidative stress from H_2O_2. As depicted in Figure 4.5, H_2O_2 (1 mM) increased the fluorescence of DCF indicating the generation of reactive oxygen species (ROS) in the cytoplasm after treatment. When cells were cotreated with H_2O_2 and SDS, rescue again was observed in a dose-dependent manner. Taken together, our findings suggest that SDS protects RBCs from the H_2O_2-elicited eryptosis through the anti-oxidative effect, suppression of Ca^{2+} influx and activation of caspase-3 activity.

(a)

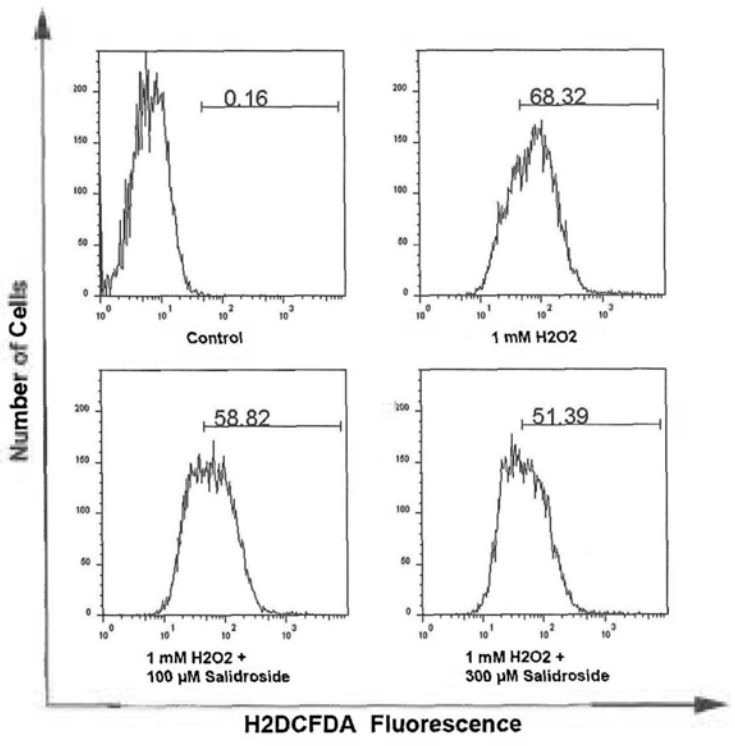

(b)

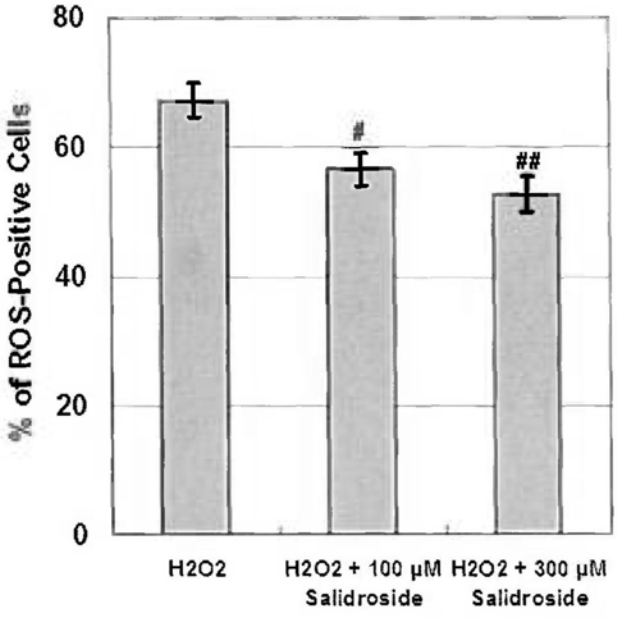

Figure 4.5 Effects of salidroside on the ROS level in erythrocytes after H_2O_2 treatment. Erythrocytes were treated with medium alone, H_2O_2 (1 mM) in the presence or absence of salidroside (300 µM) as indicated at 37 °C, 5% CO_2 for 24 hours. Level of ROS was then determined using H2DCFDA. Figure represents the % of cell population in the selected region (**a**). Mean ± SD (bar-chart), n=3. $^{\#}P < 0.01$, $^{*}P < 0.05$, compared to the H_2O_2-treated group (**b**).

4.7 Discussion

During ascent to high altitude, the low alveolar oxygen tension (~4% O_2 vs. 16% O_2 at sea level) or hypoxia was shown to promote the production of ROS from mitochondria (Chandel *et al.*, 1998; Dada *et al.*, 2003; Guzy *et al.*, 2005; Lundberg *et al.*, 2009). When oxidized Hbs accumulate, they induce phospholipid oxidation and disrupt the membrane. Under this oxidative imbalance condition, RBCs are committed to senescence and to cell death (Kiefer and Snyder, 2000). Because of this, the oxidative stress from ROS is regarded as one of the major triggers of eryptosis (Barvitenko *et al.,* 2005). In this study, the apoptotic effect from the oxidative stress is well supported from our results using H_2O_2 to elicit the decrease in esterase activity, increase in PS externalization and loss of membrane integrity (Figure 4.2). All these are the very early, early and late apoptotic events during the cell death of RBCs. As these occur in cells devoid of mitochondria and nucleus, eryptosis represents a unique cell death system through the regulation at the cell membrane (Lang *et al.,* 2010).

In China and Tibet, *Rhodiola rosea* L. or SDS has long been used as blood tonic and adaptogen to treat mountain malhypoxia. The mechanism for the protection is currently unclear. Our recent study has indicated that SDS promotes erythropoiesis in the EPO-treated cells and it also reduces the degree of cell death in erythroblasts after H_2O_2 treatment through the up-regulation of protective proteins thioredoxin-1 and glutathione peroxidase-1 (Qian *et al.,* 2011). In this study, we provided another

piece of evidence using human erythrocytes that SDS was able to protect the RBCs against the H_2O_2-induced eryptosis.

In 2009, Schriner *et al.* found that SDS is able to lower the mitochondrial superoxide levels in Drosophila melanogaster (Schriner *et al.,* 2009). As human erythrocytes lose their mitochondria upon maturation through the pro-apoptotic BH3-only-like factor Nix (Schweers *et al.,* 2007), it is of interest to identify the mechanism how the SDS protects the human RBCs from eryptosis under oxidative stress. In human erythrocytes, oxidative stress activates the Ca^{2+}-permeable cation channels that stimulate Ca^{2+} entry (Lang *et al.,* 2003). It is believed that the high $[Ca^{2+}]_i$ activates the Ca^{2+}-dependent cysteine protease, μ-calpain, which degrades cytoskeleton (Lui *et al.,* 2007). In the present study, our results show that H_2O_2 increased the cytosolic Ca^{2+} level. In fact, the Ca^{2+} rise alone elicited by ionomycin was able to trigger PS externalization (Figure 4.3). In this regard, SDS could reduce both the H_2O_2- and ionomycin-mediated increase in the level of Ca^{2+} (Figure 4.3), suggesting that SDS has multiple functions in the salvation.

Although caspase-3 is more than a cysteinyl aspartate-specific protease in the programmed cell death and elicits many non-apoptotic functions (D'Amelio *et al.,* 2010), it is a common executor in the intrinsic and extrinsic apoptotic pathway in the nucleated cells. In mature erythrocytes, caspase-3 is shown to be functional (Berg *et*

al., 2001). Although devoid of the mitochondrial apoptotic regulators, the caspase-3 in human RBCs can be activated by oxidative stress (Matarrese *et al.,* 2005). This notion was confirmed again in our study that H_2O_2 was capable of activating caspase-3 in human RBCs although the effect of H_2O_2 was less than that of STS through the inhibition of protein kinase c (PKC) (Sopjani *et al.,* 2009). Again, SDS could block, at least in part, the H_2O_2- or STS-mediated activation of caspase-3 (Figure 4.4). Previous studies have indicated a role for SDS in blocking the oxidative harm from tert-butyl hydroperoxide and the poor growth condition during hypoglycemia and serum starvation (Yu *et al.,* 2007; Kanupriya *et al.,* 2005), their observations are endorsed by the evidence in our study that SDS could block the oxidative stress from the H_2O_2.

In conclusion, our findings revealed a rescue effect of SDS for the first time against the oxidative stress-mediated eryptosis in human erythrocytes through the anti-oxidative effect, suppression of Ca^{2+} rise and caspase-3 activation. This work thus confirms the ethnopharmacoloical use of *Rhodiola rosea* L. or SDS in the mitigation of anemia developed as a result of mountain hypoxia.

Chapter 5

Dual Roles of ROS and Function of G6PD during Erythropoiesis in TF-1 Cells

5.1 Introduction

Unchecked high amounts of ROS can damage cellular components, whereas moderately well-regulated ROS play crucial roles as signaling messengers in the regulation of various biological processes. For example, ROS contribute significantly to the differentiation of hematopoietic cells, but the underlying mechanisms remain unresolved. Conversely, since erythrocytes are exposed to one of the highest levels of oxidative-stress conditions in the body, regulation of oxidative stress is particularly important to erythropoiesis. During erythroid maturation, a strong antioxidant system that can counterbalance the oxygen stress is gradually developed. Glucose-6-phosphate dehydrogenase (G6PD) is a key enzyme of the anti-oxidative defense system of erythrocytes. G6PD deficiency affects more than 400 million people worldwide. In the present study, using a stable G6PD-knockdown TF-1 cell line, the dual roles of ROS and the function of G6PD during erythropoiesis were investigated.

5.2 ROS reduction did not affect the EPO-induced erythropoiesis in TF-1 cells

Results from previous work of our lab had shown that antioxidant vitamin E reduced ROS production during TF-1 erythroid differentiation, but did not affect the percentage of differentiating cells (Ge, 2009). Here we investigated the effect of another antioxidant NAC on the EPO-induced erythropoiesis. NAC is a precursor for cellular GSH biosynthesis which functions in the GPx system to diminish hydrogen

peroxide and thus reduce oxidative stress.

As shown in Figure 5.1a, incubation of TF-1 cells with EPO alone increased the ROS level with a peak at Day 4 (upper right + lower right quadrants, Day 0 : 4 : 8 = 6.6% : 61.9% : 20.3%). When cells were treated with both EPO and NAC, NAC significantly reduced the ROS level during erythropoiesis. On day 4 of TF-1 erythroid differentiation, ROS^+ population was reduced from more than 60% to less than 30%, and similar observation was obtained on day 8, from more than 20% to around 10% (Figure 5.1b1). However, when erythroid marker GPA was measured (upper right + upper left quadrants in Figure 5.1a), it was found that no significant change in the GPA level was observed in the EPO and EPO+NAC groups (Figure 5.1b2), suggesting that reduction of ROS level did not affect the EPO-induced erythropoiesis in TF-1 cells.

(a)

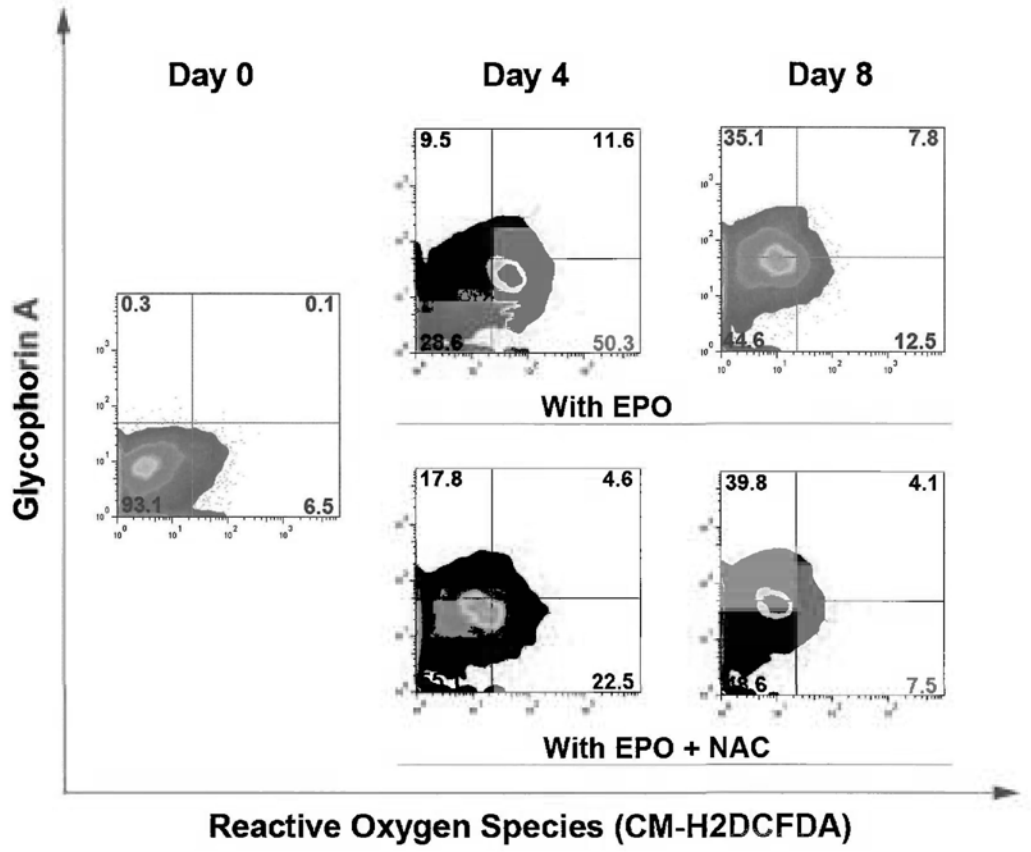
Day 0
Day 4
Day 8
Glycophorin A
0.3
0.1
93.1
6.5
9.5
11.6
28.6
50.3
35.1
7.8
4.6
12.5
With EPO
17.8
4.6
22.5
39.8
4.1
7.5
With EPO + NAC
Reactive Oxygen Species (CM-H2DCFDA)

(b1)

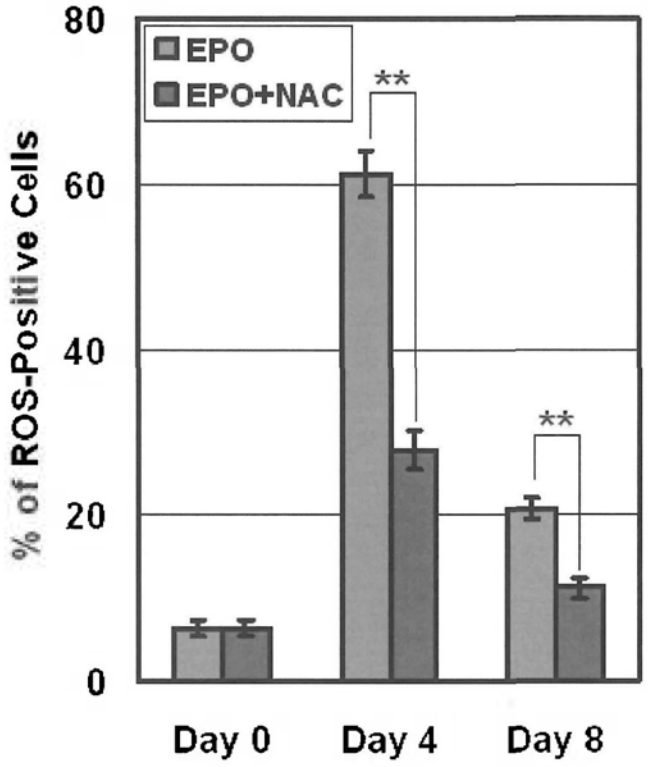
80
60
40
20
0
EPO
EPO+NAC
**
**
% of ROS-Positive Cells
Day 0
Day 4
Day 8

(b2)

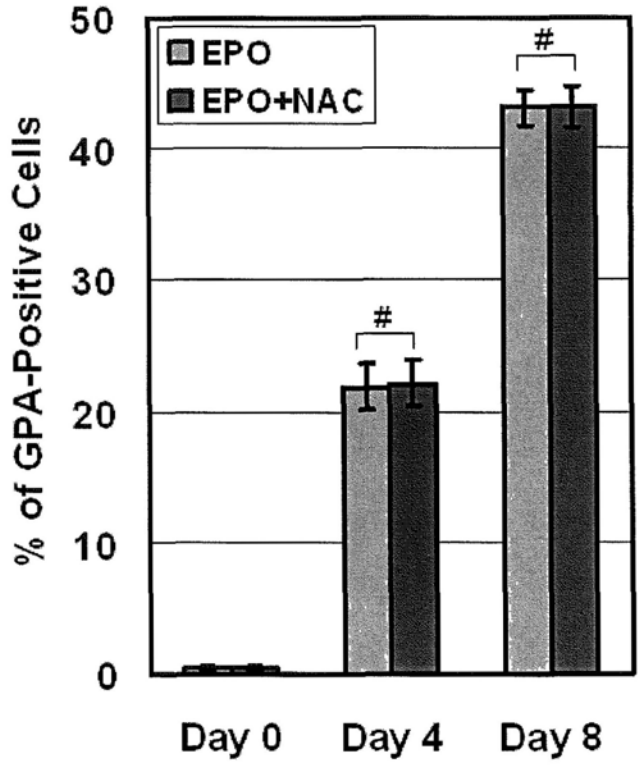

Figure 5.1 Effect of NAC on the expression of GPA and the level of ROS during TF-1 erythroid differentiation. TF-1 cells (4×10^5/ml) were treated with EPO (10 ng/ml) alone, or EPO (10 ng/ml) with NAC (5 mM) at 37 °C, 5% CO_2 for 0 to 8 days as indicated. Erythroid marker GPA and ROS were determined simultaneously by anti-GPA MAb and CM-H_2DCFDA with flow cytometry (**a**). Figure represents the % of cells found in the corresponding quadrant. Mean ± SD, n=3 (bar-chart). $^{**}P < 0.001$, $\#P > 0.5$ (**b1, b2**).

5.3 NAC treatment led to more differentiated TF-1 cells death under H_2O_2 treatment

To investigate whether ROS has effect on erythroblasts with respect to cells' endogenous antioxidant defense system, the TF-1 cells cultured with EPO alone or in combination with NAC for 0-8 days were challenged with exogenous H_2O_2 (2 mM) for 9 h before conducting the annexin-V/PI flow cytometric analysis. We reasoned that the ROS produced in TF-1 cells during erythropoiesis might trigger the development of the endogenous antioxidant defense system. The presence of NAC to remove the endogenous ROS during erythropoiesis might restrain the development of the antioxidant defense system and more cells will die when challenged with H_2O_2. In fact, more viable cells were seen in the lower left quadrant along the differentiation process in the EPO treated group (Day 0 : 2 : 4 : 6 : 8 = 45.5% : 45.3% : 57.9% : 75% : 81.8% (Figure 5.2a)).

As shown in Figure 5.2a, more and more viable cells (cells in the lower left quadrant, annexin-V^-/PI^-, 45.3% on day 2, 57.9% on day 4, 75.0% on day 6 and 81.8% on day 8) were found in the EPO-treated group along the course of differentiation, indicating that cells developed stronger anti-oxidative strength to cope with the stress from H_2O_2. However, when compared to the corresponding NAC-added group, less viable cells were found (EPO+NAC vs. EPO = 45.4% vs. 45.3% (Day 2); 51.6% vs. 57.9% (Day 4); 63.0% vs. 75.0% (Day 6); 69.2% vs. 81.8% (Day 8)), indicating that the NAC-added group did not develop such a strong

anti-oxidative strength as the EPO control group to cope with the oxidative stress from H_2O_2.

Also, as can be seen in Figure 5.2b, the number of PS-positive cells (Annexin-V^+ cells), including the early and late apoptotic cells (lower right + upper right quadrants), reduced during the EPO-mediated erythropoiesis under the H_2O_2 treatment. In the NAC-added groups, although the PS-positive cells were also reduced along the course of TF-1 differentiation, but the reduction were much less than that of the EPO control groups. This suggests the antioxidant NAC partially blocked the establishment of endogenous defense mechanism against oxidative stress.

(a)

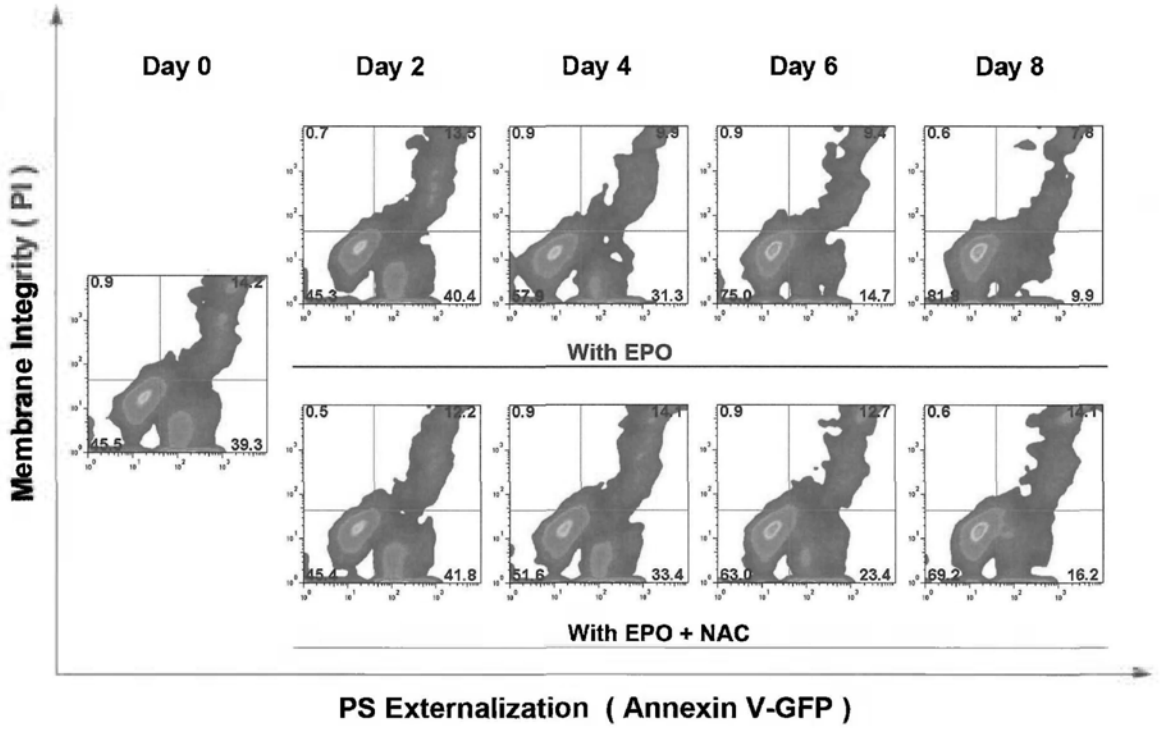
Day 0
Day 2
Day 4
Day 6
Day 8
Membrane Integrity (PI)
With EPO
With EPO + NAC
PS Externalization (Annexin V-GFP)

(b)

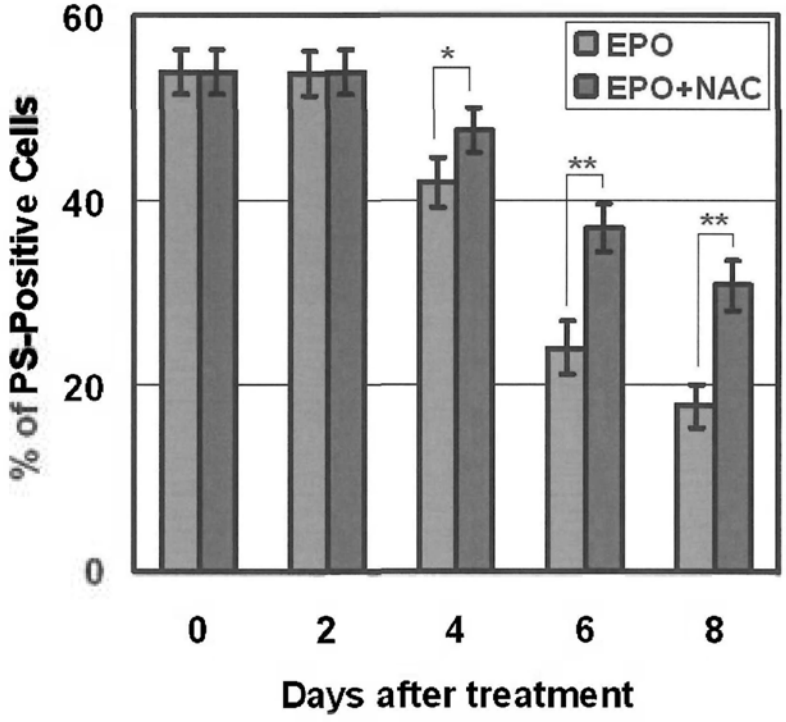
60
40
20
0
% of PS-Positive Cells
EPO
EPO+NAC
*
**
**
0
2
4
6
8
Days after treatment

Figure 5.2 Effect of NAC on H_2O_2-mediated apoptosis in TF-1 erythropoiesis. TF-1 cells (4×10^5/ml) were treated with EPO (10 ng/ml) alone, or EPO (10 ng/ml) with NAC (5 mM) at 37 °C, 5% CO_2. At the day as indicated, the cells were washed twice with ice-cold PBS and then cultured in M2 medium containing 2 mM H_2O_2 for 9 h at 37 °C, 5% CO_2 before the annexin V-GFP/PI flow cytometric assay. Number at the corner represents the % of cells found in the corresponding quadrant (**a**). Percentage of PS-positive cells (% sum in the upper- and lower-right quadrants) was shown in the bar-chart, mean ± SD, n=3, $*P < 0.05$, $**P < 0.005$ (**b**).

5.4 Antioxidant defense system was downregulated by NAC during the EPO-induced erythropoiesis in TF-1 cells

In order to explore why the presence of NAC produced more apoptotic cells during the EPO-induced erythropoiesis, we tried to detect some related antioxidant enzymes or proteins. Antioxidant enzymes such as GPx1, Trx1 and catalase play a crucial role in reducing intracellular ROS therefore protecting the cells from oxidative stress (Ghaffari, 2008). Results from previous work showed GPx1 and Trx1 were significantly upregulated during TF-1 erythroid differentiation, whereas catalase showed no observable changes (Ge, 2009). GPx1 and Trx1 are the major enzymes respectively in the GPx and Prx cellular peroxide scavenging system (Day 2009). So we examined the expression level of GPx1 and Trx1 in TF-1 cells during erythropoiesis. In addition, given the importance of NADPH in erythroid cells to scavenge peroxide, and the importance of Glut1 and G6PD in recharging NADPH, we therefore also detected the expression of Glut1 and G6PD during TF-1 erythropoiesis.

G6PD is a housekeeping gene, and as shown in Figure 5.3, the expression level of this enzyme had no observable change from day 0 to day 8 of TF-1 erythroid differentiation, whereas the expression of Glut1, GPx1 and Trx1 were upregulated along the course of TF-1 erythropoiesis (Day 0, 4, and 8) (Figure 5.4). Interestingly, under the antioxidant NAC (5 mM) treatment, the upregulation of Glut1 (the "smear-like" pattern bands was because of glycosylation of Glut1 (Montel-Hagen *et al.*, 2008)), GPx1 and Trx1 were significantly lessened, however, the level of G6PD

were still had no change. This suggests that NAC down-regulated antioxidant system related proteins Glut1, GPx1 and Trx1 and thus resulted in the reduction of antioxidant defense function in TF-1 erythroid cells.

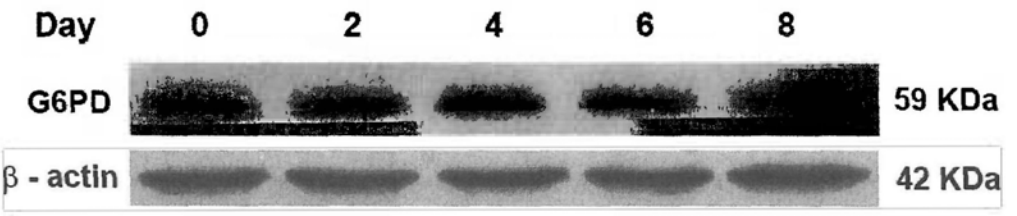

Figure 5.3 Expression of G6PD during TF-1 erythropoiesis. TF-1 cells (4×10^5/ml) were cultured with EPO (10 ng/ml) at 37 °C, 5% CO_2 for days as indicated. After cell lysis, lysates containing equal amount of proteins per lane were subjected to standard SDS-PAGE and Western blot analysis with antibodies for G6PD and β-actin (as an internal control). Reproducible results were obtained in three independent experiments.

(a)

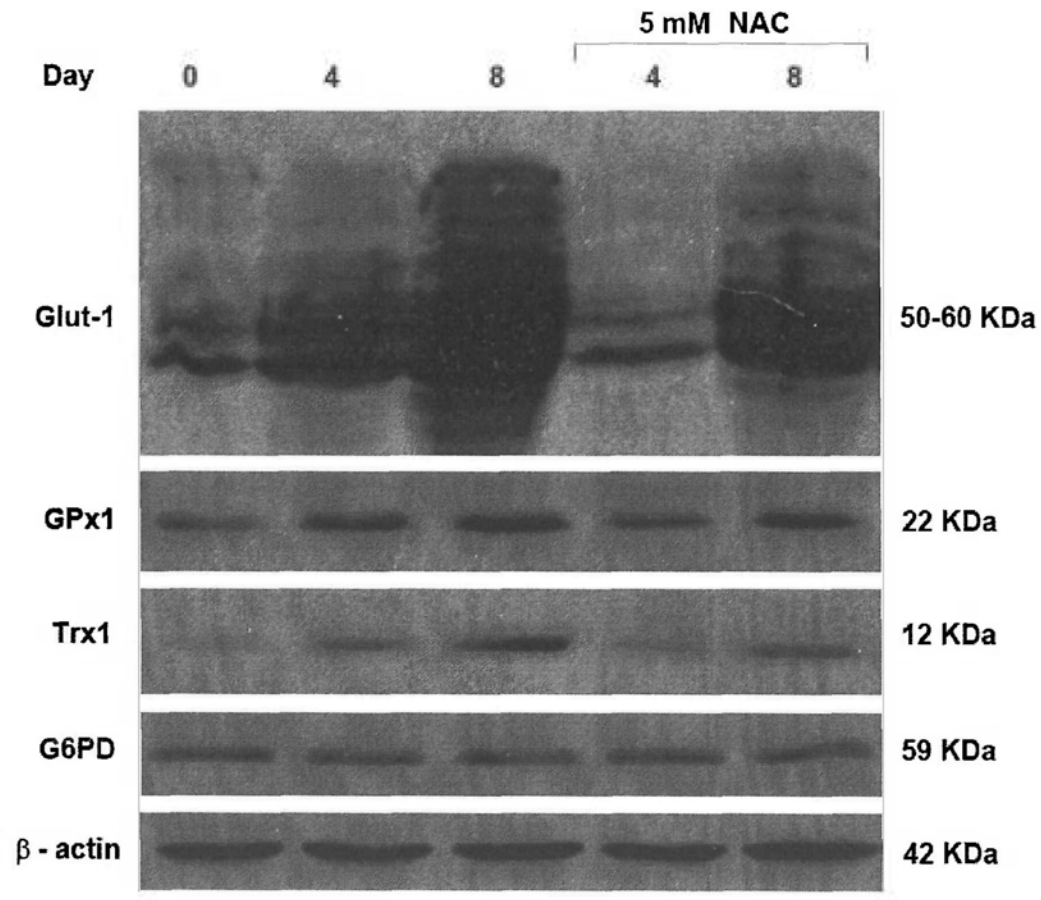
5 mM NAC
Day
0
4
8
4
8
Glut-1
50-60 KDa
GPx1
22 KDa
Trx1
12 KDa
G6PD
59 KDa
β - actin
42 KDa

(b)

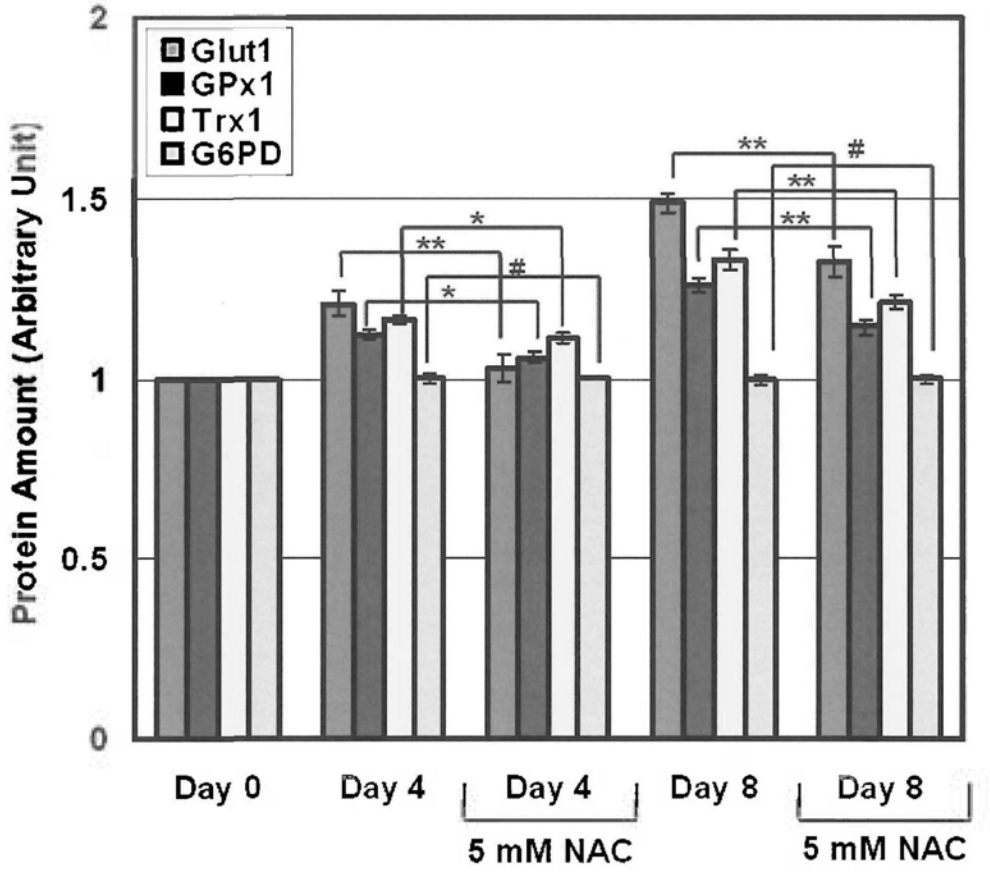

Figure 5.4 Effect of NAC on antioxidant system related proteins during TF-1 erythroid differentiation. TF-1 cells (4×10^5/ml) were treated with EPO (10 ng/ml) alone, or EPO (10 ng/ml) with NAC (5 mM) at 37 °C, 5% CO_2 for days as indicated. After cell lysis, lysates containing equal amount of proteins per lane were subjected to standard SDS-PAGE and Western blot analysis with antibodies for Glut1, GPx1, Trx1, G6PD and β-actin (as an internal control) (**a**). Results, normalized by corresponding day 0 control, are mean ± SD, n=3 (bar-chart). $*P < 0.01$, $**P < 0.005$, $\#P > 0.5$ (**b**).

5.5 Downregulation of antioxidant defense system was found in the differentiated TF-1 cells

During the TF-1 erythroid differentiation, the cell population consists of both differentiated and undifferentiated cells. In order to know whether the down-regulation of antioxidant defense system under NAC treatment was due to the differentiated cells, we separated TF-1 cells with 6 days EPO treatment into differentiated (GPA^+ cells) and undifferentiated population (GPA^- cells) by FACS cells sorting, and probed the Glut1, GPx1 and Trx1 expression again. As shown in Figure 5.5, firstly, we can see more Glut1, GPx1 and Trx1 in GPA^+ cells than that in GPA^- cells, indicating that upregulation of these proteins during TF-1 erythropoiesis were mostly from differentiated cells. Secondly, the upregulation of Glut1, GPx1 and Trx1 of the GPA^+ cells under NAC treatment were significantly lessened than that of the untreated GPA^+ cells. On the other hand, for the GPA^- cells, whether under NAC treatment or not, the expression levels of Glut1, GPx1 and Trx1 had no obvious changes, indicating that the downregulation of antioxidant defense system under NAC treatment appeared in the differentiated TF-1 cells during erythropoiesis. For the antioxidant enzyme G6PD, expression level of it remained more or less the same in the differentiated or undifferentiated cells no matter with or without the NAC treatment

(a)

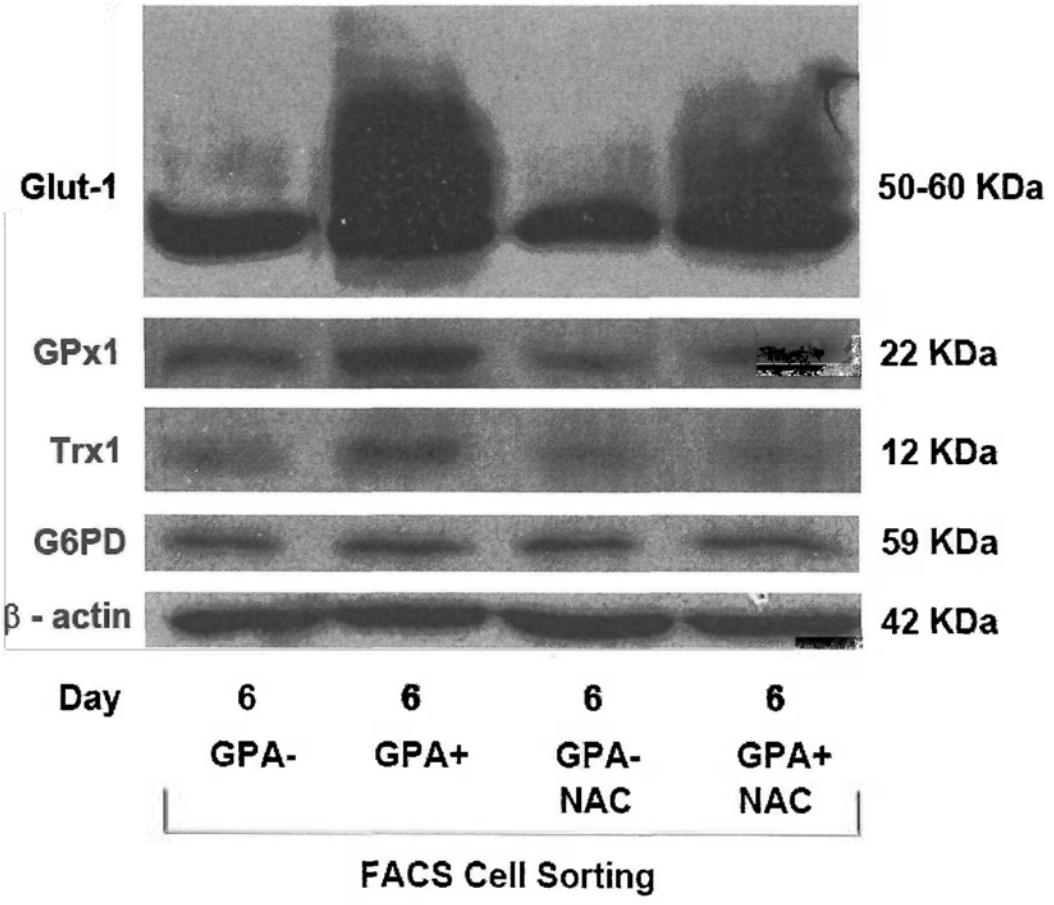
Glut-1
50-60 KDa
GPx1
22 KDa
Trx1
12 KDa
G6PD
59 KDa
β - actin
42 KDa
Day
6
6
6
6
GPA-
GPA+
GPA-
NAC
GPA+
NAC
FACS Cell Sorting

(b)

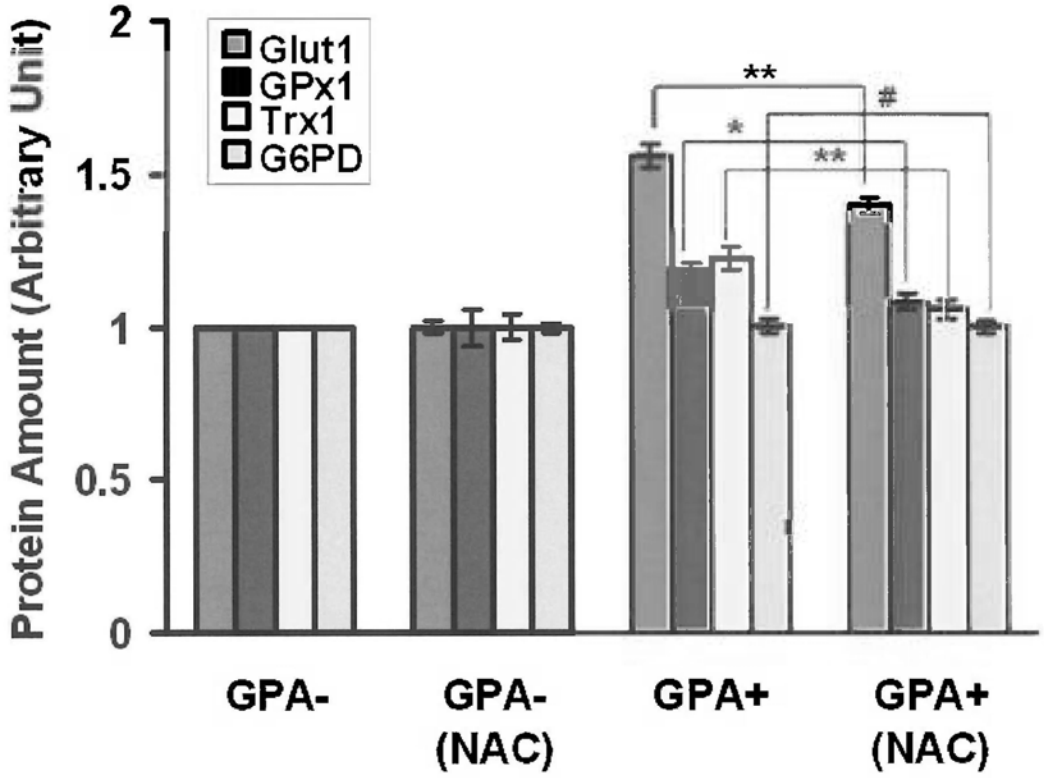

Figure 5.5 Expression level of antioxidant system related proteins in GPA^+ and GPA^- populations. TF-1 cells cultured with EPO (10 ng/ml) for 6 days were labeled with anti-GPA antibody, and then sorted by FACS cell sorting based on GPA labeling. The GPA^+ and GPA^- populations were lysed separately and subjected to Western blot analysis with antibodies for Glut1, GPx1, Trx1, G6PD and β-actin (as an internal control) (**a**). Results, normalized by corresponding day 0 control, are mean ± SD, n=3 (bar-chart). $*P < 0.01$, $**P < 0.005$, $\#P > 0.5$ (**b**).

5.6 G6PD was successfully knocked down in TF-1 cells

G6PD enzyme plays a crucial role in the antioxidant defense system of RBCs. Mechanistically, G6PD serves as the only source of the major intracellular reductant NADPH, which enables cells to counterbalance oxidative stress. Therefore G6PD deficiency becomes especially lethal in RBCs, to which any oxidative stress will result in hemolytic anemia (Elyassi and Rowshan, 2009). G6PD deficiency is the most common form of RBC enzymopathy, affecting millions of people worldwide (Paglialunga *et al.*, 2004). So we were curious to know what would happen in erythropoiesis in the absence of G6PD. We knocked down the G6PD gene in TF-1 cells by using BLOCK-iT™ Pol II miR RNAi with EmGFP as a reporter. Figure 5.6a shows TF-1 cells under confocal microscope, the upper graph is normal TF-1 cells, and the lower left graph is TF-1 cells transfected with empty EmGFP vector, then the graph on the lower right is TF-1 cells transfected with EmGFP vector expressing G6PD microRNA (EmGFP-miR-G6PD). We can see the cells in the two lower graphs emitting green fluorescence, indicating these cells were successfully transfected with EmGFP vectors which were expressing GFP. This was also subsequently confirmed by using flow cytometry, as shown in Figure 5.6b, the green histogram represents the GFP fluorescence emitted by TF-1 cells transfected with EmGFP-miR-G6PD, while the gray histogram represents that fluorescence of the normal untransfected TF-1 (X-axis, intensity of GFP fluorescence; Y-axis, number of cells). We can see the green histogram notably shifted to the right hand when compared with the gray one, suggesting the former were emitting a much stronger GFP fluorescence, which

indicates these cells were successfully transfected with EmGFP vectors.

We next examined the G6PD protein level in the G6PD microRNA (miR) expression vector transfected cells. As shown in Figure 5.7, G6PD expression was significantly reduced after transfecting cells with the G6PD microRNA vector, whereas the G6PD expression level of the cells transfected with the empty EmGFP vector was more or less the same to the control. This suggests G6PD was successfully knocked down in the TF-1 cells. Furthermore, the G6PD expression level was found similar to that of Day 0 five days after EPO treatment in the G6PD-knockdown cells. In the control and cells transfected with the empty vector, the G6PD protein level was higher and remained unchanged as usual after EPO treatment (Figure 5.7a and 5.7b).

(a)

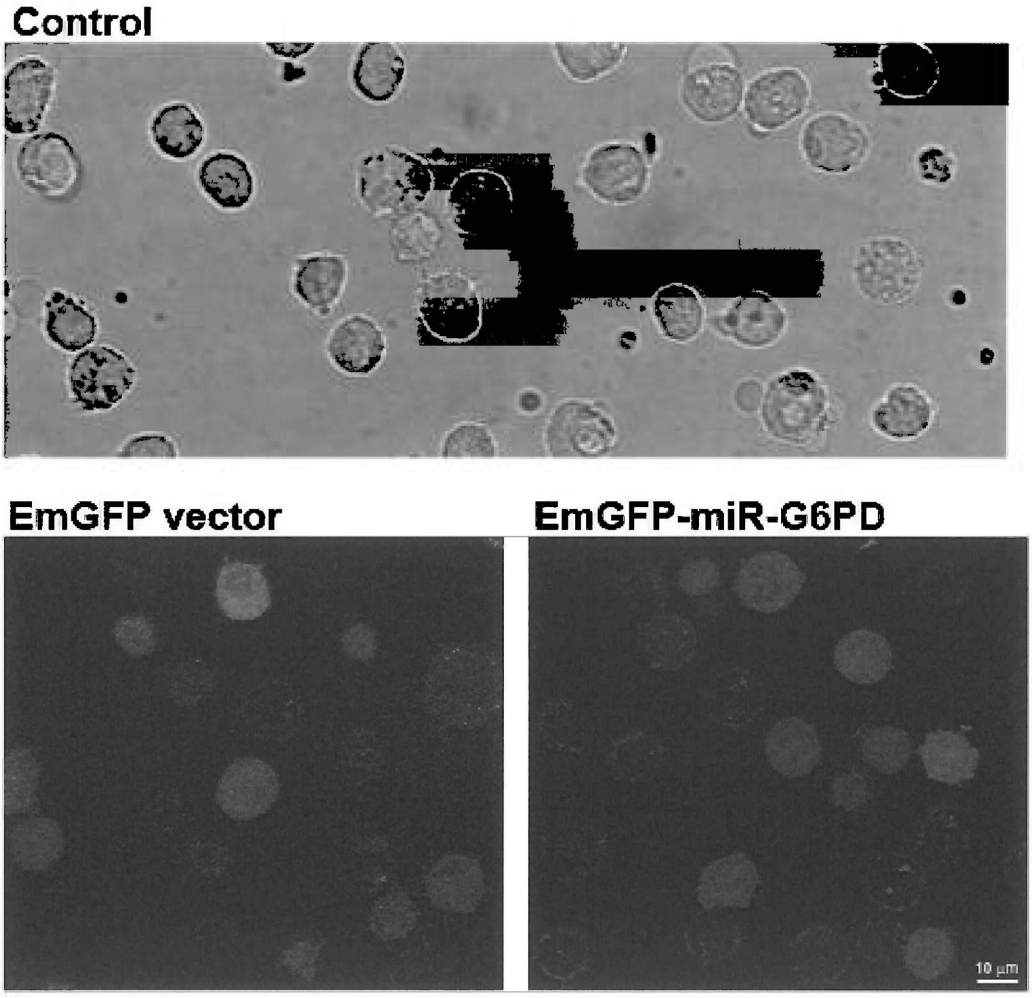

(b)

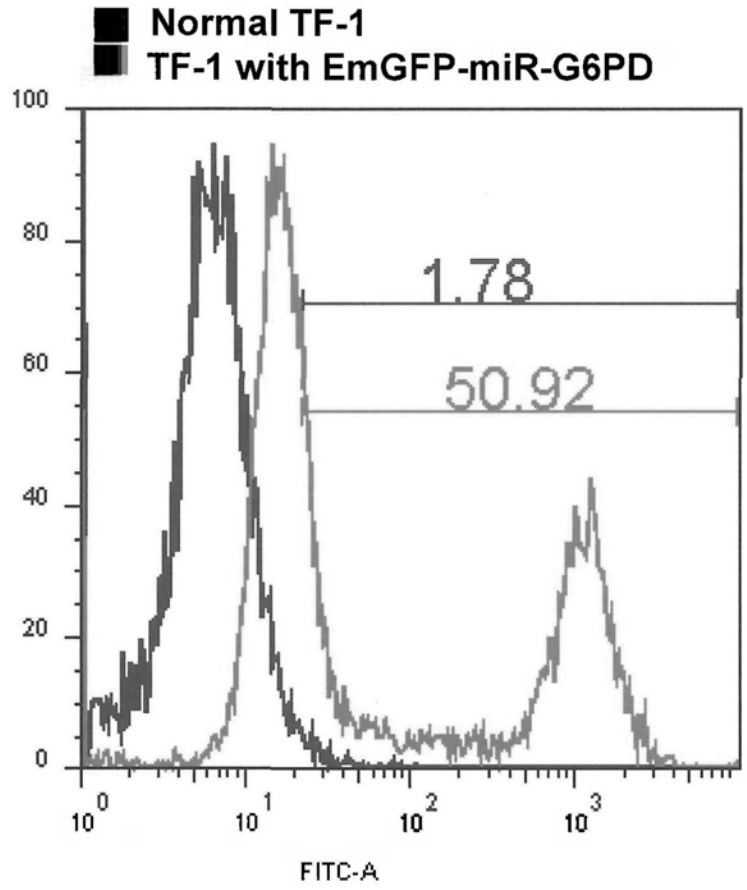

Figure 5.6 Observation of TF-1 cells with or without EmGFP vector. (**a**) by confocal: TF-1 cells transfected with empty EmGFP vector (lower left graph) or G6PD microRNA expression EmGFP vector (lower right graph) were visualized under confocal microscope, exited with 488nm laser line and measured by using a 495nm - 563nm band pass filter. Normal TF-1 cells (upper graph) were set as control. The scale bar represents the cell dimension. Images shown here were typical results in more than 3 trials. (**b**) by flow cytometry: TF-1 cells transfected with G6PD microRNA expression EmGFP vector were assayed by flow cytometry for fluorescence of FITC at channel FL-1H at log scale (green histogram). Normal TF-1 cells were set as control (gray histogram). Histograms shown here was typical result in more than 3 trials.

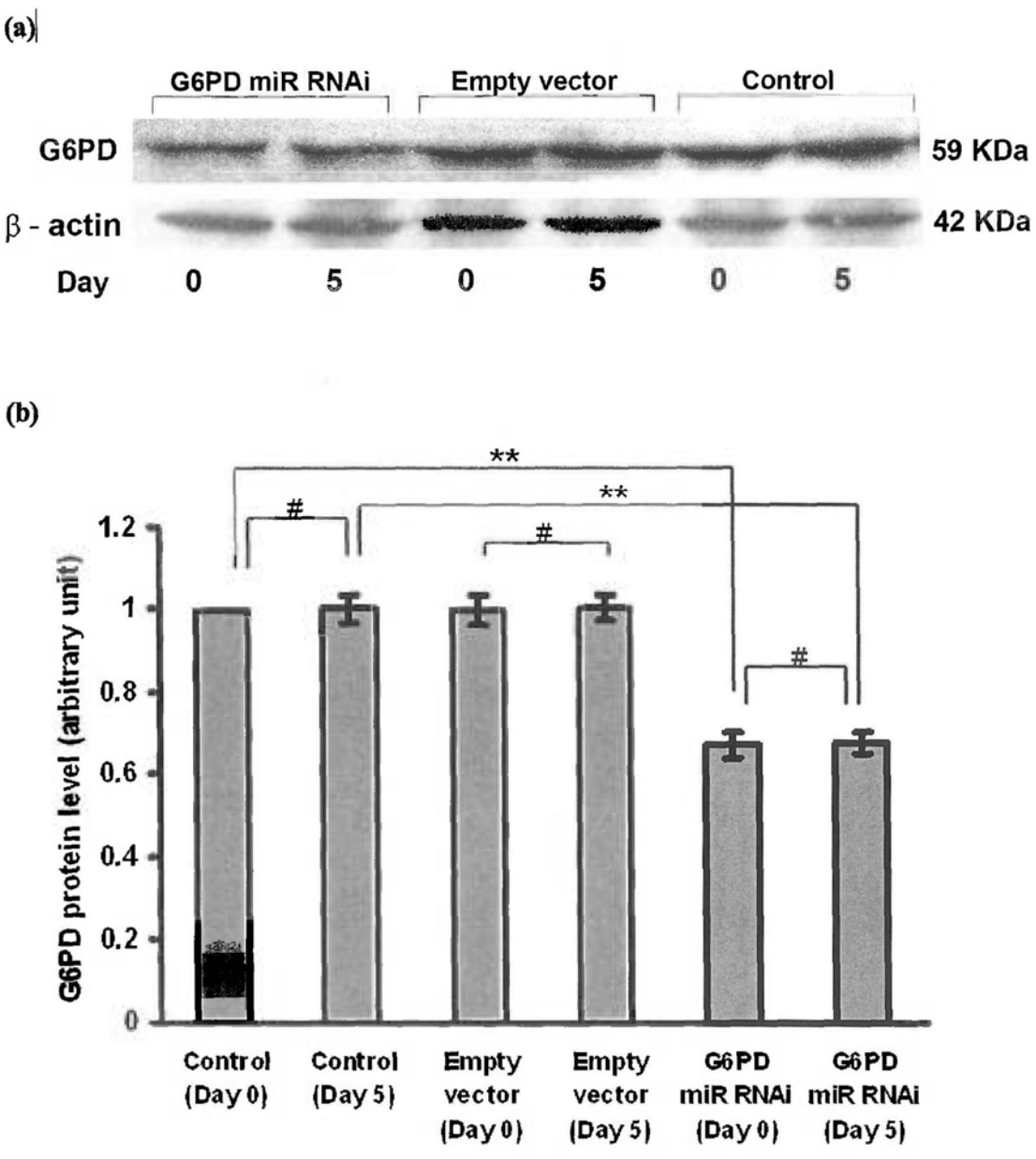

Figure 5.7 Expression level of G6PD in TF-1 cells transfected with EmGFP vector. TF-1 cells transfected with G6PD microRNA expression EmGFP vector or empty EmGFP vector or normal TF-1 cells were treated with EPO (10 ng/ml) at 37 °C, 5% CO_2 for 0 or 5 days. After cell lysis, lysates were subjected to Western blot analysis with antibodies for G6PD and β-actin (as an internal control) (**a**). Results, normalized by day 0 of normal TF-1 cells control, are mean ± SD, n=3 (bar-chart). $^{**}P < 0.001$, $\#P > 0.5$ (**b**).

5.7 NADPH level was significantly decreased in the G6PD-knockdown TF-1 cells

NADPH is the reduced form of nicotinamide adenine dinucleotide phosphate ($NADP^+$). It serves as an electron donor for many enzymatic reactions essential in biosynthetic pathways, and its production is crucial to the protection of cells from oxidative stress (Cappellini and Fiorelli, 2008). G6PD is the principal source of major intracellular NADPH (Zhang *et al.*, 2010). As shown in Figure 5.8, $NADPH/NADP^+$ ratio was significantly decreased in the G6PD-knockdown TF-1 cells when compared to that of normal cells, indicating NADPH level was reduced when G6PD was knocked down. This suggests that G6PD activity was significantly diminished in the G6PD-knockdown TF-1 cells.

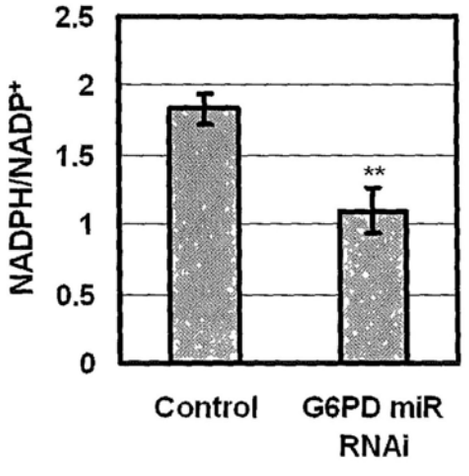

Figure 5.8 Change of $NADPH/NADP^+$ ratio after G6PD knockdown in TF-1 cells. $NADPH/NADP^+$ ratios of G6PD-knockdown TF-1 cells or normal TF-1 cells control were measured by using the corresponding quantification kit as described in the materials and methods section. The result (mean ± SD) represents three independent experiments. $^{**}P < 0.005$.

5.8 EPO-mediated erythroid differentiation was reduced in G6PD-knockdown TF-1 cells

Next, we examined the effect of G6PD-knockdown on erythropoiesis by treating G6PD-deficient TF-1 cells with EPO to see if they can undergo erythropoiesis. As shown in Figure 5.9, the percentage of erythroid marker GPA^+ cells was increased from about 2% of the total cell population on day 0 to around 38% on day 8 after EPO treatment, indicating the G6PD-deficient cells was able to commit to erythroid differentiation under EPO treatment. However, the degree of erythropoiesis was greatly reduced when compared to the normal cells. For example, on day 8 of differentiation, the percentage of GPA^+ population was 51.21% in normal erythropoiesis, while the percentage of that in G6PD-deficient erythropoiesis was only 37.86% (Figure 5.9b).

5.9 ROS level was increased during G6PD-deficient erythropoiesis

At the same time, ROS level was also detected and as shown in Figure 5.10, during G6PD-deficient erythropoiesis, ROS level was greatly increased compared to normal erythropoiesis. This is predicable since G6PD plays a crucial role in antioxidant defense system to against oxidative stress and diminish ROS level; on the other hand, this also indicates that no other additional effective endogenous anti-oxidative strength were developed to make up the deficiency of G6PD during TF-1 erythropoiesis.

(a)

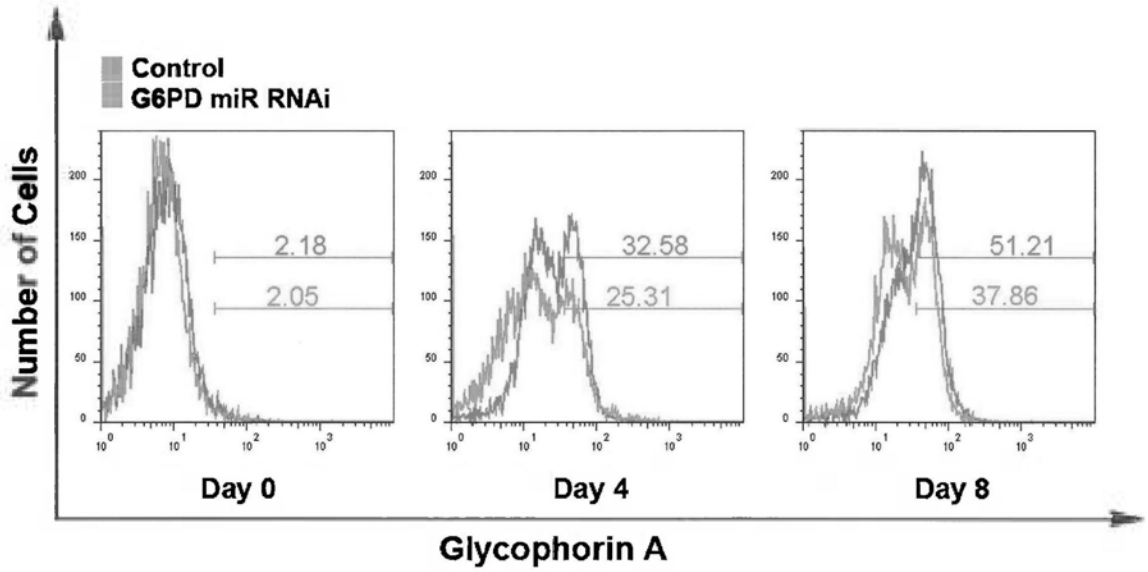

(b)

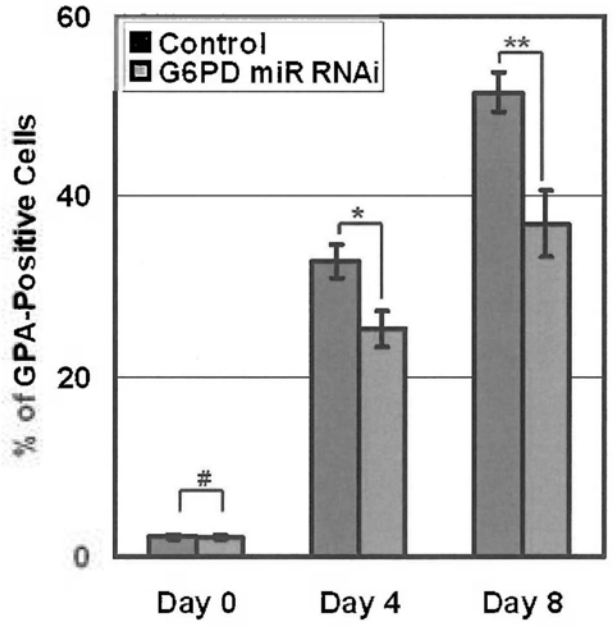

Figure 5.9 Change of GPA expression after G6PD knockdown under EPO treatment. G6PD-knockdown TF-1 cells or normal TF-1 cells control (4×10^5/ml) were treated with EPO (10 ng/ml) at 37 °C, 5% CO_2 for 0 to 8 days as indicated. Erythroid marker GPA was determined by anti-GPA MAb with flow cytometry. Figure represents the % of cells expressing erythroid marker in the selected region (**a**). Results are mean ± SD, n=3 (bar-chart). $*P < 0.01$, $**P < 0.005$, $\#P > 0.5$ (**b**).

(a)

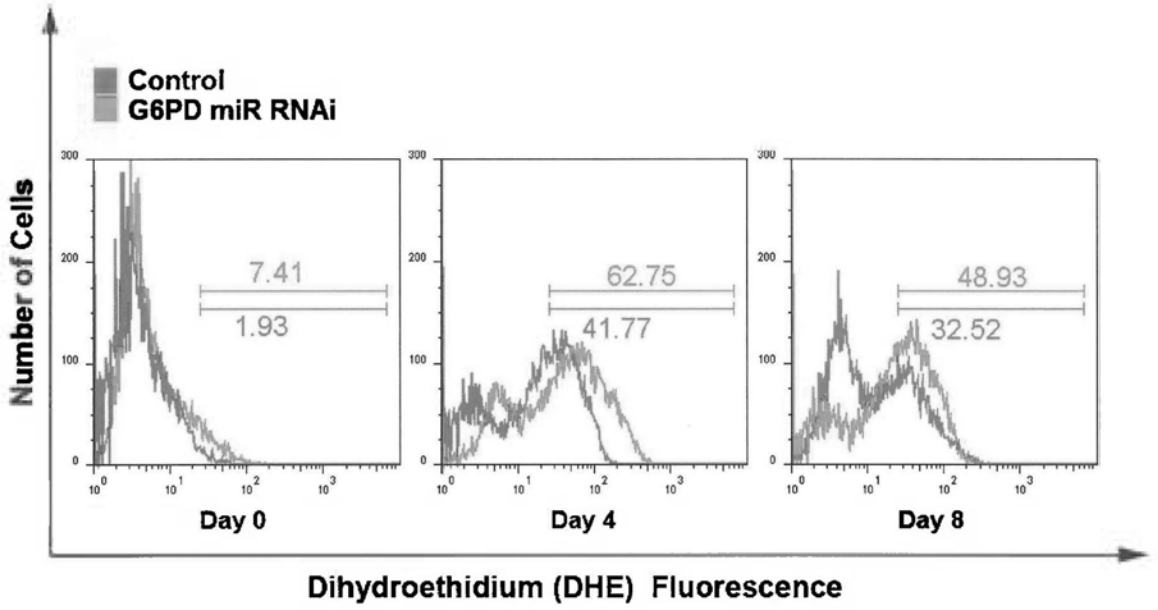

(b)

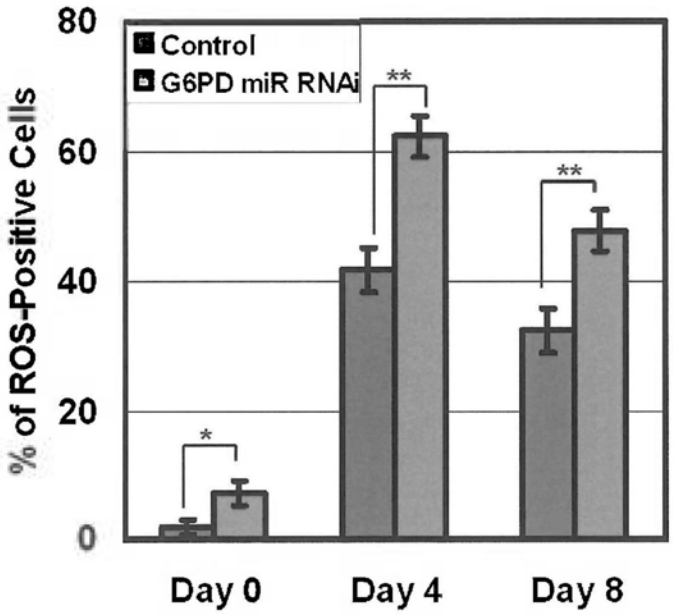

Figure 5.10 Change of ROS level after G6PD knockdown under EPO treatment. G6PD-knockdown TF-1 cells or normal TF-1 cells control (4×10^5/ml) were treated with EPO (10 ng/ml) at 37 °C, 5% CO_2 for 0 to 8 days as indicated. ROS was detected simultaneously by CM-H_2DCFDA with flow cytometry. Figure represents the % of cells in the selected region (**a**). Results are mean ± SD, n=3 (bar-chart). *$P <$ 0.05, **$P < 0.005$ (**b**).

5.10 Apoptotic cells were increased during G6PD-deficient erythropoiesis

Since ROS was raised during erythropoiesis in the G6PD-knockdown TF-1, more cells might be subjected to apoptosis in response to the high oxidative stress. We therefore examined the percentage of apoptotic cells in G6PD-knockdown TF-1 erythroid cells. As shown in Figure 5.11, much more apoptotic cells were found in the G6PD-knockdown cells when compared to the normal TF-1 (13.2% vs. 8.2% at Day 4; 11.5% vs. 7.7% at Day 8). Furthermore, the percentage of apoptotic cells in the control group had no obvious change along the course of erythroid differentiation (~8%), whereas in the G6PD-knockdown group, the trend of change in percentage of apoptotic cells was similar to that of ROS, firstly increased then declined. This observation suggests the increase in the number of apoptotic cells may be a result of the increased ROS level in G6PD-knockdown TF-1.

In Figure 5.9, we found a decrease in the erythroid differentiation in the G6PD-knockdown TF-1. With the input from Figure 5.10 and 5.11, it seems likely that the decrease is a result of (1) increase in apoptosis and (2) increase in ROS production.

(a)

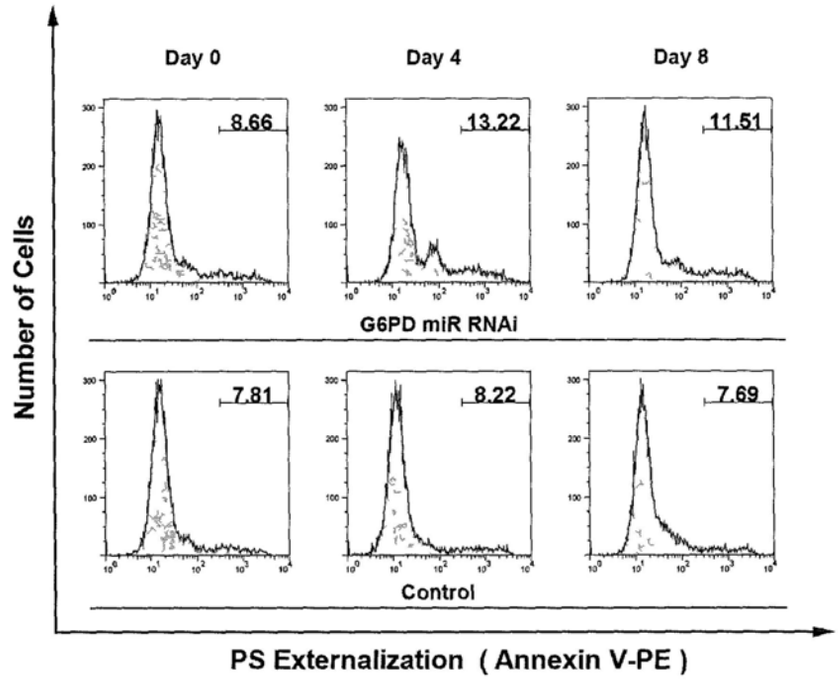

(b)

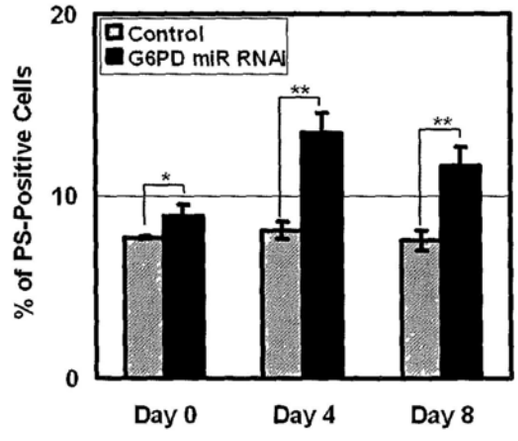

Figure 5.11 Change of percentage of dying cells after G6PD knockdown under EPO treatment. G6PD-knockdown TF-1 cells or normal TF-1 cells control (4×10^5/ml) were treated with EPO (10 ng/ml) at 37 °C, 5% CO_2 for days as indicated. Percentage of dying cells was determined by annexin V-PE dye with flow cytometric assay. Number represents the % of cells found in the selected region (**a**). Percentage of PS-positive cells was shown in the bar-chart, mean ± SD, n=3, $*P < 0.05$, $**P < 0.001$ (**b**).

5.11 Antioxidant enzymes downregulated during G6PD-deficient erythropoiesis

We were next curious to know if other enzymes or proteins of the antioxidant system were affected during erythropoiesis in the G6PD-knockdown TF-1. To this end, the expression levels of Glut1, GPx1 and Trx1 were examined. As shown in Figure 5.12, G6PD expression was reduced in the G6PD-knockdown cells and such a reduced expression was stable along the course of erythroid differentiation. Also, the antioxidant enzymes GPx1 and Trx1 were significantly down-regulated in the G6PD-knockdown TF-1 during erythropoiesis compared to that in normal erythropoiesis, suggesting that G6PD is not only responsible to defend cells against oxidative stress by producing NADPH and scavenging peroxide, but also plays a critical role in regulating other antioxidant enzymes such as GPx1 and Trx1 during TF-1 erythropoiesis. However, the expression level of Glut1 had no observed alteration between G6PD-knockdown TF-1 and normal parental cells during erythropoiesis.

(a)

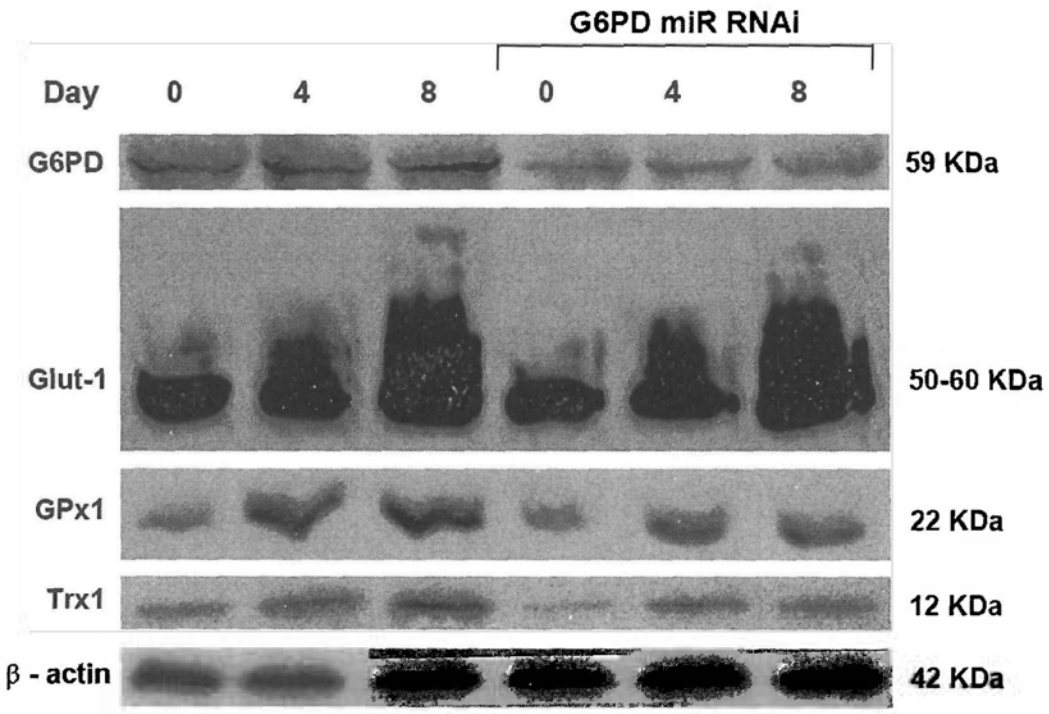
G6PD miR RNAi
Day 0 4 8 0 4 8
G6PD
59 KDa
Glut-1
50-60 KDa
GPx1
22 KDa
Trx1
12 KDa
β - actin
42 KDa

(b1)

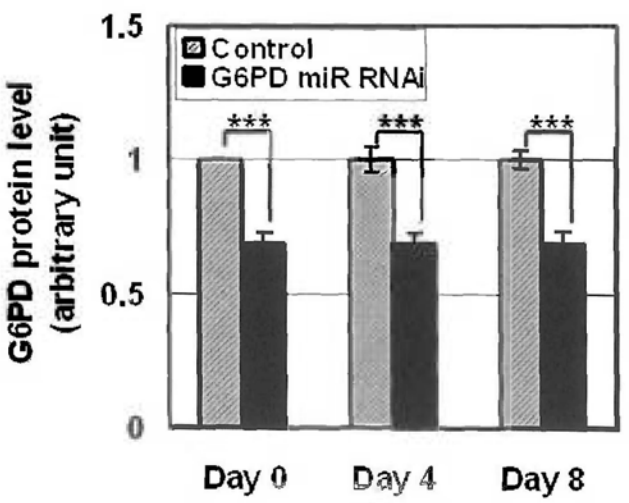
Control
G6PD miR RNAi
G6PD protein level (arbitrary unit)
1.5
1
0.5
0
***
***
***
Day 0
Day 4
Day 8

(b2)

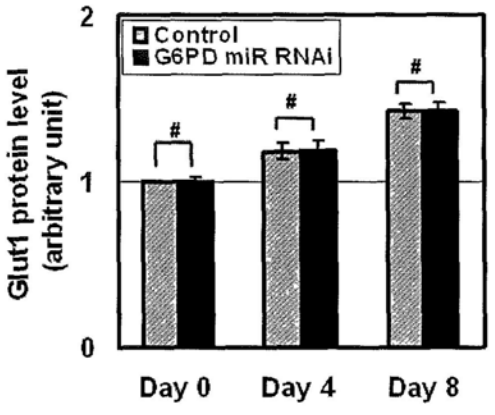

(b3)

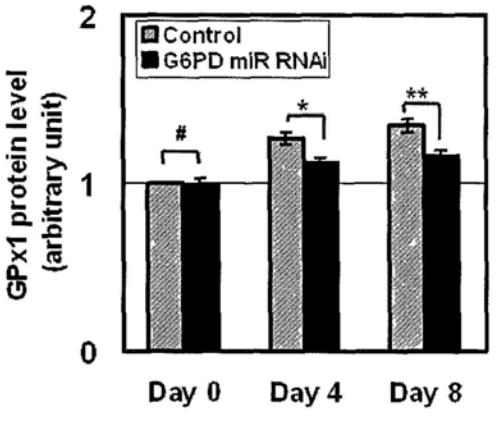

(b4)

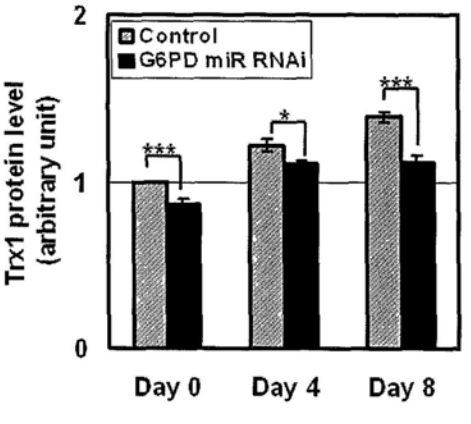

Figure 5.12 Change of antioxidant system related proteins after G6PD knockdown under EPO treatment. G6PD-knockdown TF-1 cells or normal TF-1 cells control (4×10^5/ml) were treated with EPO (10 ng/ml) at 37 °C, 5% CO_2 for days as indicated. After cell lysis, lysates were subjected to standard SDS-PAGE and Western blot analysis with antibodies for G6PD, Glut1, GPx1, Trx1 and β-actin (as an internal control) (**a**). Results, normalized by corresponding day 0 control, are mean ± SD, n=3 (bar-chart). *$P < 0.01$, **$P < 0.005$, ***$P < 0.001$, #$P > 0.5$ (**b1, b2, b3, b4**).

5.12 Vulnerable antioxidant defense system during G6PD-deficient erythropoiesis

As revealed previously in Figure 5.2, the number of dying cells (PS-positive cells) after H_2O_2-treatment was reduced along the course of erythropoiesis. This indicates that TF-1 cells developed endogenous defense mechanism against oxidative stress during erythroid differentiation. To further investigate the capability of counteracting exogenous oxidative challenge during erythroid differentiation in the G6PD-knockdown cells, we performed the H_2O_2-treatment experiment with the G6PD-knockdown cells again.

As shown in Figure 5.13, more dying cells (PS-positive cells) were found in the G6PD-knockdown group when compared to that of the normal erythropoiesis. For example, on day 0 of differentiation, about 55% dying cells were observed in the normal group under H_2O_2 treatment, while that number was up to ~70% of the G6PD-knockdown group. Moreover, along the course the erythroid differentiation, for the normal group, the number of dying cells was notably decreased to ~25% on day 8, but for the G6PD-knockdown group, that number was as high as 50%. Similarly, Figure 5.14 shows that under H_2O_2 treatment, the number of dead cells (PI-positive cells) of normal TF-1 erythropoiesis group was ~14% of day 0 and diminished to ~8% of day 8, while during G6PD-deficient erythropoiesis group, that number was ~20% on day 0 and ~16% on day 8.

Although the number of dying or dead cells under H_2O_2 treatment was decreased a bit along the course of erythropoiesis in the G6PD-knockdown group, which indicates that an endogenous antioxidant defense system was also partially developed as compared to normal TF-1 erythropoiesis, G6PD-knockdown erythroid cells had a much weaker antioxidant defense system and were much more vulnerable to oxidative stress. This might be another cause of why less differentiated cells were obtained in the G6PD-knockdown TF-1 (Figure 5.9) when compared to that of normal TF-1.

(a)

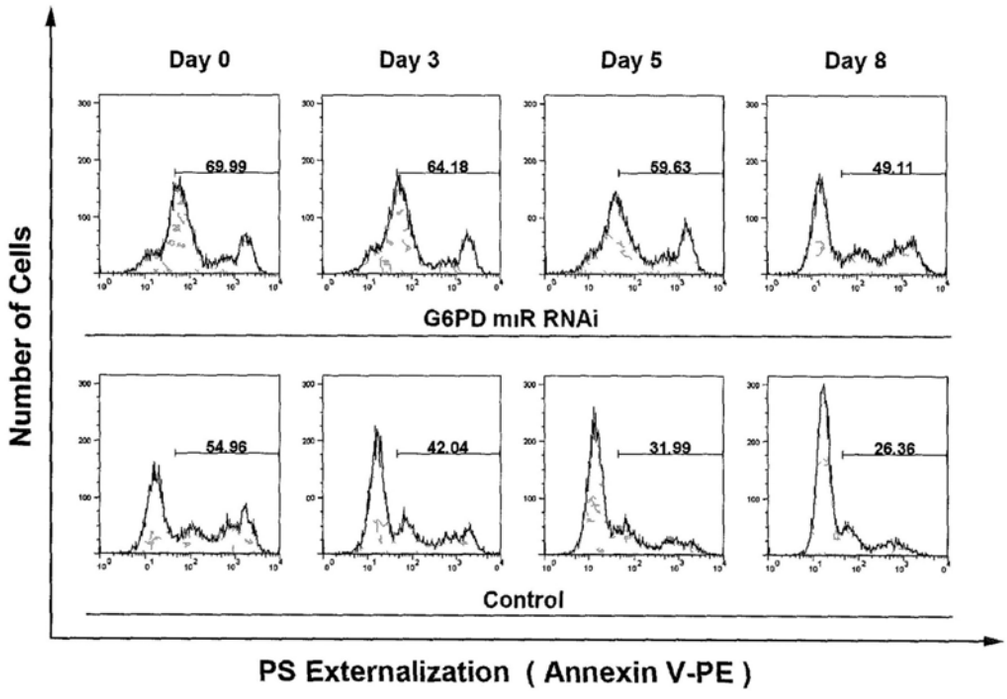
Day 0
Day 3
Day 5
Day 8
69.99
64.18
59.63
49.11
G6PD miR RNAi
54.96
42.04
31.99
26.36
Control
Number of Cells
PS Externalization (Annexin V-PE)

(b)

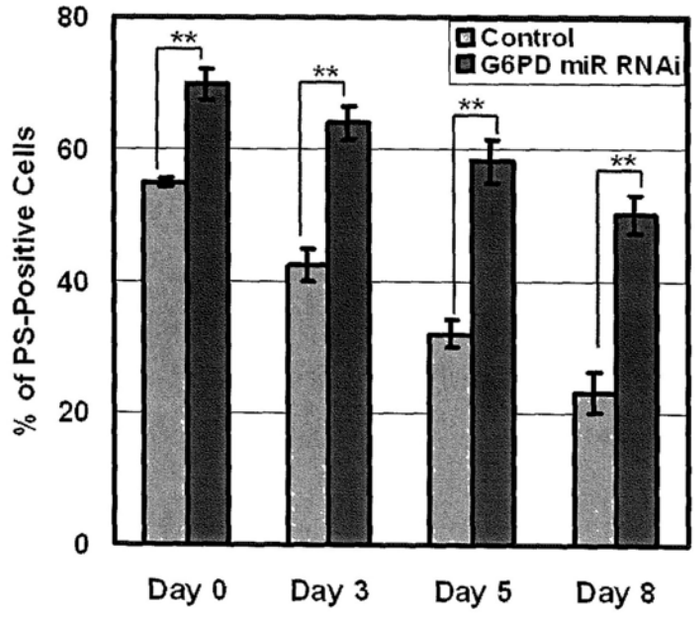
80
60
40
20
0
% of PS-Positive Cells
Control
G6PD miR RNAi
**
**
**
**
Day 0
Day 3
Day 5
Day 8

Figure 5.13 Variation of percentage of dying cells after G6PD knockdown under H_2O_2 treatment. G6PD-knockdown TF-1 cells or normal TF-1 cells control (4×10^5/ml) were treated with EPO (10 ng/ml) at 37 °C, 5% CO_2. At the day as indicated, the cells were washed twice with ice-cold PBS and then cultured in M2 medium containing 2 mM H_2O_2 for 9 h at 37 °C, 5% CO_2 before the annexin V-PE flow cytometric assay (**a**). Number represents the % of cells found in the selected region. Percentage of PS-positive cells was shown in the bar-chart, mean ± SD, n=3, $^{**}P < 0.001$ (**b**).

(a)

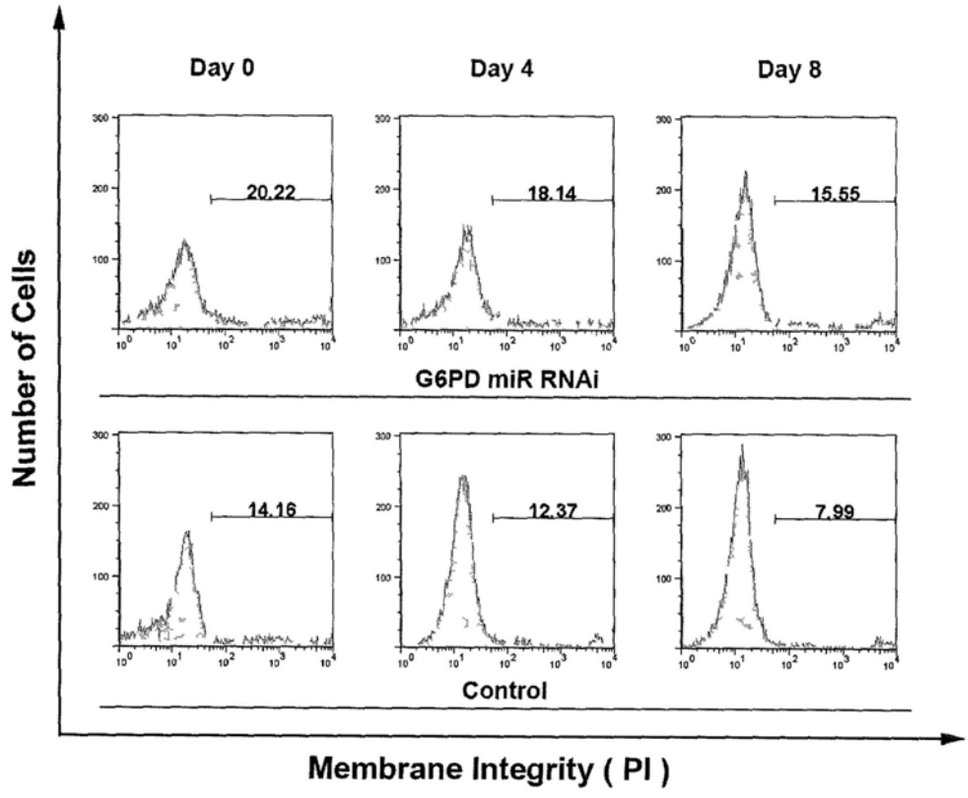
Day 0
Day 4
Day 8
20.22
18.14
15.55
G6PD miR RNAi
14.16
12.37
7.99
Control
Number of Cells
Membrane Integrity (PI)

(b)

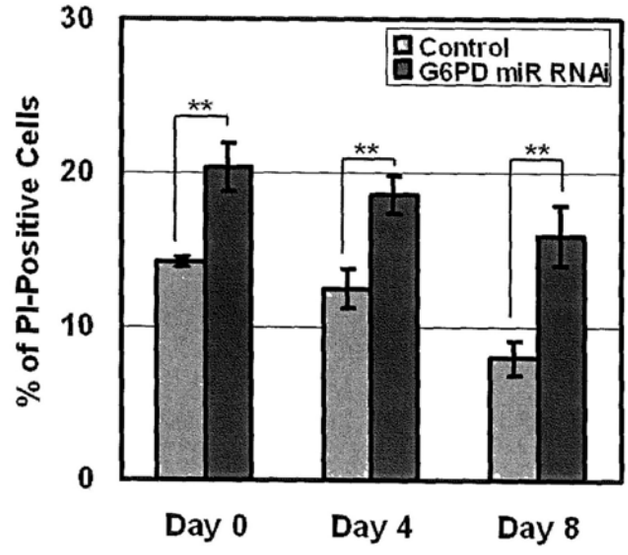
30
20
10
0
Control
G6PD miR RNAi
**
**
**
% of PI-Positive Cells
Day 0
Day 4
Day 8

Figure 5.14 Variation of percentage of dead cells after G6PD knockdown under H_2O_2 treatment. G6PD-knockdown TF-1 cells or normal TF-1 cells control (4×10^5/ml) were treated with EPO (10 ng/ml) at 37 °C, 5% CO_2. At the day as indicated, the cells were washed twice with ice-cold PBS and then cultured in M2 medium containing 2 mM H_2O_2 for 9 h at 37 °C, 5% CO_2 before the PI flow cytometric assay. Number represents the % of cells found in the selected region (**a**). Percentage of PI-positive cells was shown in the bar-chart, mean ± SD, n=3, $^{**}P < 0.005$ (**b**).

5.13 Salidroside attenuated H_2O_2-induced apoptosis in G6PD-knockdown TF-1 cells

As aforementioned, Figure 5.13 and 5.14 reveal that G6PD-knockdown erythroid cells had a much weaker antioxidant defense system and were much more vulnerable to oxidative stress when compared with the normal TF-1 erythroid cells. On the other hand, as indicated previously in chapter 3 and 4, salidroside was able to rescue the H_2O_2-treated RBCs from eryptosis and protect TF-1 erythroblasts against oxidative stress. Hence, we were curious to know whether SDS could also protect G6PD-knockdown erythroid cells against oxidative stress. To this end, we conducted the H_2O_2-challenge experiment with salidroside-treated G6PD-knockdown TF-1 cells, and then performed MTT and annexin-V assay.

As shown in Figure 5.15, taking the viability of Day 0 of the normal TF-1 cells without H_2O_2 treatment as 100%, under H_2O_2 treatment, the viability of Day 0 of normal TF-1 cells was about 50%, whereas the G6PD-knockdown cells was only about 35%; and the viability of normal TF-1 was increased to nearly 80% at Day 8 of erythroid differentiation, while that percentage for G6PD-knockdown cells was only gradually increased to ~50% at Day 8. This indicates firstly G6PD-knockdown cells were much more susceptible to H_2O_2-treatment; secondly the normal TF-1 developed an endogenous antioxidant defense system during erythropoiesis and the G6PD-knockdown cells also partially developed that system. These findings were consistent with the result of Figure 5.13 and 5.14. For the SDS-treated

G6PD-knockdown TF-1 group, the viability was raised to more than 60% at Day 8, while as mentioned above, that percentage of untreated G6PD-knockdown TF-1 was less than 50%, suggesting SDS defended G6PD-knockdown erythroid TF-1 cells from H_2O_2-challenge during G6PD-deficient erythropoiesis.

Figure 5.16 also reveals the similar result, in which we can see apoptotic cells (PS-positive cells) were significantly decreased in the salidroside-treated group (G6PD-knockdown with EPO vs. G6PD-knockdown with EPO and SDS = 63.1% vs. 53.4% (Day 3); 57.5% vs. 43.7% (Day 5); 48.6% vs. 33.6% (Day 8)), indicating SDS attenuated H_2O_2-induced apoptosis in G6PD-knockdown TF-1 cells during erythroid differentiation.

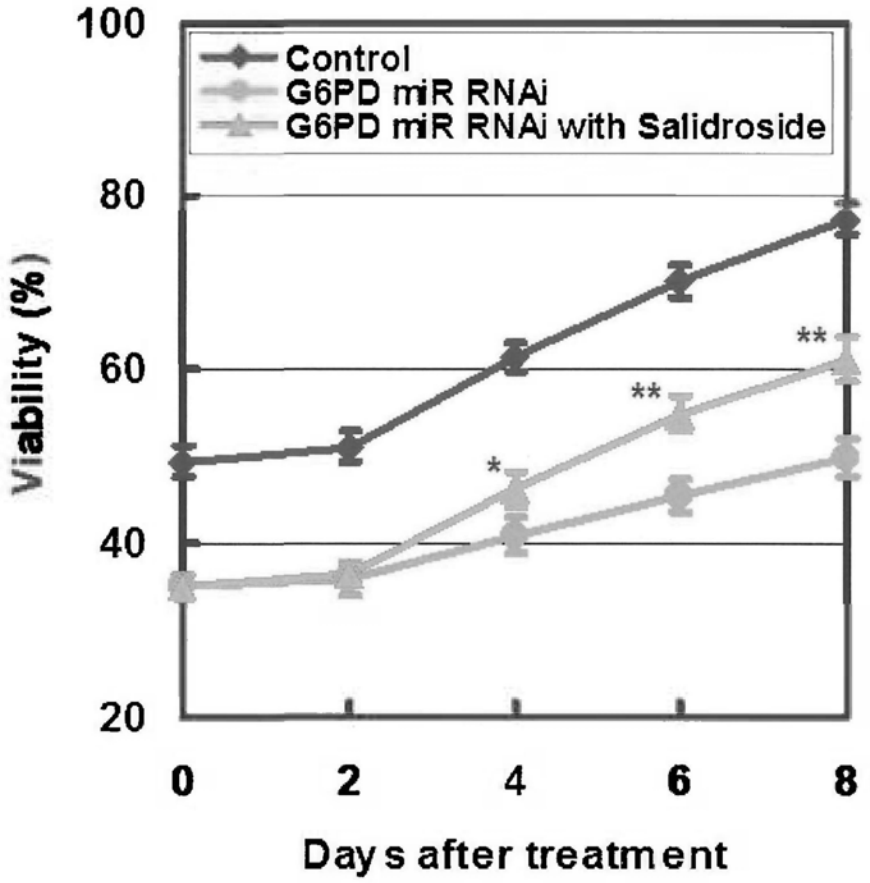

Figure 5.15 Effect of salidroside on the viability in G6PD-knockdown TF-1 cells under H_2O_2 treatment. G6PD-knockdown TF-1 cells or normal TF-1 cells control (4×10^5/ml) were treated with EPO (10 ng/ml) or EPO (10 ng/ml) and salidroside (100 μM) at 37 °C, 5% CO_2. At the day as indicated, the cells were washed twice with ice-cold PBS and then cultured in M2 medium containing 2 mM H_2O_2 for 9 h at 37 °C, 5% CO_2. Then cell viability (% of the Day 0 normal TF-1 cells without H_2O_2 treatment) was measured by MTT assay. Results are mean ± SD, n=3. Student's *t-test*, G6PD miR RNAi with Salidroside *versus* G6PD miR RNAi, on the corresponding day, $*P < 0.05$, $**P < 0.005$.

(a)

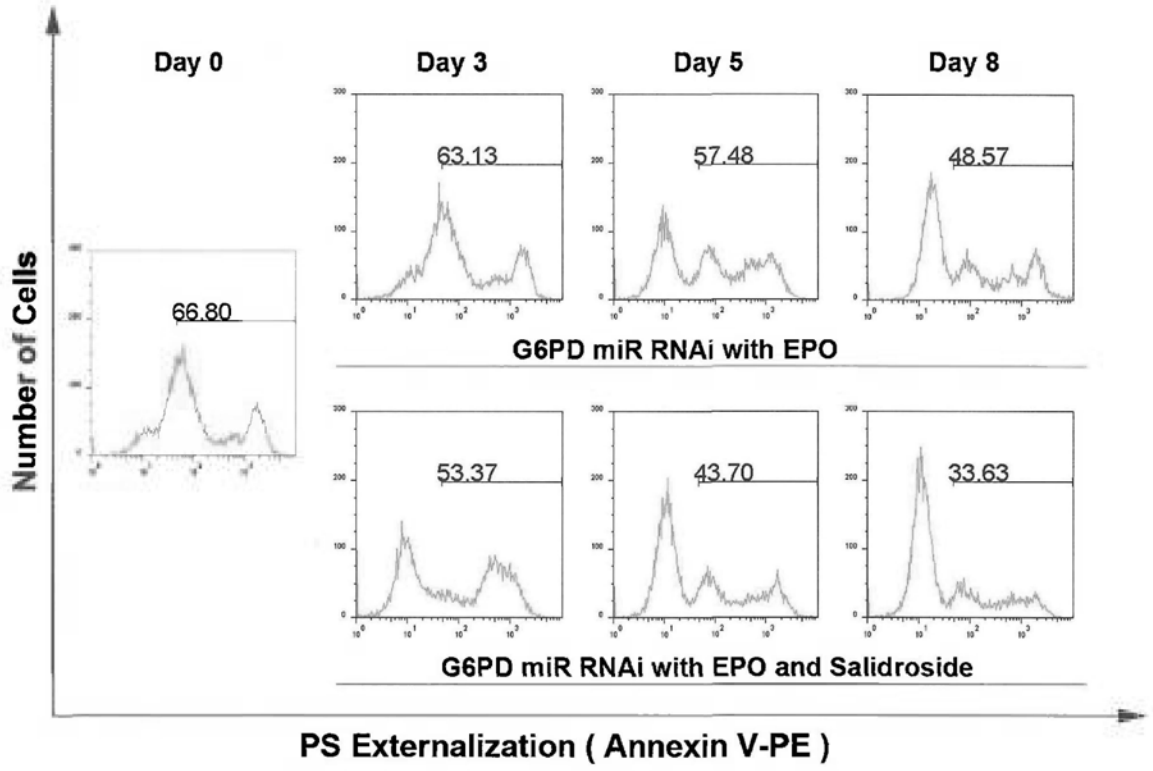
Day 0
Day 3
Day 5
Day 8
66.80
63.13
57.48
48.57
G6PD miR RNAi with EPO
53.37
43.70
33.63
G6PD miR RNAi with EPO and Salidroside
Number of Cells
PS Externalization (Annexin V-PE)

(b)

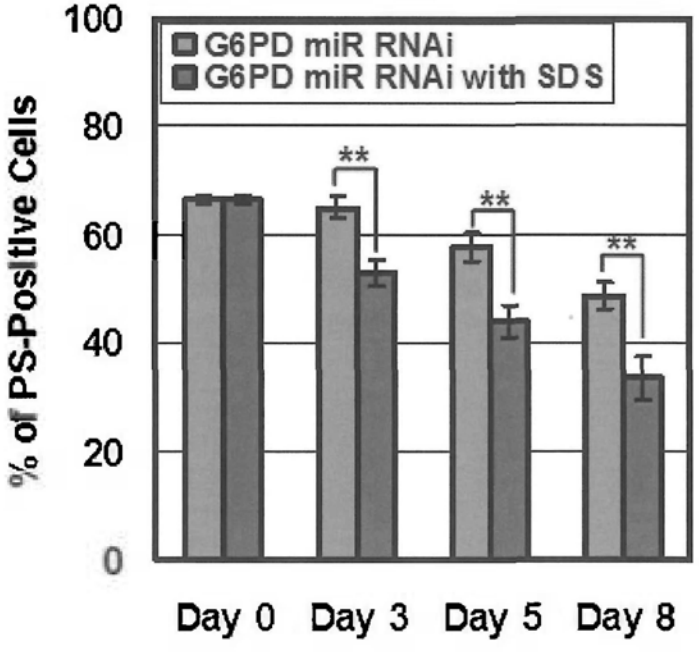
G6PD miR RNAi
G6PD miR RNAi with SDS
% of PS-Positive Cells
100
80
60
40
20
0
**
**
**
Day 0
Day 3
Day 5
Day 8

Figure 5.16 Effect of salidroside on H_2O_2-induced apoptosis in G6PD-knockdown TF-1 cells. G6PD-knockdown TF-1 cells (4×10^5/ml) were treated with EPO (10 ng/ml) or EPO (10 ng/ml) and salidroside (100 μM) at 37 °C, 5% CO_2. At the day as indicated, the cells were washed twice with ice-cold PBS and then cultured in M2 medium containing 2 mM H_2O_2 for 9 h at 37 °C, 5% CO_2 before the annexin V-PE flow cytometric assay. Number represents the % of cells found in the selected region (**a**). Percentage of PS-positive cells was shown in the bar-chart, mean ± SD, n=3, $^{**}P < 0.005$ (**b**).

5.14 Discussion

Our previous work has shown that ROS was produced with a peak at day 4 and subsequently decreased at day 6 and day 8 during TF-1 erythroid differentiation. At the same time, erythroid markers were increased and endogenously protective anti-oxidative mechanism was simultaneously activated (Qian *et al.*, 2011). We now show that the ROS level reduced by antioxidant NAC did not affect the EPO-induced erythroid marker's production in TF-1 cells (Figure 5.1), indicating that ROS does not play a leading role in erythropoiesis. On the other hand, NAC-treatment experiments show that the activation of anti-oxidative defense system was partially restrained under the reduced ROS level condition (Figure 5.2, 5.4 and 5.5). This suggests that ROS plays a role in the establishment of endogenous defense system against oxidative stress. These findings further confirm and foster the observations from our previous work (Ge, 2009).

G6PD is a key enzyme of anti-oxidative defense system of RBCs. As early as 1995, Pandolfi *et al.* reported that G6PD is essential for defense against oxidative stress by using G6PD knockout mice. In 2004, Paglialunga *et al.* reported that G6PD activity is indispensable for definite erythropoiesis. Mechanistically, G6PD plays a key role in the regeneration of NADPH and maintenance of cellular redox balance in erythrocytes (Cappellini and Fiorelli, 2008). In our G6PD-knockdown TF-1 cells, $NADPH/NADP^+$ ratio was significantly decreased (Figure 5.8), suggesting the cells' capability of regenerating NADPH was notably reduced, which indicates the G6PD

activity was remarkably diminished. Under EPO inducement, the G6PD-knockdown TF-1 cells was able to commit to erythroid differentiation but the percentage of differentiated cells was significantly reduced (Figure 5.9). On the other hand, the ROS level and percentage of apoptotic cells were notably increased in the G6PD-knockdown erythropoiesis group (Figure 5.10, 5.11). These observations indicate that the decreased efficacy of producing erythroid cells in G6PD-knockdown group may be due to the increase in apoptosis and ROS production.

GPx1 is one of the major anti-ROS defense enzymes in erythroid cells. This enzyme employs NADPH, generated from the hexose monophosphate shunt through G6PD, as the electron donor and glutathione as the ROS scavenger (Ghaffari, 2008). Also, Trx1 is able to eliminate the H_2O_2 produced intracellularly (Kang *et al.*, 1998). Its action is similar to the GPx system, which also utilizes NADPH as the reducing power. Our previous work has revealed that GPx1 and Trx1 were up-regulated during erythropoiesis (Qian *et al.*, 2011), here we show that in G6PD-knockdown erythropoiesis, GPx1 and Trx1 were significantly down-regulated when compared with control, indicating that G6PD also plays a role in regulating other antioxidant enzymes such as GPx1 and Trx1 during TF-1 erythropoiesis (Figure 5.12). This observation is consistent with previous reports showing that GPx activity was significantly decreased in G6PD-deficient mice (Xu *et al.*, 2010) and G6PD-deficient patients' cord blood (Tho *et al.*, 1988). In addition, it also has been reported that a decay of G6PD activity may have negative effect on antioxidant enzymes such as

GPx (Ninfali *et al.*, 1991; Ozmen *et al.*, 2005). However, that Trx1 enzyme is also linked to G6PD activity has not been reported yet. The explanation for these connections between G6PD and GPx1/Trx1 may be the decrease in NADPH level under subnormal G6PD activity condition, because both GPx1 and Trx1 are dependent on NADPH for function. With the decreased antioxidant enzymes including G6PD, GPx1 and Trx1, and the lower NADPH level, it is not surprising why G6PD-knockdown erythroblasts were much more vulnerable to H_2O_2-induced oxidative stress challenge (Figure 5.13, 5.14).

On the other hand, the expression level of Glut1 had no observed alteration between G6PD-knockdown TF-1 and normal parental cells during erythropoiesis (Figure 5.12). This is in contrast to the observations in Figure 5.5 & 5.9 which indicate that the Glut1 upregulation was only found in differentiated TF-1 cells, and there were less differentiated cells in G6PD-knockdown erythropoiesis. Therefore presumably, the Glut1 expression should be downregulated in the G6PD-knockdown erythroblasts. Nevertheless, we should not forget another factor ROS and its changes between G6PD-deficient erythropoiesis and normal erythropoiesis. Whether ROS plays a role in the regulation of Glut1 during TF-1 erythropoiesis might be an interesting question to ask.

As mentioned before, SDS has long been used as a blood tonic and adaptogen in traditional Chinese and Tibetan medicine. It has been reported to have various

pharmacological properties and one of them is anti-oxidative effect (Kanupriya *et al.*, 2005; Yu *et al.*, 2007). Using TF-1 cells, we showed that SDS, in conjunction with EPO, was able to protect G6PD-knockdown erythroblasts from H_2O_2 -induced cell death (Figure 5.15, 5.16).

In summary, our work firstly provides evidence that ROS plays a role in the establishment of endogenous anti-oxidative defense system in TF-1 erythroid differentiation. Secondly, our findings reveal that the major antioxidant enzyme G6PD also functions in the regulation of other antioxidant enzymes such as GPx1 and Trx1. Thirdly, the traditional medicine SDS is able to protect G6PD-knockdown erythroblasts from H_2O_2-induced oxidative stress, and up to now, this medicine has not reported to have any adverse side-effects (Darbinyan *et al.*, 2007). Therefore, our work provides support to the idea that SDS can be used for helping G6PD-deficient patients.

Chapter 6

Regulation of ROS on Glut1 during Erythropoiesis in TF-1 Cells

6.1 Introduction

Glucose is the only fuel utilized in human erythrocytes and Glut1 is the sole glucose transporter in the red cell membrane that delivers glucose into the cells. Moreover, Glucose undergoes oxidation via the pentose phosphate pathway thereby generating reductant NADPH and hence provides the majority of reducing equivalents against oxidative stress in human erythrocytes. Therefore the glucose transporter Glut1 plays an extraordinarily critical role in human erythrocytes. However, the regulation of Glut1 during erythropoiesis is poorly understood. Employing commonly used erythropoiesis model TF-1 cells, the pathway by which Glut1 is regulated during erythroid maturation was investigated.

6.2 Glut1 expression was upregulated during erythropoiesis

As shown in Figure 6.1a, gradually increased expression level of Glut1 with glycosylation (the "smear-like" pattern, (Montel-Hagen *et al.*, 2008)) was observed in the TF-1 cells when treated with EPO for 2 to 8 days. The Glut1 band intensity was normalized by control and the mean ± SD (n=3) from different groups and the results were summarized in Figure 6.1a2. As can be seen, a time-dependent increase in Glut1 was found. The Western blot in Figure 6.1a determined both the Glut1 on the cell surface and those found intracellularly. To measure the former, cell surface Glut1 was detected using EGFP-conjugated Glut1 ligand by flow cytometric analysis (Figure 6.1b). As can be seen, a remarkable up-regulation of Glut1 on cell surface was observed along the course of EPO-induced erythroid differentiation.

(a1)

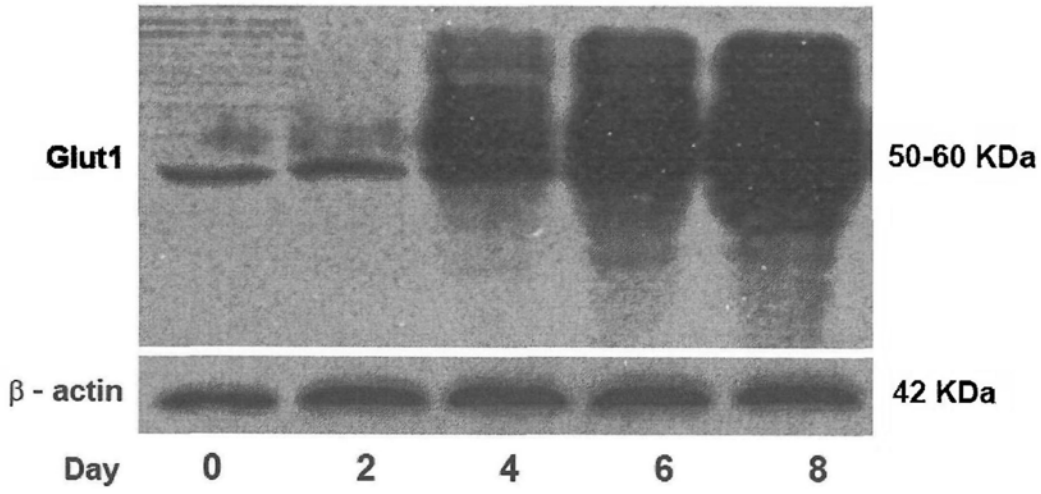
Glut1
50-60 KDa
β - actin
42 KDa
Day 0 2 4 6 8

(a2)

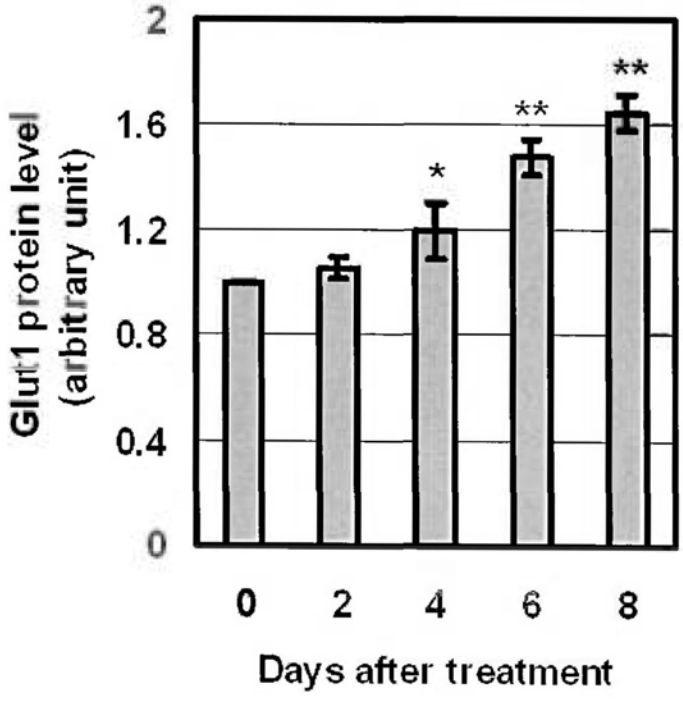
Glut1 protein level (arbitrary unit)
2
1.6
1.2
0.8
0.4
0
*
**
**
0 2 4 6 8
Days after treatment

(b1)

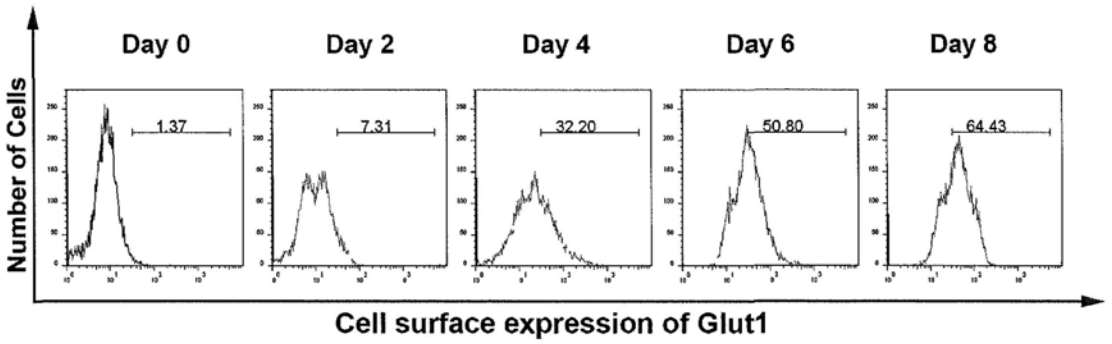

(b2)

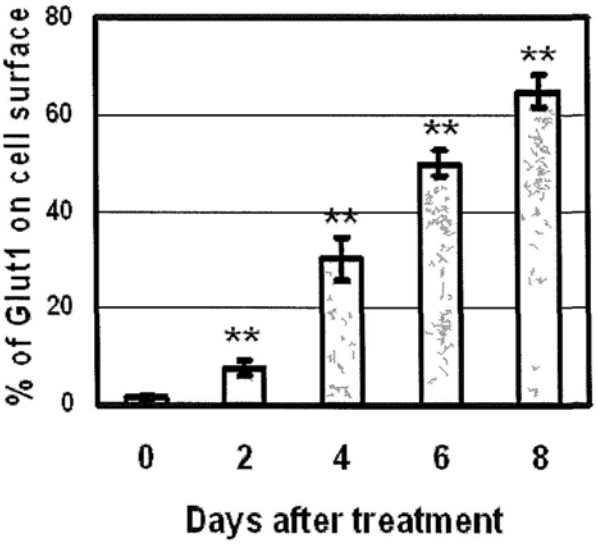

Figure 6.1 Expression of Glut1 during erythropoiesis in TF-1 cells. TF-1 cells (4×10^5/ml) were cultured with EPO (10 ng/ml) at 37 °C, 5% CO_2 for days as indicated. After cell lysis, lysates containing equal amount of proteins per lane were subjected to standard SDS-PAGE and Western blot analysis with antibodies for Glut1 and β-actin (as an internal control) (**a1**). Cell surface expression of Glut1 was determined by EGFP-Glut1 ligand with flow cytometry. Figure represents the % of cells in the selected region (**b1**). Results in bar charts were normalized by corresponding control at day 0. Mean ± SD, n=3. $*P < 0.05$, $**P < 0.005$, compared to corresponding day 0 control (**a2, b2**).

6.3 Upregulation of Glut1 is important for erythropoiesis

The correlation between Glut1 up-regulation and erythropoiesis was then investigated by associating the cell surface Glut1 expression level with erythroid marker expression. The cells were treated with EGFP-conjugated Glut1 ligand binding assay together with staining of erythroid lineage marker GPA using APC-conjugated antibody. As can be seen in Figure 6.2, only 0.04% of cells were found in the two right quadrants for cell surface expression of Glut1 on day 0 suggesting that no cell surface expression of Glut1 was detected at the beginning of erythropoiesis in TF-1 cells. Along the course of erythroid differentiation, the percentage of cells with simultaneous cell surface expression of Glut1 and GPA expression increased in a time-dependent manner from 0% at day 0 to 56.7% at day 8 (Figure 6.2, upper right quadrants, Day 0 : 2 : 5 : 8 = 0% : 2.9% : 29.6% : 56.7%), and most of the GPA^+ cells were Glut1 positive in later phase of development, indicating that up-regulation of Glut1 is associated with erythroid differentiation. Moreover, previous work of our lab has showed that inhibition of Glut1 by levofloxacin partially blocked the TF-1 erythropoiesis without affecting cell viability (Ge, 2009), suggesting that up-regulation of Glut1 is important for erythropoiesis.

(a)

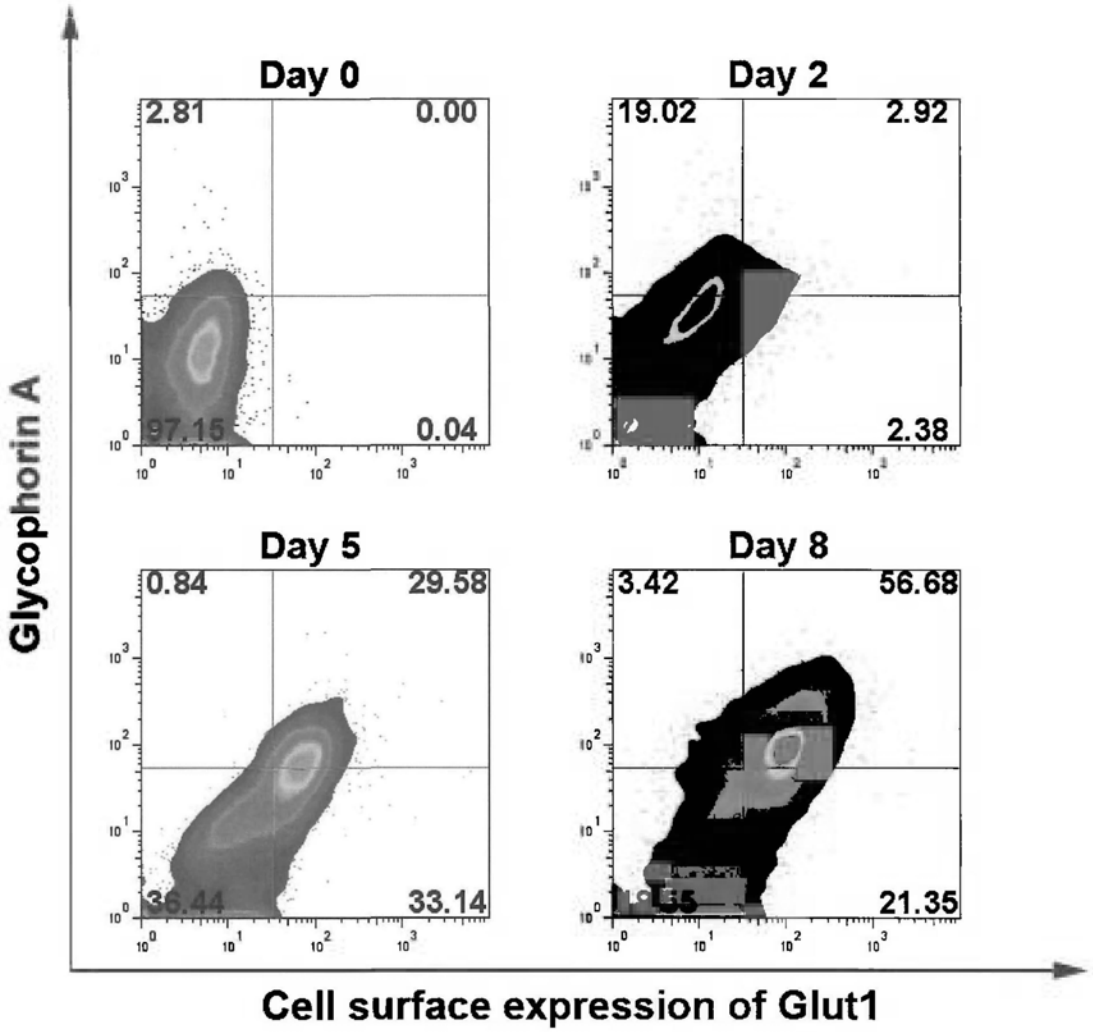
Day 0
2.81
0.00
97.15
0.04
Day 2
19.02
2.92
2.38
Day 5
0.84
29.58
33.14
Day 8
3.42
56.68
21.35
Glycophorin A
Cell surface expression of Glut1

(b)

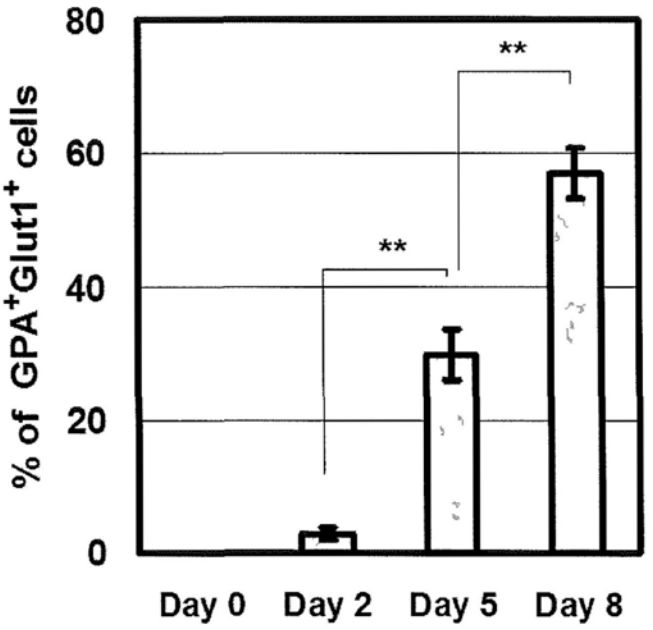

Figure 6.2 Expressions of cell surface Glut1 and erythroid marker GPA during erythropoiesis in TF-1 cells. TF-1 cells (4×10^5/ml) were cultured with EPO (10 ng/ml) at 37 °C, 5% CO_2 for days as indicated. Expression of cell surface Glut1 and erythroid marker GPA were determined simultaneously by EGFP-Glut1 ligand and anti-GPA MAb with flow cytometry. Figure represents the % of cells found in the corresponding quadrant (**a**). Mean ± SD, n=3 (bar-chart). $^{**}P < 0.001$ (**b**).

6.4 Reduction in ROS level resulted in a decrease in Glut1 level

Given the importance of Glut1 up-regulation during erythropoiesis, we were interested in the pathway by which Glut1 is up-regulated in erythroid differentiation. Our previous report had revealed that ROS production was increased with a peak at day 4 during the EPO-induced TF-1 erythropoiesis (Qian *et al.*, 2011) and similar results were shown in Figure 6.3. Coincidently, prominent up-regulation of Glut1 was also obtained at day 4 after EPO treatment. Therefore, we were curious to know if ROS plays a role in the up-regulation of Glut1 during erythropoiesis. We reduced ROS production in TF-1 erythropoiesis by employing an antioxidant EUK-134, which is a synthetic superoxide dismutase and catalase mimetic to prevent oxidative stress (Rong *et al.*, 1999), and observed whether the up-regulation of Glut1 had changes.

As shown in Figure 6.4a and 6.4b, compared with the control group, the cells co-treated with EUK-134 and EPO significantly reduced the ROS production (EPO+EUK-134 vs. EPO = 20.2% vs. 27.7% (Day 2); 39.5% vs. 48.5% (Day 4); 27.8% vs. 42.3% (Day 6); 20.6% vs. 30.5% (Day 8)), suggesting that the EUK-134 functioned well as an antioxidant in the TF-1 erythropoiesis. Simultaneously, the expression level of Glut1 was also examined by flow cytometric assay and Western blot analysis for detecting cell surface expression of Glut1 and total cell expression of Glut1 respectively. As shown in Figure 6.5, the cell surface expression level of Glut1 in the group co-treated with EUK-134 and EPO were notably decreased when compared with the EPO control group (EPO vs. EPO+EUK-134 = 7.9% vs. 6.9%

(Day 2); 32.0% vs. 25.7% (Day 4); 50.3% vs. 40.8% (Day 6); 65.7% vs. 50.8% (Day 8)). Also, the total cell expression level of Glut1 in the EUK-134-added group were significantly reduced when compared with the corresponding control group (Figure 6.6). Moreover, the mRNA level of Glut1 was also measured and much less mRNA of Glut1 were found in the EUK-134 and EPO co-treatment group than that of EPO control group (Figure 6.7). Collectively, the ROS level reduced by antioxidant EUK-134 resulted in a decrease in Glut1 level, including the cell surface expression, the total cell expression and the mRNA levels, indicating that ROS play a role in the up-regulation of Glut1 during erythroid differentiation.

(a)

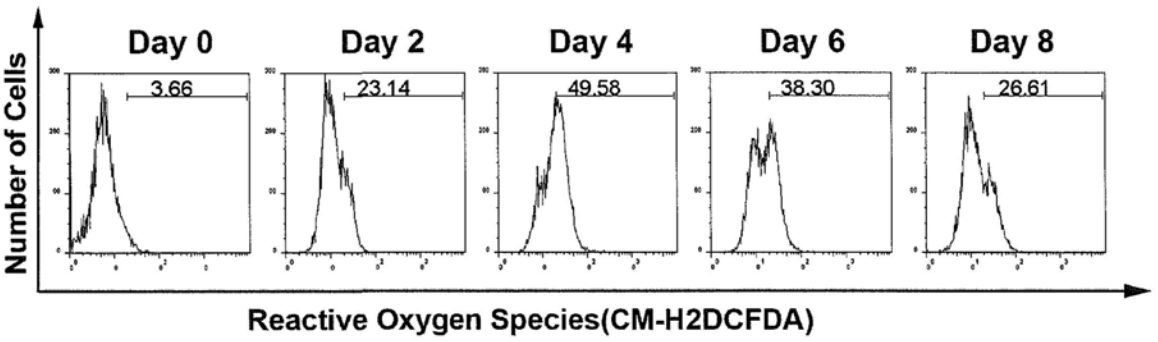

(b)

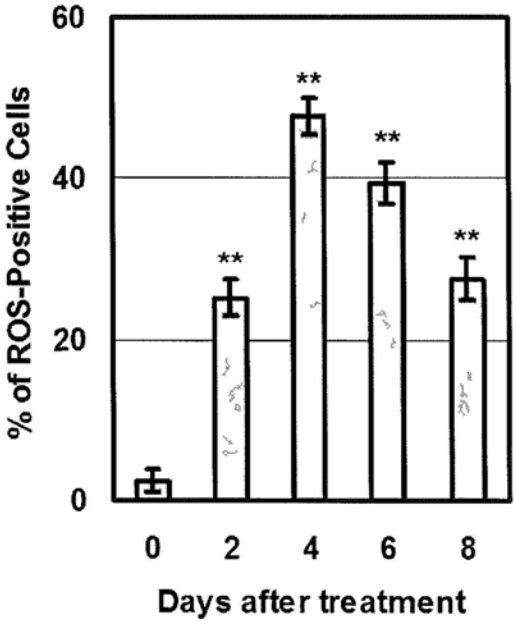

Figure 6.3 Changes of ROS level during erythropoiesis in TF-1 cells. TF-1 cells (4×10^5/ml) were cultured with EPO (10 ng/ml) at 37 °C, 5% CO_2 for days as indicated. ROS levels were determined by CM-H_2DCFDA with flow cytometry. Figure represents the % of cells found in the selected region (**a**). Mean ± SD, n=3 (bar-chart). $^{**}P < 0.001$, compared to day 0 control (**b**).

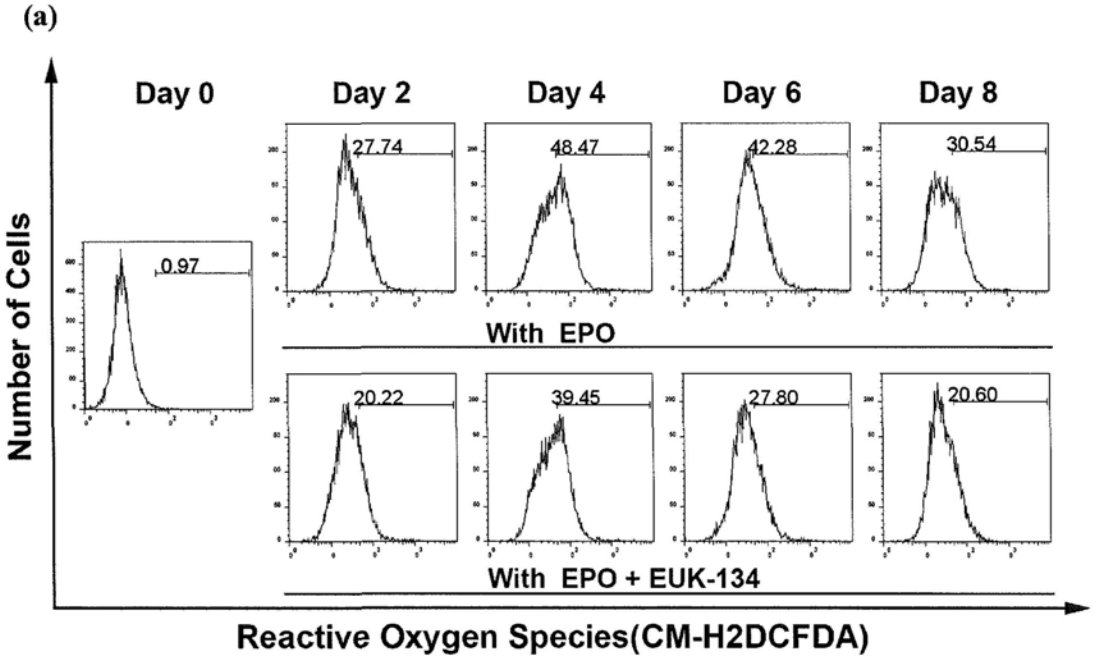

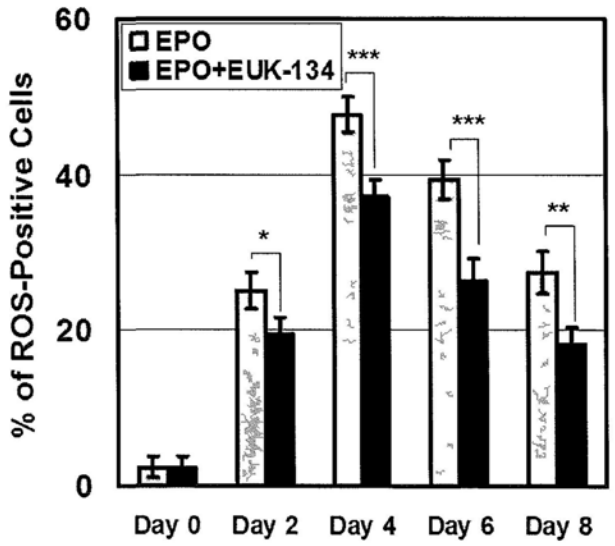

Figure 6.4 Effect of EUK-134 on the level of ROS during erythroid differentiation in TF-1 cells. TF-1 cells (4×10^5/ml) were treated with EPO (10 ng/ml) alone, or EPO (10 ng/ml) with EUK-134 (50 μM) at 37 °C, 5% CO_2 for 0 to 8 days as indicated. ROS levels were determined by CM-H_2DCFDA with flow cytometry. Figure represents the % of cells found in the selected region (**a**). Mean ± SD, n=3 (bar-chart). $*P < 0.05$, $**P < 0.01$, $***P < 0.005$ (**b**).

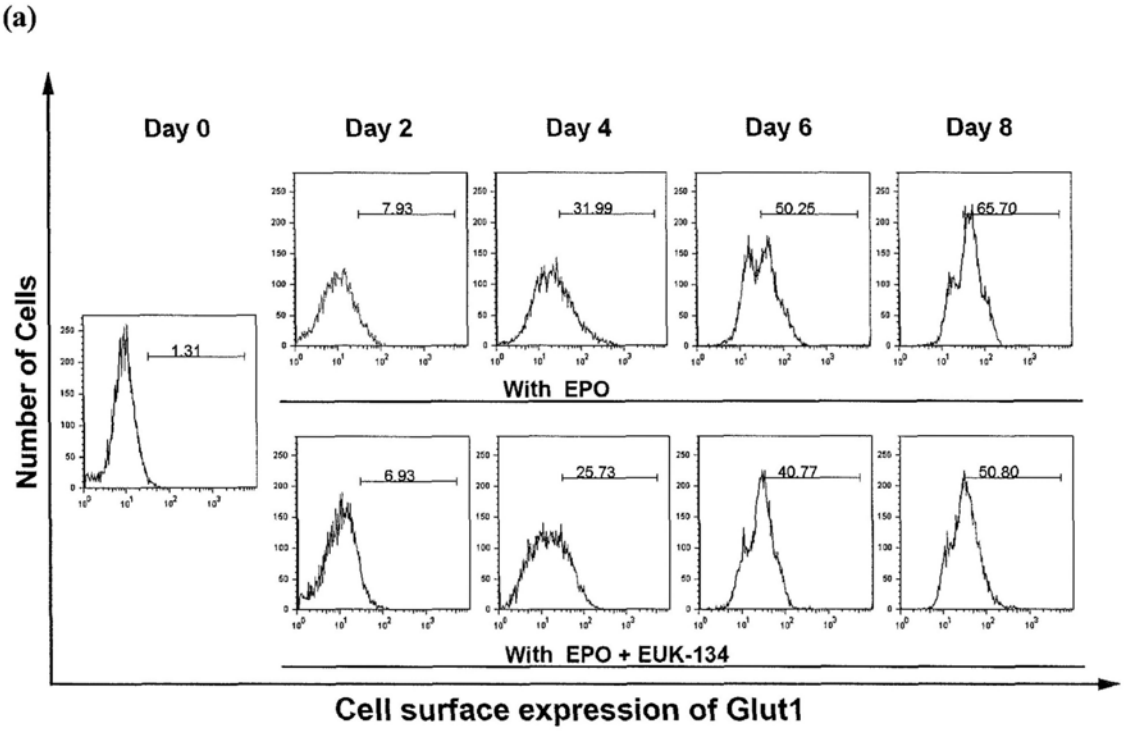

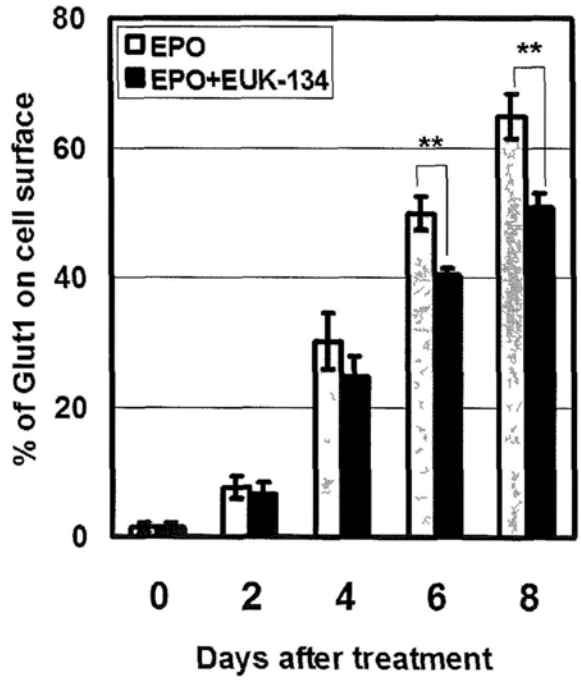

Figure 6.5 Effect of EUK-134 on the cell surface expression of Glut1 during erythropoiesis in TF-1 cells. TF-1 cells (4×10^5/ml) were treated with EPO (10 ng/ml) alone, or EPO (10 ng/ml) with EUK-134 (50 μM) at 37 °C, 5% CO_2 for 0 to 8 days as indicated. Cell surface expression of Glut1 was determined by EGFP-Glut1 ligand with flow cytometry. Figure represents the % of cells found in the selected region (**a**). Mean ± SD, n=3 (bar-chart). $^{**}P < 0.005$ (**b**).

(a)

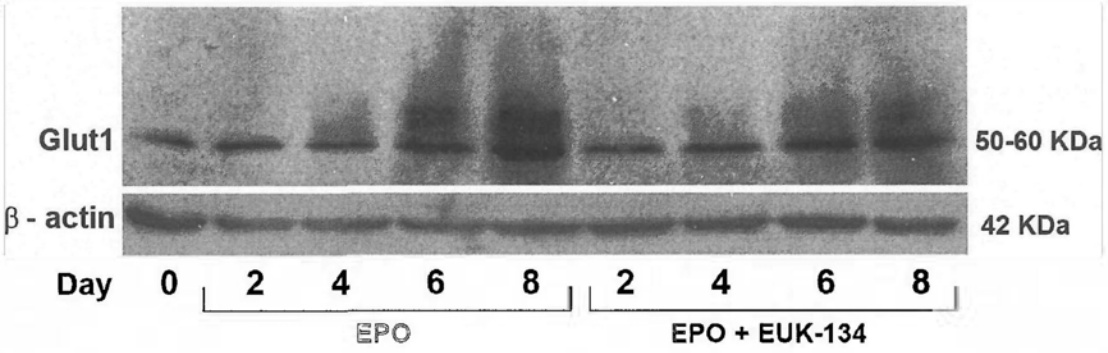

(b)

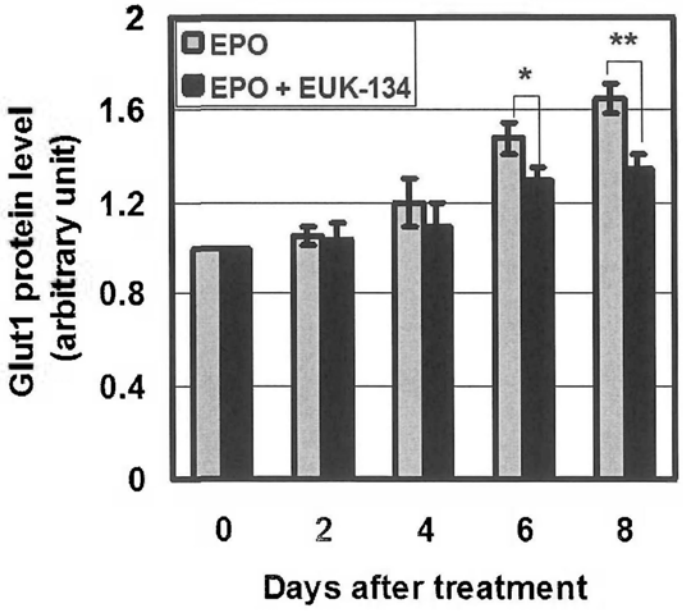

Figure 6.6 Effect of EUK-134 on the expression level of Glut1 in TF-1 cells during erythropoiesis. TF-1 cells (4×10^5/ml) were treated with EPO (10 ng/ml) alone, or EPO (10 ng/ml) with EUK-134 (50 μM) at 37 °C, 5% CO_2 for 0 to 8 days as indicated. After cell lysis, lysates containing equal amount of proteins per lane were subjected to standard SDS-PAGE and Western blot analysis with antibodies for Glut1 and β-actin (as an internal control) (**a**). Mean ± SD, n=3 (bar-chart). $*P < 0.05$, $**P < 0.01$ (**b**).

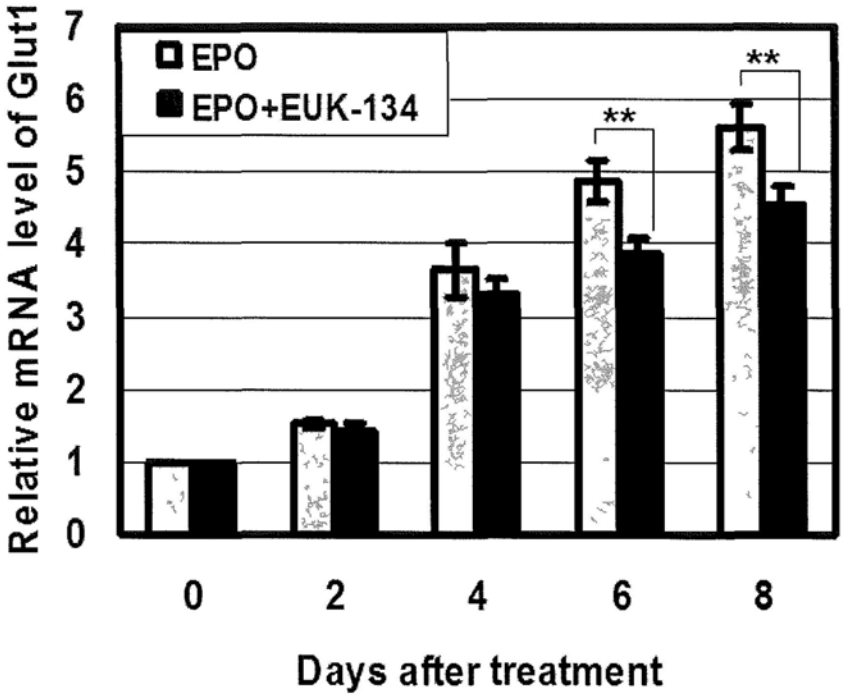

Figure 6.7 Effect of EUK-134 on the mRNA level of Glut1 in TF-1 cells during erythropoiesis. TF-1 cells (4×10^5/ml) were treated with EPO (10 ng/ml) alone, or EPO (10 ng/ml) with EUK-134 (50 μM) at 37 °C, 5% CO_2 for 0 to 8 days as indicated. RNA were extracted on alternative days from 2 x 10^6 TF-1 cells. After 1st strand cDNA synthesis, the cDNA were used as template for real-time PCR using specific primers designed for Glut1 and β-actin as described in Chapter 2. β-actin was used as a house keeping gene for normalization. Mean ± SD, n=3. $^{**}P < 0.01$.

6.5 ROS may regulate Glut1 expression through HIF-1α

It has been revealed that ROS have important roles in the regulation of a variety of biological processes (Veal *et al.*, 2007). For example, ROS can regulate HIF-1 stability and transcriptional activity in cells (Pouyssegur and Mechta-Grigoriou, 2006). Moreover, HIF-1 is considered to be the major regulator of about 100 physiologically important genes (Kietzmann and Gorlach, 2005), and *Glut1*, which encodes glucose transporter 1, is one of these genes that are regulated by HIF-1 (Chen *et al.*, 2001). Therefore, considered together, we were wondering if it is possible that ROS regulate Glut1 through the HIF-1 in erythropoiesis. In order to verify this hypothesis, we examined the expression level of HIF-1α (the regulated subunit of HIF-1) during erythropoiesis. Firstly, the expression of HIF-1α along the course of TF-1 erythroid differentiation was detected by Western blot analysis and results are shown in Figure 6.8. As can be seen, a time-dependent increase in the expression level of HIF-1α was observed in the cells with treated with EPO for 2 to 8 days. Then the expression of HIF-1α under reduced ROS level condition in erythroid cells was examined. It has been shown in Figure 6.4 that the ROS production was significantly reduced under EUK-134 treatment in the TF-1 erythropoiesis, and as expected, the expression level of HIF-1α in the EUK-134 and EPO co-treated group were also remarkably decreased when compared with the EPO control group (Figure 6.9). In addition, the mRNA level of HIF-1α in the EUK-134 and EPO co-treated group was significantly reduced as well (Figure 6.10). These observations suggest that ROS also play a role in the up-regulation of HIF-1α during erythroid differentiation. It is

noteworthy that the trend of changes in HIF-1α expression under reduced ROS production condition was similar to that of Glut1 expression, and as mentioned above, HIF-1α is a known regulator of Glut1, so taken together, it is possible that ROS regulate Glut1 expression through the HIF-1α in erythropoiesis.

(a)

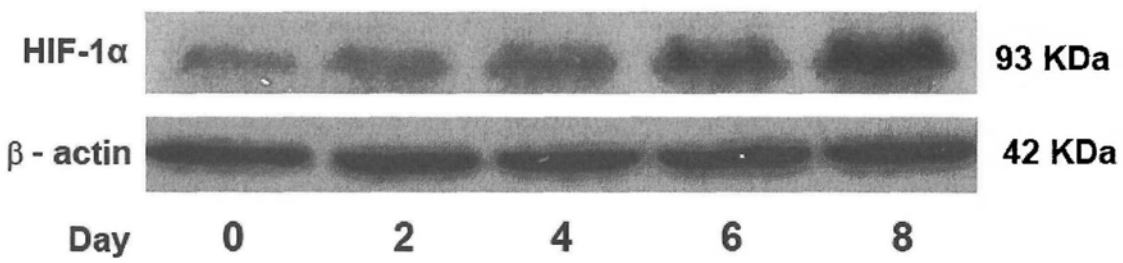

(b)

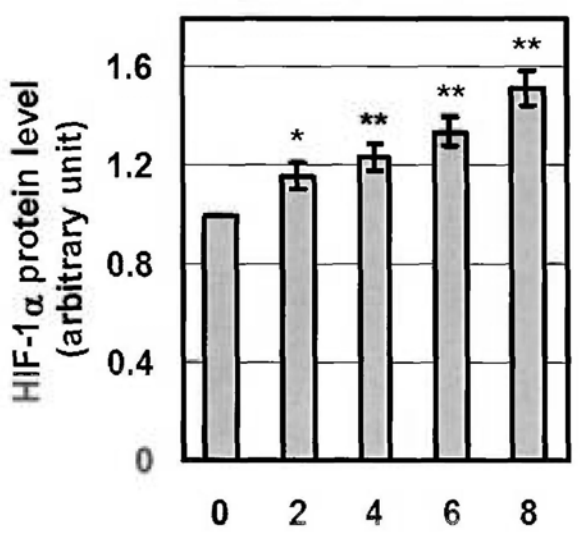

Figure 6.8 Expression of HIF-1α during erythropoiesis in TF-1 cells. TF-1 cells (4×10^5/ml) were cultured with EPO (10 ng/ml) at 37 °C, 5% CO_2 for days as indicated. After cell lysis, lysates containing equal amount of proteins per lane were subjected to standard SDS-PAGE and Western blot analysis with antibodies for HIF-1α and β-actin (as an internal control) (**a**). Results were normalized by corresponding day 0 controls. Mean ± SD, n=3 (bar-chart). *$P < 0.01$, **$P < 0.005$, compared to day 0 control (**b**).

(a)

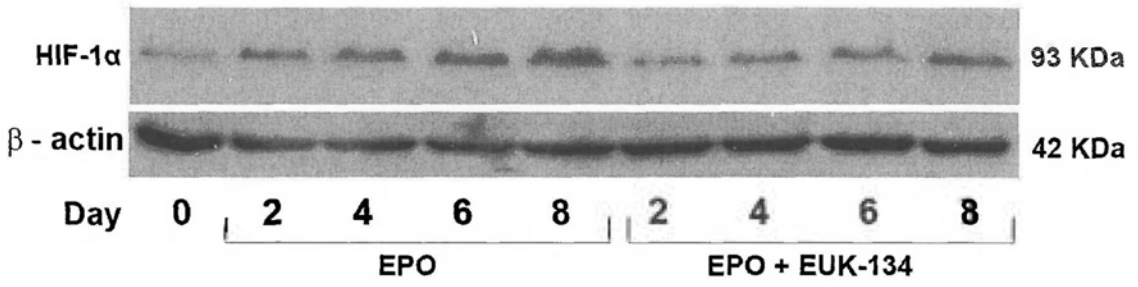

(b)

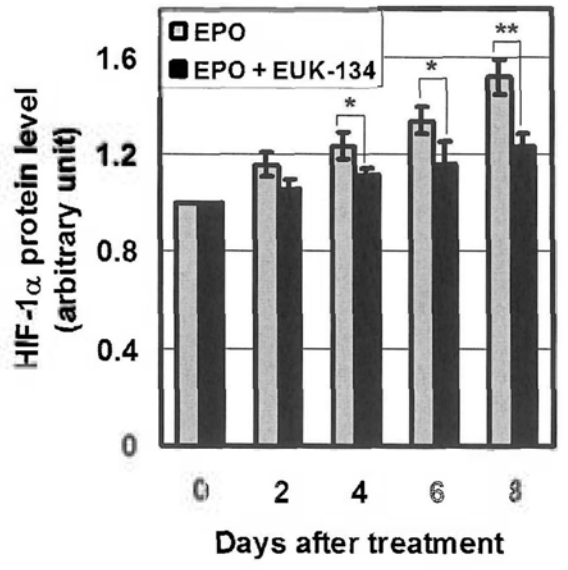

Figure 6.9 Effect of EUK-134 on the expression of HIF-1α proteins during erythropoiesis in TF-1 cells. TF-1 cells (4×10^5/ml) were treated with EPO (10 ng/ml) alone, or EPO (10 ng/ml) with EUK-134 (50 μM) at 37 °C, 5% CO_2 for 0 to 8 days as indicated. After cell lysis, lysates containing equal amount of proteins per lane were subjected to standard SDS-PAGE and Western blot analysis with antibodies for HIF-1α and β-actin (as an internal control) (**a**). Results were normalized by corresponding day 0 controls. Mean ± SD, n=3 (bar-chart). $*P < 0.05$, $**P < 0.005$ (**b**).

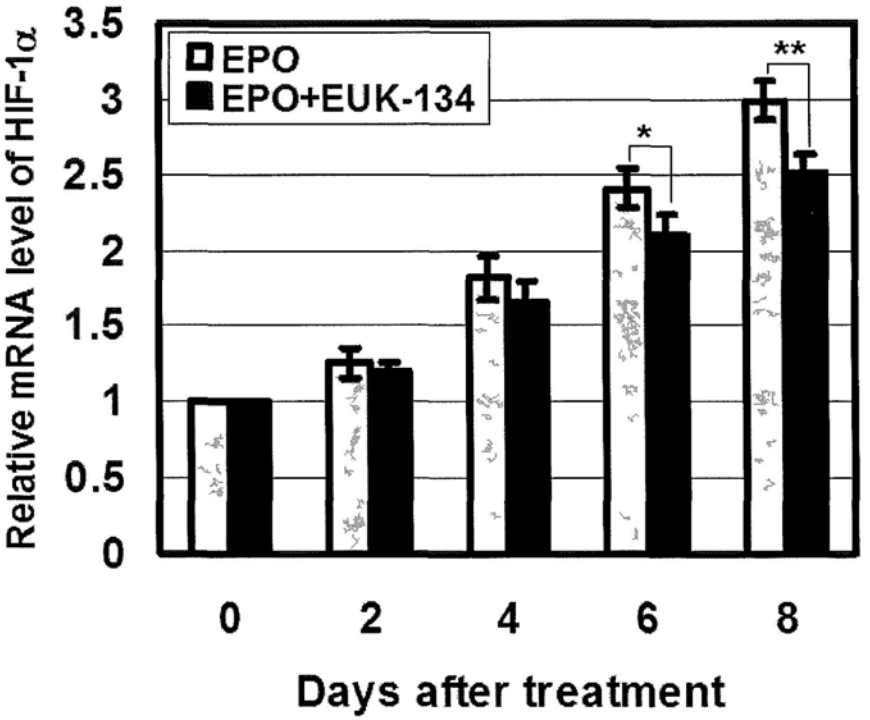

Figure 6.10 Effect of EUK-134 on the mRNA level of HIF-1α during erythropoiesis in TF-1 cells. TF-1 cells (4×10^5/ml) were treated with EPO (10 ng/ml) alone, or EPO (10 ng/ml) with EUK-134 (50 μM) at 37 °C, 5% CO_2 for 0 to 8 days as indicated RNA were extracted on alternative days from 2 x 10^6 TF-1 cells. After 1st strand cDNA synthesis, the cDNA were used as template for Real-Time PCR using specific primers designed for HIF-1α and β-actin as described in Chapter 2. β-actin was used as a house keeping gene for normalization. Mean ± SD, n=3 (bar-chart). *$P < 0.05$, **$P < 0.01$.

6.6 Elevated ROS up-regulated the expression of HIF-1α and Glut1

For further investigation, we raised ROS level by adding exogenous H_2O_2 into TF-1 erythroid cells and then tested whether there were changes in HIF-1α expression in cells. As shown in Figure 6.11a, ROS production was elevated in a dose-dependent manner when the TF-1 erythroid cells were treated with H_2O_2 in a range from 0 to 100 μM for 15 min. Then the transcriptional activity and expression level of HIF-1α was evaluated in these H_2O_2-treated cells. As can be seen in Figure 6.11b & 6.11c, HIF-1α protein expression and mRNA levels were increased in a dose-dependent manner with a peak at 50 μM when the cells were treated with H_2O_2 in a range from 0 to 100 μM for 3 hours. These observations firstly suggest that ROS can regulate HIF-1α expression in erythroid cells; secondly, the upregulation of ROS on HIF-1α seems to be within a certain range, when the ROS was increased to a certain level, the HIF-1α accumulation did not continue increasing but declined instead. Subsequently, the cell surface expression of Glut1 was detected by utilizing EGFP-Glut1 ligand with flow cytometric analysis. As depicted in Figure 6.11d & 6.11e, the cell surface expression and mRNA level of Glut1 were gradually increased when the TF-1 erythroid cells were treated with the H_2O_2 in a range from 0 to 50 μM for 3 hours. However, similar to the trend in HIF-1α, when the H_2O_2 concentration was raised to 100 μM, the protein and mRNA level of Glut1 did not increase continuously. These results indicate that HIF-1α plays a role in the regulation of Glut1 expression during erythroid differentiation. Taken together, these findings further reveal that ROS

induced the HIF-1α expression and functioned as a regulator for the Glut1 expression during erythroid differentiation.

(a1)

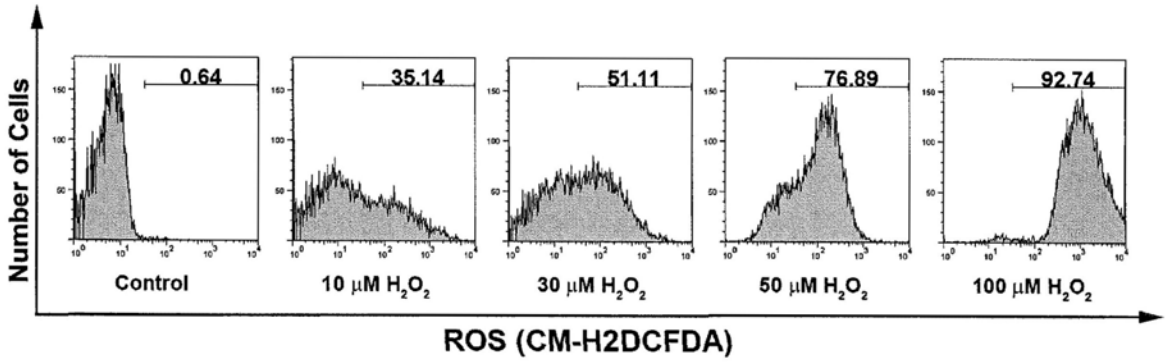

(a2)

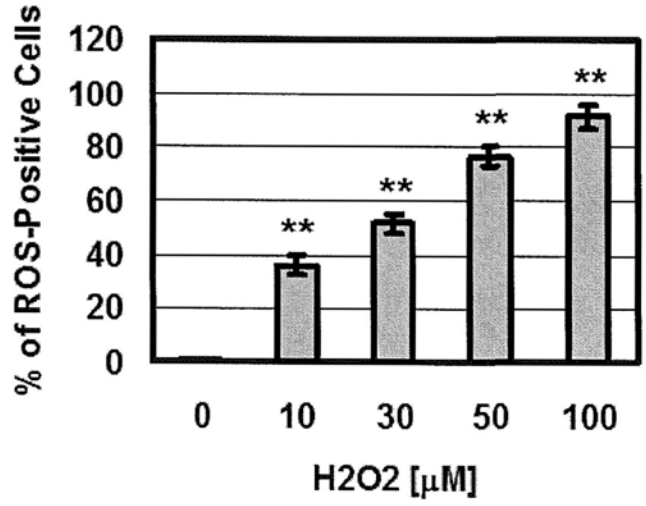

(b1)

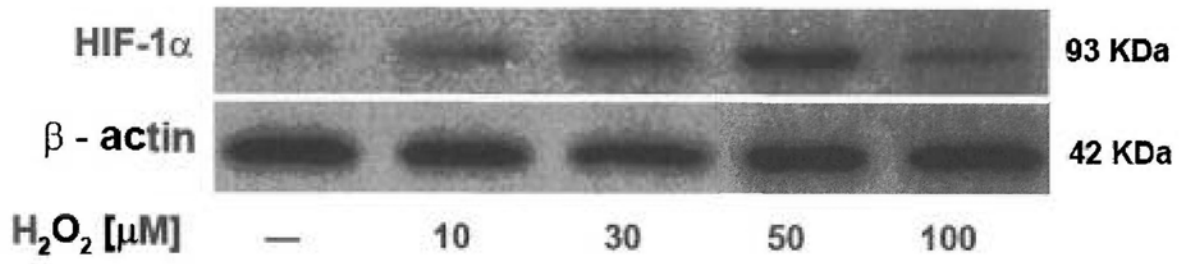
HIF-1α
β - actin
93 KDa
42 KDa
H2O2 [μM]
—
10
30
50
100

(b2)

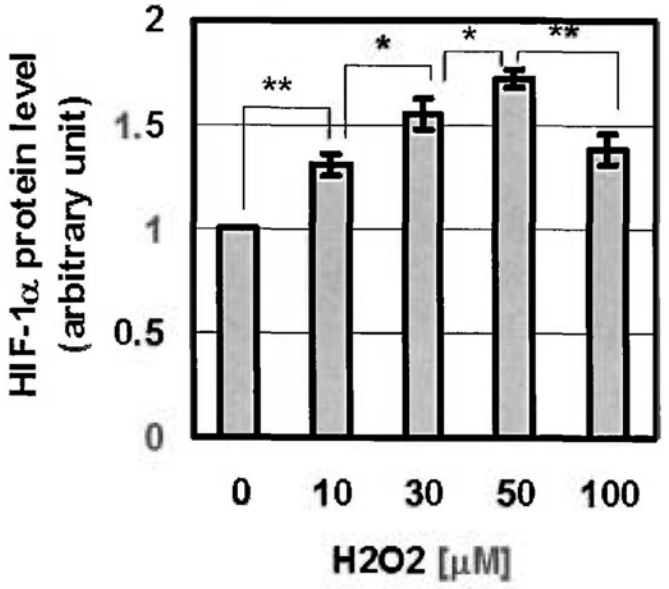
HIF-1α protein level (arbitrary unit)
2
1.5
1
0.5
0
**
*
*
**
0
10
30
50
100
H2O2 [μM]

(c)

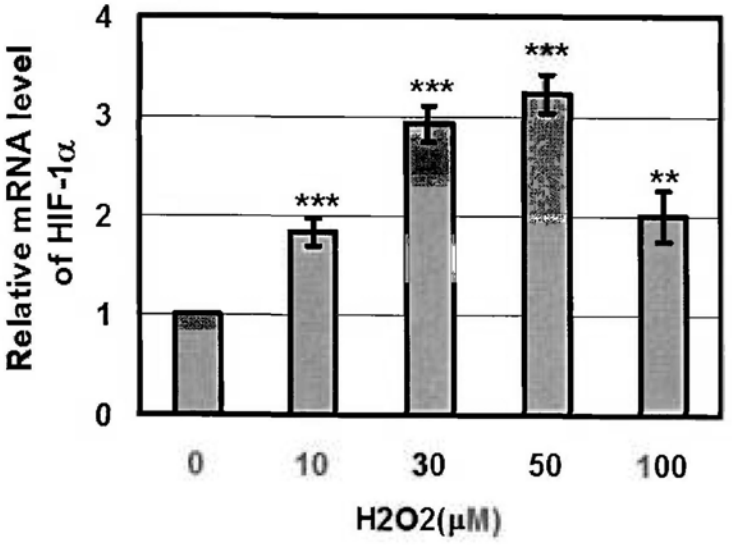
Relative mRNA level of HIF-1α
4
3
2
1
0
***
***
***
**
0
10
30
50
100
H2O2(μM)

(d1)

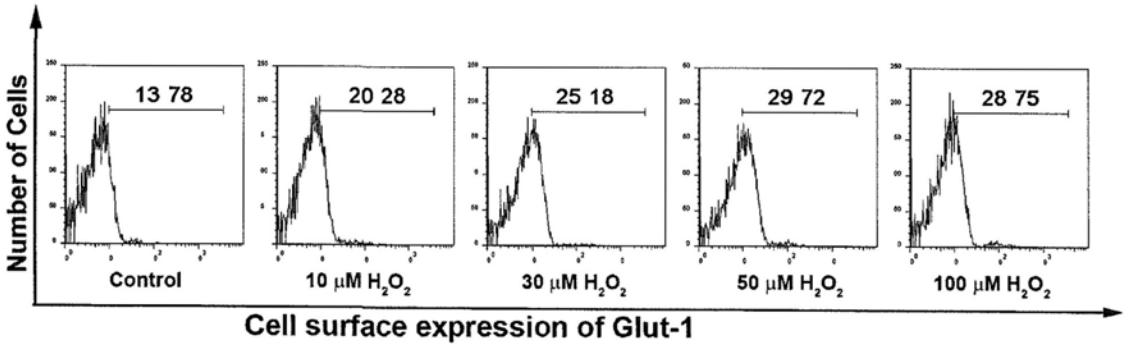
Number of Cells
13 78
20 28
25 18
29 72
28 75
Control
10 μM H2O2
30 μM H2O2
50 μM H2O2
100 μM H2O2
Cell surface expression of Glut-1

(d2)

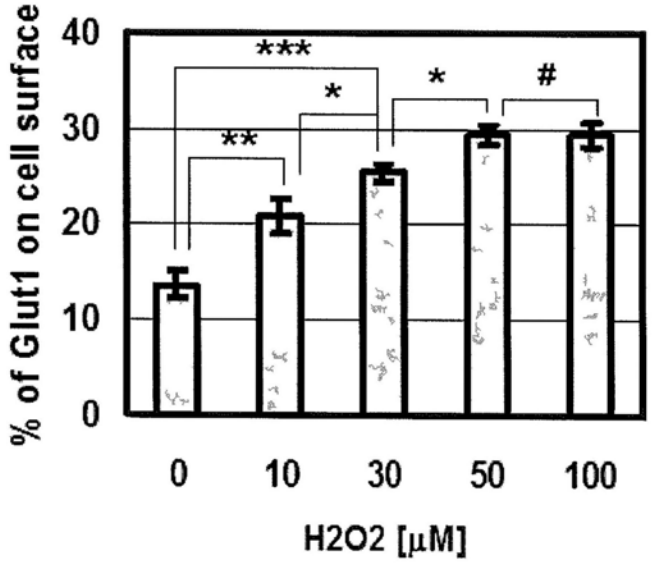
% of Glut1 on cell surface
40
30
20
10
0
***
**
*
*
#
0
10
30
50
100
H2O2 [μM]

(e)

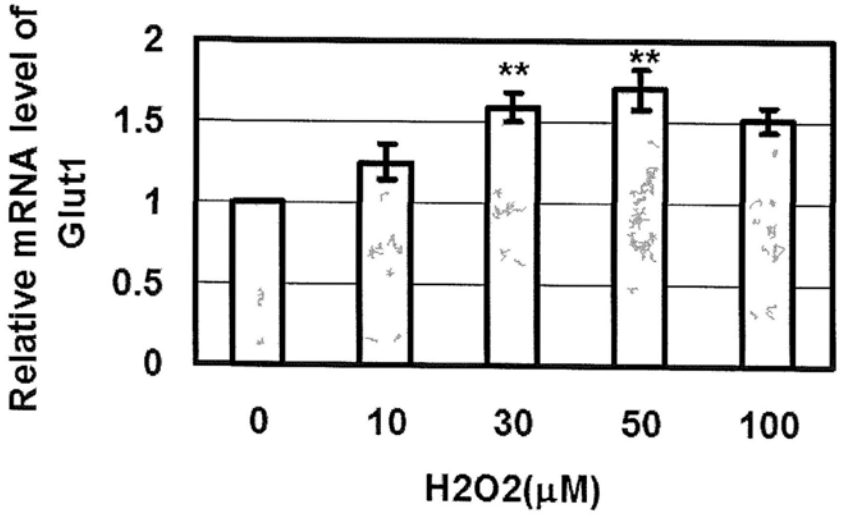
Relative mRNA level of Glut1
2
1.5
1
0.5
0
**
**
0
10
30
50
100
H2O2(μM)

Figure 6.11 Changes of ROS, HIF-1α and Glut1 under H_2O_2 treatment in TF-1 erythroid cells. TF-1 cells (4×10^5/ml) with EPO treatment for one day were challenged with various concentrations of H_2O_2 as indicated. After 15 min, ROS level was determined by CM-H_2DCFDA with flow cytometry (**a1**). Mean ± SD, n=3 (bar-chart). $^{**}P < 0.001$, compared to the group without H_2O_2 treatment (**a2**). After 3 hours, expression levels of HIF-1α protein were determined by Western blot analysis (**b1**). Mean ± SD, n=3 (bar-chart). $^{*}P < 0.05$, $^{**}P < 0.005$ (**b2**). After 3 hours, mRNA levels of HIF-1α were determined by real-time PCR analysis. Mean ± SD, n=3. $^{**}P < 0.005$, $^{***}P < 0.001$, compared to the group without H_2O_2 treatment (**c**). After 3 hours, cell surface expression of Glut1 was determined by EGFP-Glut1 ligand with flow cytometry (**d1**). Mean ± SD, n=3 (bar-chart). $^{*}P < 0.05$, $^{**}P < 0.01$, $^{***}P < 0.001$, $\#P > 0.5$ (**d2**). After 3 hours, mRNA levels of Glut1 were determined by Real-Time PCR analysis. Mean ± SD, n=3. $^{**}P < 0.005$, compared to the group without H_2O_2 treatment (**e**).

6.7 Inhibition of HIF-1α suppressed the up-regulation of Glut1

To further verify the regulation role of HIF-1α on Glut1 in erythropoiesis, we utilized PX-478, a HIF-1α inhibitor (Koh *et al.*, 2008; Palayoor *et al.*, 2008), to treat TF-1 erythroid cells. As shown in Figure 6.12a, the HIF-1α expression level was decreased in a time-dependent manner in the day 5 EPO-treated TF-1 erythroid cells when treated with PX-478 (20 μM) for 0-24 hours. On the contrary, the HIF-1α expression in the PX-478 untreated day 5 EPO cells was gradually increased in the next 24 hours (Figure 6.12a). Similar observations were also found in the mRNA levels of HIF-1α (Figure 6.12b), suggesting that PX-478 functioned well as a HIF-1α inhibitor in TF-1 erythroid cells. Then Glut1 expression of the cells under identical PX-478 treatment was examined and as expected, the Glut1 up-regulation was remarkably suppressed in the cells treated with PX-478 for 24 hours when compared with the corresponding control (Figure 6.12c). Also, the mRNA level of Glut1 was decreased in the PX-478 treated cells as well (Figure 6.12d). These observations indicate that HIF-1α plays an important role in the up-regulation of Glut1 during erythroid differentiation.

(a1)

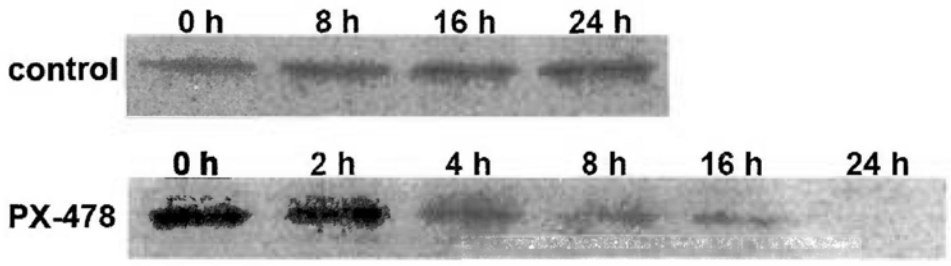

blot: anti HIF-1α

(a2)

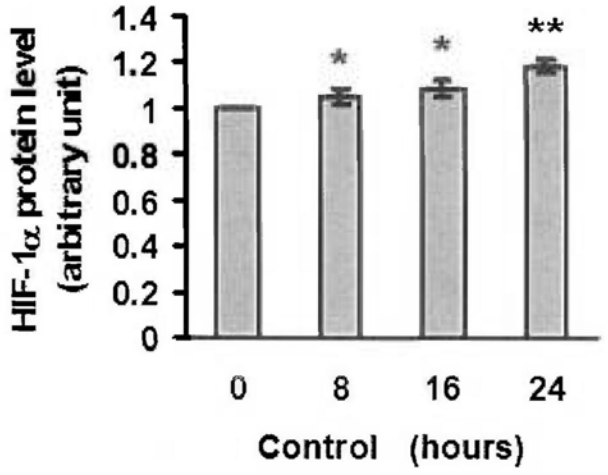

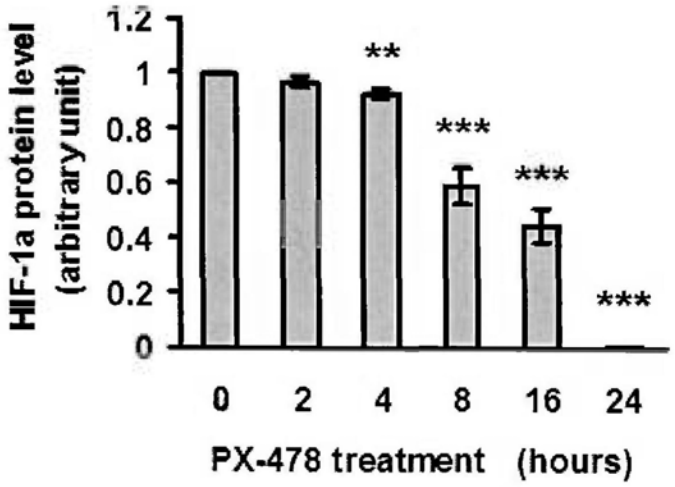

(b)

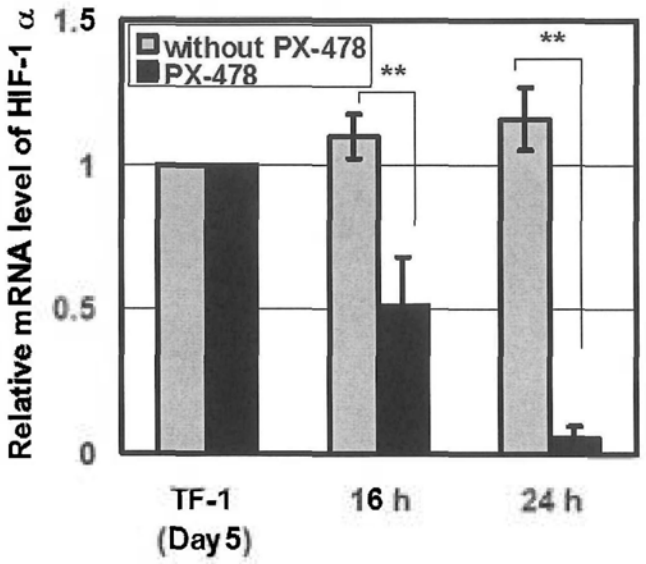
Relative mRNA level of HIF-1 α
1.5
1
0.5
0
without PX-478
PX-478
**
**
TF-1
(Day 5)
16 h
24 h

(c1)

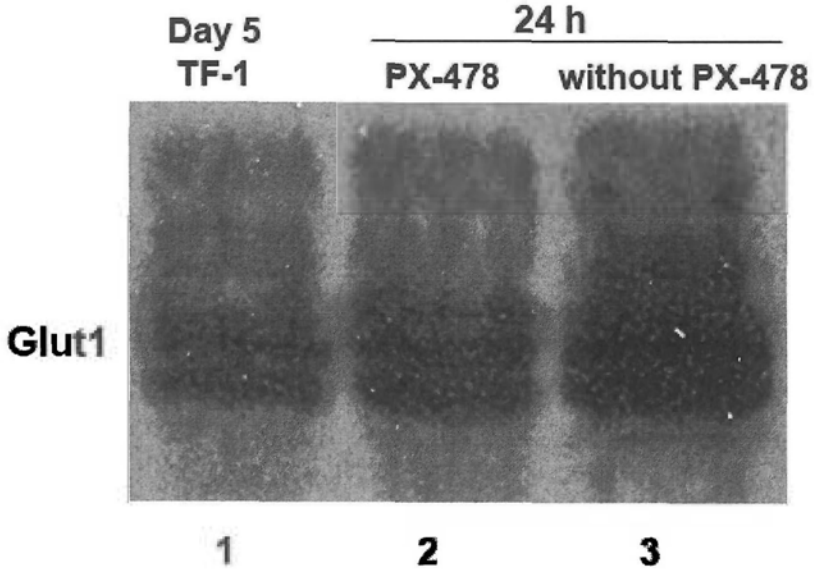
Day 5
TF-1
24 h
PX-478
without PX-478
Glut1
1
2
3

(c2)

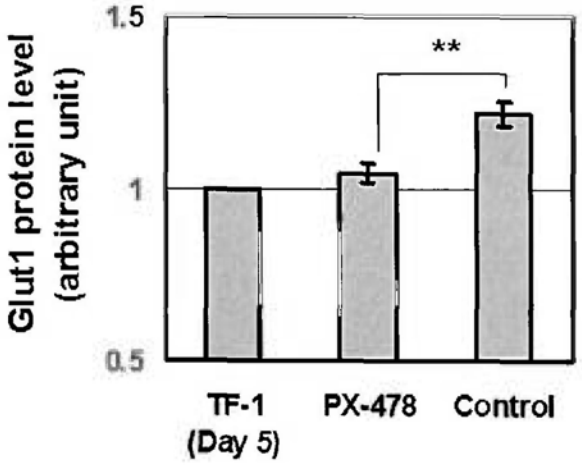
Glut1 protein level
(arbitrary unit)
1.5
1
0.5
**
TF-1
(Day 5)
PX-478
Control

(d)

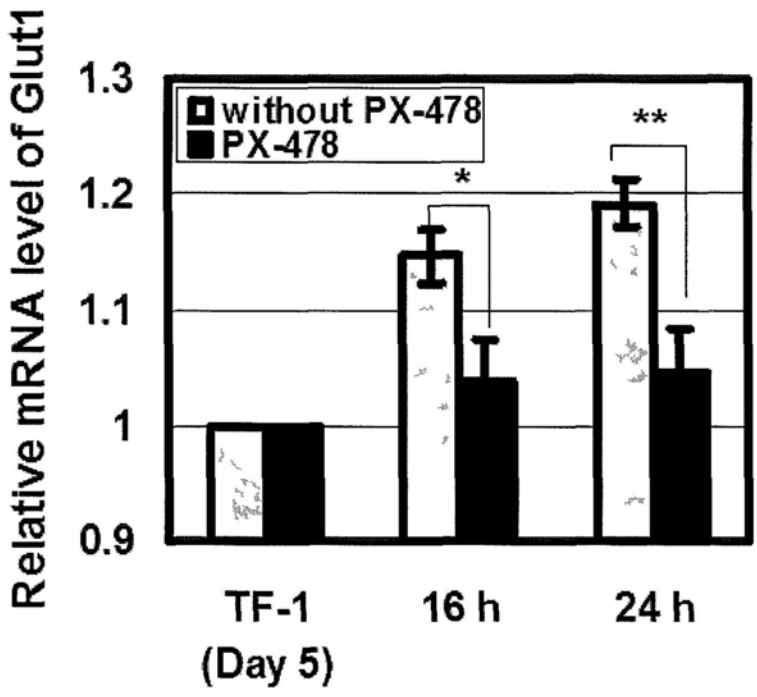

Figure 6.12 Changes of HIF-1α and Glut1 under PX-478 treatment in TF-1 erythroid cells. TF-1 cells (4×10^5/ml) with EPO treatment for 5 days were treated with PX-478 (20 μM) for different hours as indicated, and untreated TF-1 cells were served as control. Expression levels of HIF-1α protein were determined by Western blot analysis after different hours as indicated (**a1**). Results were normalized by corresponding HIF-1α protein level at 0 hour (bar-chart) (**a2**). HIF-1α mRNA levels were determined by Real-Time PCR analysis after different hours as indicated. Results were normalized by corresponding Day 5 TF-1 cells (bar-chart) (**b**). Expression levels of Glut1 protein were determined by Western blot analysis after 24 hours (**c1**). Results were normalized by corresponding Day 5 TF-1 cells (bar-chart) (**c2**). Glut1 mRNA levels were determined by Real-Time PCR analysis after different hours as indicated. Results were normalized by corresponding Day 5 TF-1 cells (bar-chart). Mean ± SD, n=3. $*P < 0.05$, $**P < 0.005$, $***P < 0.001$ (**d**).

6.8 Discussion

Although HIF-1 has initially been described as a transcription factor regulated by hypoxia, there is now increasing evidence that HIF-1 is also responsive to a variety of non-hypoxic stimuli (Duyndam *et al.*, 2001; Gao *et al.*, 2002; Hirota *et al.*, 2004; Kietzmann and Gorlach, 2005; Kietzmann *et al.*, 2003; Richard *et al.*, 2000; Treins *et al.*, 2002). Besides, several lines of emerging evidence indicate that intracellular ROS level was elevated upon exposure to hypoxia (Chandel *et al.*, 1998; Guzy *et al.*, 2005; Mansfield *et al.*, 2005). Furthermore, it is reported that mitochondrial ROS generation is required for hypoxic stabilization of HIF-1α protein (Klimova and Chandel, 2008). In the past decade, the role of ROS in the regulation of HIF-1 in well-oxygenated cells has been hotly reported. For example, increased levels of HIF-1α protein under normoxia have been detected in H_2O_2-treated aortic smooth muscle cells (Gorlach *et al.*, 2001) and Hep3B cells (Guzy *et al.*, 2005; Mansfield *et al.*, 2005). Here in our study, HIF-1α protein expression and mRNA level were increased in TF-1 cells after the exposure to exogenous H_2O_2, in a dose-dependent manner in low H_2O_2 dosage (10-50 μM), but subsided at high concentration (100 μM) (Figure 11b & 11c). These results suggest that only small change in the redox state is required to induce the HIF-1α activation. Therefore, H_2O_2 within a certain level is sufficient to activate HIF-1α expression in TF-1 erythroid cells. Similar results were also found in other types of cells such as Hep3B cells (Guzy *et al.*, 2005; Mansfield *et al.*, 2005) and human vascular smooth muscle cells (VSMCs) (Gorlach *et al.*, 2001).

Further, antioxidant-treatments were demonstrated to diminish the HIF-1α protein accumulation in VSMCs (Gorlach *et al.*, 2001), macrophages (Shatrov *et al.*, 2003), osteoblasts (Kim *et al.*, 2002), HepG2 cells (Tacchini *et al.*, 2001) and human ovary, cancer cells (Duyndam *et al.*, 2001).

ROS are produced and serve as important mediators in a variety of physiological processes, such as differentiation (Ghaffari, 2008; Veal *et al.*, 2007). It is reported that HIF-1α can be induced by differentiation of monocytes to macrophages (Frede *et al.*, 2006; Oda *et al.*, 2006; Westra *et al.*, 2010). Our previous work has revealed that ROS was produced with a peak at day 4 during the TF-1 erythroid differentiation (Qian *et al.*, 2011), which is also shown in Figure 6.3. Here we show that during the TF-1 differentiation the HIF-1α expression and transcriptional activity were elevated as well (Figure 6.8, 6.10). Moreover, this elevation was attenuated by the treatment with antioxidant EUK-134 (a catalase mimetic and can scavenge H_2O_2 (Rong *et al.*, 1999)) (Figure 6.9, 6.10). Our results are consistent with the findings from other groups that over-expression or exogenous addition of catalase prevented HIF-1α accumulation in cells (BelAiba *et al.*, 2004; Pouyssegur and Mechta-Grigoriou, 2006; Richard *et al.*, 2000). Taken together, our findings suggest that the ROS produced during erythropoiesis induced HIF-1α activation.

The underlying mechanism by which ROS increased HIF-1α expression under normoxia has been complicated. HIF-1α protein is regulated by PHD (prolyl hydroxylase domain) enzymes (Bruick and McKnight, 2001; Epstein *et al.*, 2001; Ivan *et al.*, 2002). In the presences of three necessary cofactors, which are O_2, 2-oxoglutarate (2-OG) and Fe(II), the PHD enzymes catalyze hydroxylation of HIF-1α and thus lead to its degradation. In the absence of O_2, PHD enzymes lose their activity and therefore HIF-1α proteins are no longer degraded and accumulated in cells (Pouyssegur and Mechta-Grigoriou, 2006). This is one of the mechanisms by which HIF-1α is accumulated under hypoxia or anoxia. In 2004, Gerald *et al.* reported that enhanced H_2O_2 levels promote the oxidation of Fe(II) to Fe(III), and thus decrease the activity of PHD enzymes and lead to the stabilization of HIF-1α. Further, Fe(II) supplementation reduces the steady-state HIF-1α levels in junD-/- fibroblasts suffering from chronic oxidative stress. This is one possible mechanism by which ROS increased the HIF-1α expression. However, ROS not just promoted the accumulation of HIF-1α proteins, but also increased mRNA level of HIF-1α (Bonello *et al.*, 2007), which is shown in our study as well (Figure 6.11). Besides, for the differentiation-induced HIF-1α accumulation, mRNA levels were also increased, as shown in Figure 6.10 of our study and several other groups such as Westra *et al.* (2010) and Oda *et al.* (2006). The mechanisms by which HIF-1α transcriptional activity is regulated are not clearly identified. It has been reported that the regulation of ROS on HIF-1α involves PHDs, ERK pathway, p38 pathway and PKB pathway

(Kietzmann and Gorlach, 2005). Hence, much further works are needed to be done before we understand the exact mechanisms.

Glut1 is a downstream target of HIF-1α (Chen *et al.*, 2001), and it is activated during TF-1 erythropoiesis (Figure 6.1). Inhibition of HIF-1α resulted in decreased Glut1 mRNA level and diminished Glut1 protein synthesis (Figure 6.12). The upregulation of Glut1 is important for the erythroid differentiation (Figure 6.2) and inhibition of Glut1 partially blocked the TF-1 erythropoiesis without affecting cell viability (Ge, 2009). Glut1 is responsible for transporting glucose into erythroid cells to provide energy requirements. Further, it has been reported that Glut1 is able to translocate vitamin C precursor into cells as well (Montel-Hagen *et al.*, 2008). Therefore, apart from the energy point of view, Glut1 may also enhance the vitamin C uptake thereby playing a role in the anti-oxidation in erythroid cells. This hypothesis may be verified by performing glucose uptake assay and vitamin C assay during erythropoiesis.

Moreover, antioxidant treatment attenuated the up-regulation of Glut1 during TF-1 erythroid differentiation (Figure 6.5, 6.6, 6.7), suggesting a role of ROS on the regulation of Glut1. Glut1 is a hypoxia-regulated and stress-inducible protein, and Glut1 mRNA and protein expression were increased by hypoxia (Behrooz and Ismail-Beigi, 1997; Ebert *et al.*, 1995; Ouiddir *et al.*, 1999). In Figure 5.12 of Chapter 5, the Glut1 expression was unexpectedly unchanged although the number of differentiated cells was decreased in G6PD-knockdown erythropoiesis. Taking the

role of ROS into consideration, it is possible that the elevated ROS level in G6PD-knockdown cells stimulated the Glut1 expression, and this speculation could be proved by sorting out differentiated cells in G6PD-knockdown erythropoiesis and normal erythropoiesis and then probing their expression levels of Glut1.

In conclusion, this study provides evidence that the ROS generated during erythroid differentiation can regulate Glut1 expression through modulating HIF-1α expression in the erythropoiesis in TF-1 cells.

Chapter 7

General Discussion

RBCs are one of the most essential cell types of the body. They are constantly traveling through the body delivering oxygen and scavenging waste. RBC disorders are associated with a variety of other diseases, and the interplay of them would aggravate each other. For example, the RBC enzymatic defect G6PD deficiency is reported to play a role in both hypertension and diabetes (Gaskin et al., 2001). Conversely, diabetes could impair G6PD function and the decreased G6PD activity is associated with diabetic nephropathy and the malfunction of vascular endothelial cells (Carette *et al.*, 2011; Xu *et al.*, 2005). Moreover, the RBCs of diabetes patients usually cannot function well because of the abnormal glucose metabolism. In many diabetic complications such as diabetic retinopathy (DR) and diabetic nephropathy (DN), the expression levels of Glut1 are found seriously abnormal, which are down-regulated in DR and up-regulated in DN (Badr *et al.*, 2000; Fernandes *et al.*, 2004; Mogyorosi and Ziyadeh, 1999). Collectively, these reports indicate that G6PD deficiency, abnormal Glut1 level and diabetic complications are connected, and the possible reason that connects them is the oxidative stress in RBCs (Gaskin *et al.*, 2001; Xu *et al.*, 2005). Nevertheless, the mechanism underlying their relationships remains unclear. Our findings reveal that firstly G6PD is not only responsible for producing the reductant NADPH, but also plays a role in the regulation of other antioxidant enzymes such as GPx1 and Trx1 in erythropoiesis; secondly, Glut1 is regulated by ROS through HIF-1α during RBC development, both of which are shown in Figure 7.1 & 7.2.

As indicated in Figure 7.1, G6PD is the key enzyme of the pentose phosphate pathway that provides reducing agent NADPH for reduction in mature human RBCs. NADPH enables cells to scavenge peroxide via the GPx and Trx/Prx systems. From the G6PD-knockdown TF-1 cells, we found that apart from the decrease in NADPH and the increase in ROS level during erythropoiesis, the antioxidant enzymes GPx1 and Trx1 are notably down-regulated. These observations suggest that G6PD plays a role in regulating these two enzymes to control the NADPH and ROS level. Besides, SDS is able to protect G6PD-knockdown erythroblasts from the H_2O_2-induced cell death.

The effect of ROS on the expression of Glut1 through HIF-1α during RBC development is shown in Figure 7.2. Mechanistically, HIF-1α together with HIF-1β subunit promotes the gene expression of Glut1 and other genes such as EPO, VEGF, TGF-β. The fate of HIF-1α subunit is regulated by the hydroxylation of HIF-1α through the PHD enzyme in the presence of Fe^{2+}, 2-OG and O_2. Hydroxylated HIF-1α is then recognized by VHL for degradation. ROS convert Fe^{2+} to Fe^{3+} and thus lead to the inactivation of PHD enzyme allowing for stabilization of HIF-1α, and therefore activate a variety of HIF-1 target genes including Glut1. In TF-1 cells, we verified such a ROS →HIF-1α →Glut1 pathway during erythropoiesis.

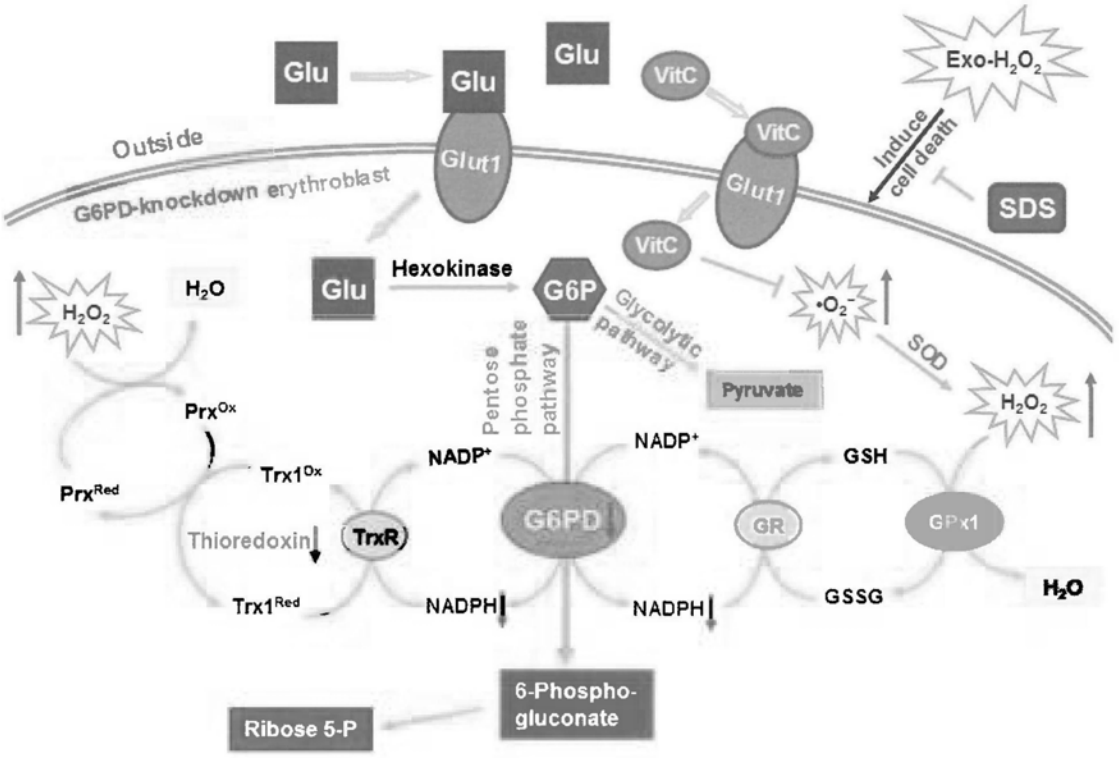

Figure 7.1 The role of G6PD during erythropoiesis in TF-1 cells.
G6PD is the key enzyme of the pentose phosphate pathway that provides NADPH for reduction. NADPH enables cells to scavenge peroxide via the GPx and Trx/Prx systems. In G6PD-knockdown TF-1 cells, we found that apart from the decrease in NADPH and the increase in ROS level during erythropoiesis, the antioxidant enzymes GPx1 and Trx1 are notably down-regulated, indicating G6PD plays a role in regulating these two enzymes. Besides, SDS is able to protect G6PD-knockdown erythroblasts from the H_2O_2-induced cell death.

Abbreviations: Glu, glucose; Glut1, glucose transporter type 1; G6P, Glucose 6-phosphate; G6PD, Glucose 6-phosphate dehydrogenase; GPx1, glutathione peroxidase; GSH, glutathione; GR, glutathione reductase; GSSG, oxidised glutathione; Trx1, thioredoxin-1; TrxR, thioredoxin reductase; Prx, peroxiredoxin; SOD, superoxide dismutase; $^{\cdot}O_2^-$, superoxide anion; H_2O_2, hydrogen peroxide; $NADP^+$, nicotinamide adenine dinucleotide phosphate; NADPH, reduced nicotinamide adenine dinucleotide phosphate; Ribose 5-P, ribose 5-phosphate; VitC, vitamin C; SDS, salidroside; Exo-H_2O_2, exogenous hydrogen peroxide; ROS, reactive oxygen species. " ↑ " indicates increase; " ↓ " indicates decrease.

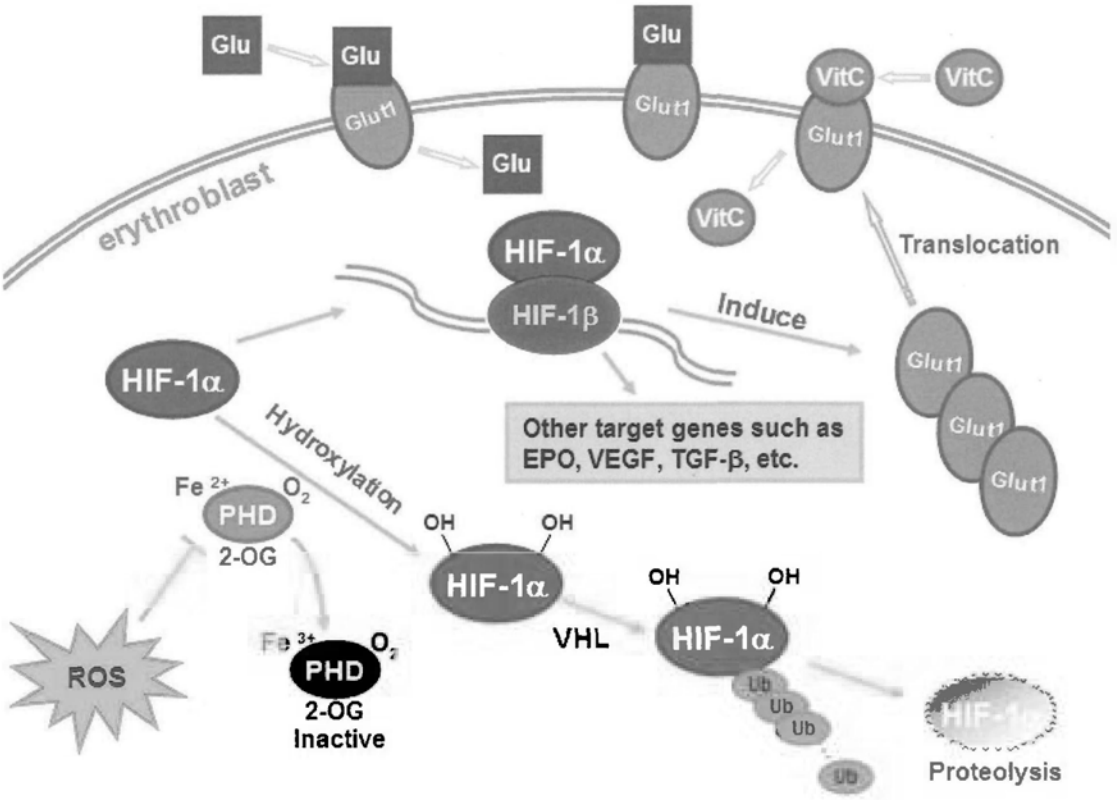

Figure 7.2 ROS regulate Glut1 through HIF-1α during erythropoiesis in TF-1 cells.

Mechanistically, HIF-1α subunit is hydroxylated by PHD enzyme in the presence of Fe^{2+}, 2-OG and O_2, and thereby recognized by VHL for degradation. ROS convert Fe^{2+} to Fe^{3+} and thus lead to the inactivation of PHD enzyme allowing for stabilization of HIF-1α, and therefore activate a variety of HIF-1 target genes including Glut1. In TF-1 cells, we verified such a ROS →HIF-1α →Glut1 pathway during erythropoiesis.

Abbreviations: ROS, reactive oxygen species; HIF-1α, hypoxia-inducible factor-1 α; 2-OG, 2-oxoglutarate; PHD, prolyl hydroxylase domain enzyme; VHL, von Hippel Lindau; HIF-1β, hypoxia-inducible factor-1 β; Glu, glucose; Glut1, glucose transporter type 1; VitC, vitamin C; EPO, erythropoietin; TGF–β, transforming growth factor beta; VEGF, vascular endothelial growth factor.

Since G6PD deficiency, abnormal Glut1 level and diabetic complications are all correlated, our findings may benefit the further investigations in RBC disorders and diabetic complications. The HIF pathway is a potential therapeutic target and recent clinical trials attempt to pharmacologically inhibit HIF degradation in order to increase EPO synthesis in patients (Fandrey, 2008). Given the importance of Glut1 in a lot of diseases such as diabetic complications and Glut1 deficiency syndrome (Gordon and Newton, 2003; Zintzaras and Stefanidis, 2005), the method for modulating Glut1 expression is worth exploring. The finding of the ROS →HIF-1α →Glut1 pathway during erythropoiesis provides a consideration for searching potential therapeutic way for regulating Glut level to prevent or treat these diseases.

Besides, we found that the traditional medicine SDS is able to promote erythroid differentiation in the EPO-treated TF-1 cells, and at the same time up-regulate antioxidant enzymes thus protecting erythroblasts against oxidative stress. Moreover, SDS can also rescue mature human RBCs from hydrogen peroxide-induced cell death through the anti-oxidative effect and suppression of $[Ca^{2+}]_i$ rise and caspase-3 activation (Figure 7.3). Taken together, these effects of SDS suggest that this medicine can be used to help the patients preventing anemia after cancer chemotherapy and treating mountain malhypoxia. Furthermore, SDS is able to exert protective effect against oxidative stress-induced cell death during erythropoiesis in G6PD-knockdown TF-1 cells (Figure 7.1). This finding indicates that SDS can be a consideration for helping G6PD-deficient patients.

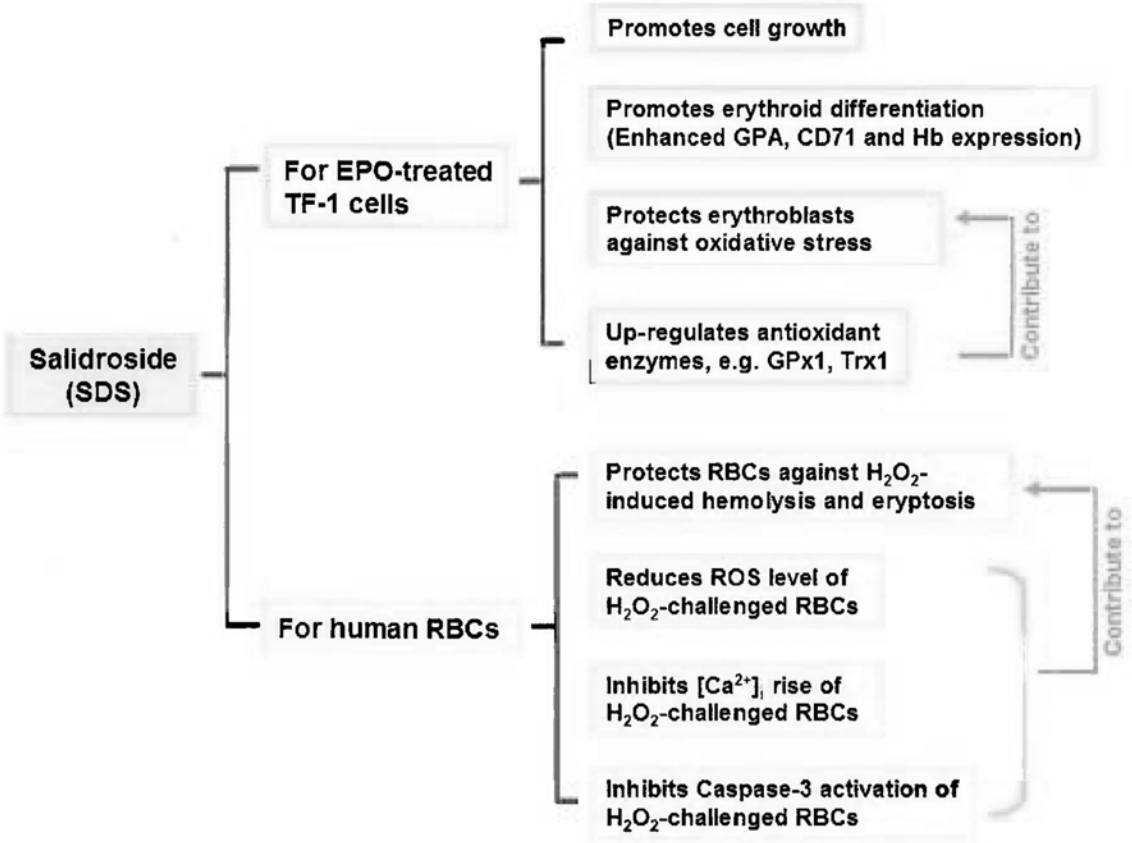

Figure 7.3 Effect of SDS on erythropoiesis and erythrocytes.
Abbreviations: SDS, salidroside; EPO, erythropoietin; GPA, glycophorin A; CD71, transferrin receptor; ROS, reactive oxygen species; RBCs, red blood cells/erythrocytes; Hb, hemoglobin; GPx1, glutathione peroxidase; Trx1, thioredoxin-1; H_2O_2, hydrogen peroxide.

In conclusion, the findings of this study may contribute to treating RBC disorders such as anemia, G6PD-deficient disease, and diabetic complications.

References

Aispuru, G.R., Aguirre, M.V., Aquino-Esperanza, J.A., Lettieri, C.N., Juaristi, J.A. and Brandan, N.C., 2008. Erythroid expansion and survival in response to acute anemia stress: the role of EPO receptor, GATA-1, Bcl-xL and caspase-3. Cell Biology International 32, 966-978.

Akel, S., Bertolette, D., Petrow-Sadowski, C. and Ruscetti, F.W., 2007. Levels of Smad7 regulate Smad and mitogen activated kinases (MAPKs) signaling and controls erythroid and megakaryocytic differentiation of erythroleukemia cells. Platelets 18, 566-578.

Ambros, V., 2004. The functions of animal microRNAs. Nature 431, 350-355.

Bacon, N.C., Wappner, P., O'Rourke, J.F., Bartlett, S.M., Shilo, B., Pugh, C.W. and Ratcliffe, P.J., 1998. Regulation of the Drosophila bHLH-PAS protein Sima by hypoxia: functional evidence for homology with mammalian HIF-1 alpha. Biochemical and Biophysical Research Communications 249, 811-816.

Badr, G.A., Tang, J., Ismail-Beigi, F. and Kern, T.S., 2000. Diabetes downregulates GLUT1 expression in the retina and its microvessels but not in the cerebral cortex or its microvessels. Diabetes 49, 1016-1021.

Bartel, D.P., 2004. MicroRNAs: genomics, biogenesis, mechanism, and function. Cell 116, 281-297.

Barvitenko, N.N., Adragna, N.C. and Weber, R.E., 2005. Erythrocyte signal transduction pathways, their oxygenation dependence and functional significance. Cellular Physiology and Biochemistry 15, 1-18.

Battistelli, M., De Sanctis, R., De Bellis, R., Cucchiarini, L., Dacha, M. and Gobbi, P., 2005. Rhodiola rosea as antioxidant in red blood cells: ultrastructural and hemolytic behaviour. European Journal of Histochemistry 49, 243-254.

Berg, C.P., Engels, I.H., Rothbart, A., Lauber, K., Renz, A., Schlosser, S.F., Schulze-Osthoff, K. and Wesselborg, S., 2001. Human mature red blood cells express caspase-3 and caspase-8, but are devoid of mitochondrial regulators of apoptosis. Cell Death and Differentiation 8, 1197-1206.

Behrooz, A. and Ismail-Beigi, F., 1997. Dual control of glut1 glucose transporter gene expression by hypoxia and by inhibition of oxidative phosphorylation. Journal of Biological Chemistry 272, 5555-5562.

BelAiba, R.S., Djordjevic, T., Bonello, S., Flugel, D., Hess, J., Kietzmann, T. and Gorlach, A., 2004. Redox-sensitive regulation of the HIF pathway under non-hypoxic conditions in pulmonary artery smooth muscle cells. Biological Chemistry 385, 249-257.

Bieber, E., 2001. Erythropoietin, the biology of erythropoiesis and epoetin alfa. An overview. Journal of Reproductive Medicine 46, 521-530.

Bonello, S., Zahringer, C., BelAiba, R.S., Djordjevic, T., Hess, J., Michiels, C., Kietzmann, T. and Gorlach, A., 2007. Reactive oxygen species activate the HIF-1alpha promoter via a functional NFkappaB site. Arteriosclerosis, Thrombosis, and Vascular Biology 27, 755-761.

Bratosin, D., Estaquier, J., Petit, F., Arnoult, D., Quatannens, B., Tissier, J.P., Slomianny, C., Sartiaux, C., Alonso, C., Huart, J.J., Montreuil, J. and Ameisen, J.C., 2001. Programmed cell death in mature erythrocytes: a model for investigating death effector pathways operating in the absence of mitochondria. Cell Death and Differentiation 8, 1143-1156.

Bratosin, D., Mitrofan, L., Palii, C., Estaquier, J. and Montreuil, J., 2005. Novel fluorescence assay using calcein-AM for the determination of human erythrocyte viability and aging. Cytometry A 66, 78-84.

Bruick, R.K. and McKnight, S.L., 2001. A conserved family of prolyl-4-hydroxylases that modify HIF. Science 294, 1337-1340.

Buck, I., Morceau, F., Cristofanon, S., Heintz, C., Chateauvieux, S., Reuter, S., Dicato, M. and Diederich, M., 2008. Tumor necrosis factor alpha inhibits erythroid differentiation in human erythropoietin-dependent cells involving p38 MAPK pathway, GATA-1 and FOG-1 downregulation and GATA-2 upregulation. Biochemical Pharmacology 76, 1229-1239.

Cai, L., Wang, H., Li, Q., Qian, Y. and Yao, W., 2008. Salidroside inhibits H2O2-induced apoptosis in PC12 cells by preventing cytochrome c release and inactivating of caspase cascade. Acta Biochim Biophys Sin (Shanghai) 40, 796-802.

Cappellini, M.D. and Fiorelli, G., 2008. Glucose-6-phosphate dehydrogenase deficiency. Lancet 371, 64-74.

Carette, C., Dubois-Laforgue, D., Gautier, J.F. and Timsit, J., 2011. Diabetes mellitus and glucose-6-phosphate dehydrogenase deficiency: from one crisis to another. Diabetes and Metabolism 37, 79-82.

Chandel, N.S., Maltepe, E., Goldwasser, E., Mathieu, C.E., Simon, M.C. and Schumacker, P.T., 1998. Mitochondrial reactive oxygen species trigger hypoxia-induced transcription. Proceedings of the National Academy of Sciences of the United States of America 95, 11715-11720.

Chen, C., Pore, N., Behrooz, A., Ismail-Beigi, F. and Maity, A., 2001. Regulation of glut1 mRNA by hypoxia-inducible factor-1. Interaction between H-ras and hypoxia. Journal of Biological Chemistry 276, 9519-9525.

Chenais, B., Andriollo, M., Guiraud, P., Belhoussine, R. and Jeannesson, P., 2000. Oxidative stress involvement in chemically induced differentiation of K562

cells. Free Radical Biology and Medicine 28, 18-27.

Chun, Y.S., Kim, M.S. and Park, J.W., 2002. Oxygen-dependent and -independent regulation of HIF-1alpha. Journal of Korean Medical Science 17, 581-588.

Cimen, M.Y., 2008. Free radical metabolism in human erythrocytes. Clinica Chimica Acta 390, 1-11.

Clarke, R.B., 2005. Isolation and characterization of human mammary stem cells. Cell Proliferation 38, 375-386.

D'Amelio, M., Cavallucci, V. and Cecconi, F., 2010. Neuronal caspase-3 signaling: not only cell death. Cell Death and Differentiation 17, 1104-1114.

Dada, L.A., Chandel, N.S., Ridge, K.M., Pedemonte, C., Bertorello, A.M. and Sznajder, J.I., 2003. Hypoxia-induced endocytosis of Na,K-ATPase in alveolar epithelial cells is mediated by mitochondrial reactive oxygen species and PKC-zeta. Journal of Clinical Investigation 111, 1057-1064.

Darbinyan, V., Aslanyan, G., Amroyan, E., Gabrielyan, E., Malmstrom, C. and Panossian, A., 2007. Clinical trial of Rhodiola rosea L. extract SHR-5 in the treatment of mild to moderate depression. Nord J Psychiatry 61, 343-348.

Darbinyan, V., Kteyan, A., Panossian, A., Gabrielian, E., Wikman, G. and Wagner, H., 2000. Rhodiola rosea in stress induced fatigue--a double blind cross-over study of a standardized extract SHR-5 with a repeated low-dose regimen on the mental performance of healthy physicians during night duty. Phytomedicine 7, 365-371.

Day, B.J., 2009. Catalase and glutathione peroxidase mimics. Biochemical Pharmacology 77, 285-296.

De Sanctis, R., De Bellis, R., Scesa, C., Mancini, U., Cucchiarini, L. and Dacha, M., 2004. In vitro protective effect of Rhodiola rosea extract against hypochlorous acid-induced oxidative damage in human erythrocytes. BioFactors 20, 147-159.

Dennery, P.A., 2007. Effects of oxidative stress on embryonic development. Birth Defects Res C Embryo Today 81, 155-162.

Devaskar, S.U. and Mueckler, M.M., 1992. The mammalian glucose transporters. Pediatric Research 31, 1-13.

Duyndam, M.C., Hulscher, T.M., Fontijn, D., Pinedo, H.M. and Boven, E., 2001. Induction of vascular endothelial growth factor expression and hypoxia-inducible factor 1alpha protein by the oxidative stressor arsenite. Journal of Biological Chemistry 276, 48066-48076.

Ebert, B.L., Firth, J.D. and Ratcliffe, P.J., 1995. Hypoxia and mitochondrial inhibitors regulate expression of glucose transporter-1 via distinct Cis-acting sequences. Journal of Biological Chemistry 270, 29083-29089.

Elyassi, A.R. and Rowshan, H.H., 2009. Perioperative management of the glucose-6-phosphate dehydrogenase deficient patient: a review of literature. Anesthesia Progress 56, 86-91.

Epstein, A.C., Gleadle, J.M., McNeill, L.A., Hewitson, K.S., O'Rourke, J., Mole, D.R., Mukherji, M., Metzen, E., Wilson, M.I., Dhanda, A., Tian, Y.M., Masson, N., Hamilton, D.L., Jaakkola, P., Barstead, R., Hodgkin, J., Maxwell, P.H., Pugh, C.W., Schofield, C.J. and Ratcliffe, P.J., 2001. C. elegans EGL-9 and mammalian homologs define a family of dioxygenases that regulate HIF by prolyl hydroxylation. Cell 107, 43-54.

Fandrey, J., 2008. Erythropoiesis--once more HIF! Blood 112, 931-932.

Fernandes, R., Carvalho, A.L., Kumagai, A., Seica, R., Hosoya, K., Terasaki, T., Murta, J., Pereira, P. and Faro, C., 2004. Downregulation of retinal GLUT1 in diabetes by ubiquitinylation. Molecular Vision 10, 618-628.

Finkel, T. and Holbrook, N.J., 2000. Oxidants, oxidative stress and the biology of ageing. Nature 408, 239-247.

Fiorentini, D., Prata, C., Maraldi, T., Zambonin, L., Bonsi, L., Hakim, G. and Landi, L., 2004. Contribution of reactive oxygen species to the regulation of Glut1 in two hemopoietic cell lines differing in cytokine sensitivity. Free Radical Biology and Medicine 37, 1402-1411.

Föller, M., Huber, S.M. and Lang, F., 2008. Erythrocyte programmed cell death. IUBMB Life 60, 661-668.

Frede, S., Stockmann, C., Freitag, P. and Fandrey, J., 2006. Bacterial lipopolysaccharide induces HIF-1 activation in human monocytes via p44/42 MAPK and NF-kappaB. Biochemical Journal 396, 517-527.

Friedman, J.S., Rebel, V.I., Derby, R., Bell, K., Huang, T.T., Kuypers, F.A., Epstein, C.J. and Burakoff, S.J., 2001. Absence of mitochondrial superoxide dismutase results in a murine hemolytic anemia responsive to therapy with a catalytic antioxidant. Journal of Experimental Medicine 193, 925-934.

Gao, N., Jiang, B.H., Leonard, S.S., Corum, L., Zhang, Z., Roberts, J.R., Antonini, J., Zheng, J.Z., Flynn, D.C., Castranova, V. and Shi, X., 2002. p38 Signaling-mediated hypoxia-inducible factor 1alpha and vascular endothelial growth factor induction by Cr(VI) in DU145 human prostate carcinoma cells. Journal of Biological Chemistry 277, 45041-45048.

Gaskin, R.S., Estwick, D. and Peddi, R., 2001. G6PD deficiency: its role in the high prevalence of hypertension and diabetes mellitus. Ethnicity and Disease 11, 749-754.

Ge, D.T., 2009. The Role of reactive oxygen species during erythropoiesis: an in vitro model using TF-1 cells. MPhil Thesis, CUHK.

Gerald, D., Berra, E., Frapart, Y.M., Chan, D.A., Giaccia, A.J., Mansuy, D., Pouyssegur, J., Yaniv, M. and Mechta-Grigoriou, F., 2004. JunD reduces tumor angiogenesis by protecting cells from oxidative stress. Cell 118, 781-794.

Ghaffari, S., 2008. Oxidative stress in the regulation of normal and neoplastic hematopoiesis. Antioxid Redox Signal 10, 1923-1940.

Gordon, N. and Newton, R.W., 2003. Glucose transporter type1 (GLUT-1) deficiency. Brain and Development 25, 477-480.

Gorlach, A., Diebold, I., Schini-Kerth, V.B., Berchner-Pfannschmidt, U., Roth, U., Brandes, R.P., Kietzmann, T. and Busse, R., 2001. Thrombin activates the hypoxia-inducible factor-1 signaling pathway in vascular smooth muscle cells: Role of the p22(phox)-containing NADPH oxidase. Circulation Research 89, 47-54.

Green, D.R. and Kroemer, G., 2004. The pathophysiology of mitochondrial cell death. Science 305, 626-629.

Guzy, R.D., Hoyos, B., Robin, E., Chen, H., Liu, L., Mansfield, K.D., Simon, M.C., Hammerling, U. and Schumacker, P.T., 2005. Mitochondrial complex III is required for hypoxia-induced ROS production and cellular oxygen sensing. Cell Metab 1, 401-408.

Harman, D., 1956. Aging: a theory based on free radical and radiation chemistry. Journals of Gerontology 11, 298-300.

Helgerson, A.L. and Carruthers, A., 1987. Equilibrium ligand binding to the human erythrocyte sugar transporter. Evidence for two sugar-binding sites per carrier. Journal of Biological Chemistry 262, 5464-5475.

Hirota, K., Fukuda, R., Takabuchi, S., Kizaka-Kondoh, S., Adachi, T., Fukuda, K. and Semenza, G.L., 2004. Induction of hypoxia-inducible factor 1 activity by muscarinic acetylcholine receptor signaling. Journal of Biological Chemistry 279, 41521-41528.

Ho, Y.S., Xiong, Y., Ma, W., Spector, A. and Ho, D.S., 2004. Mice lacking catalase develop normally but show differential sensitivity to oxidant tissue injury. Journal of Biological Chemistry 279, 32804-32812.

Hu, X., Lin, S., Yu, D., Qiu, S., Zhang, X. and Mei, R., 2010. A preliminary study: the anti-proliferation effect of salidroside on different human cancer cell lines. Cell Biology and Toxicology 26, 499-507.

Ingley, E., Tilbrook, P.A. and Klinken, S.P., 2004. New insights into the regulation of erythroid cells. IUBMB Life 56, 177-184.

Ivan, M., Haberberger, T., Gervasi, D.C., Michelson, K.S., Gunzler, V., Kondo, K., Yang, H., Sorokina, I., Conaway, R.C., Conaway, J.W. and Kaelin, W.G., Jr., 2002. Biochemical purification and pharmacological inhibition of a

mammalian prolyl hydroxylase acting on hypoxia-inducible factor. Proceedings of the National Academy of Sciences of the United States of America 99, 13459-13464.

Jaakkola, P., Mole, D.R., Tian, Y.M., Wilson, M.I., Gielbert, J., Gaskell, S.J., Kriegsheim, A., Hebestreit, H.F., Mukherji, M., Schofield, C.J., Maxwell, P.H., Pugh, C.W. and Ratcliffe, P.J., 2001. Targeting of HIF-alpha to the von Hippel-Lindau ubiquitylation complex by O2-regulated prolyl hydroxylation. Science 292, 468-472.

Jacobs-Helber, S.M. and Sawyer, S.T., 2004. Jun N-terminal kinase promotes proliferation of immature erythroid cells and erythropoietin-dependent cell lines. Blood 104, 696-703.

Jain, M., Brenner, D.A., Cui, L., Lim, C.C., Wang, B., Pimentel, D.R., Koh, S., Sawyer, D.B., Leopold, J.A., Handy, D.E., Loscalzo, J., Apstein, C.S. and Liao, R., 2003. Glucose-6-phosphate dehydrogenase modulates cytosolic redox status and contractile phenotype in adult cardiomyocytes. Circulation Research 93, e9-16.

Jeney, V., Balla, J., Yachie, A., Varga, Z., Vercellotti, G.M., Eaton, J.W. and Balla, G., 2002. Pro-oxidant and cytotoxic effects of circulating heme. Blood 100, 879-887.

Johnson, R.M., Goyette, G., Jr., Ravindranath, Y. and Ho, Y.S., 2005. Hemoglobin autoxidation and regulation of endogenous H2O2 levels in erythrocytes. Free Radical Biology and Medicine 39, 1407-1417.

Jiang, H., Guo, R. and Powell-Coffman, J.A., 2001. The Caenorhabditis elegans hif-1 gene encodes a bHLH-PAS protein that is required for adaptation to hypoxia. Proceedings of the National Academy of Sciences of the United States of America 98, 7916-7921.

Kang, S.W., Chae, H.Z., Seo, M.S., Kim, K., Baines, I.C. and Rhee, S.G., 1998. Mammalian peroxiredoxin isoforms can reduce hydrogen peroxide generated in response to growth factors and tumor necrosis factor-alpha. Journal of Biological Chemistry 273, 6297-6302.

Kanupriya, Prasad, D., Sai Ram, M., Kumar, R., Sawhney, R.C., Sharma, S.K., Ilavazhagan, G., Kumar, D. and Banerjee, P.K., 2005. Cytoprotective and antioxidant activity of Rhodiola imbricata against tert-butyl hydroperoxide induced oxidative injury in U-937 human macrophages. Molecular and Cellular Biochemistry 275, 1-6.

Kelly, G.S., 2001. Rhodiola rosea: a possible plant adaptogen. Alternative Medicine Review 6, 293-302..

Kiefer, C.R. and Snyder, L.M., 2000. Oxidation and erythrocyte senescence. Current Opinion in Hematology 7, 113-116.

Kietzmann, T. and Gorlach, A., 2005. Reactive oxygen species in the control of hypoxia-inducible factor-mediated gene expression. Seminars in Cell & Developmental Biology 16, 474-486.

Kietzmann, T., Samoylenko, A., Roth, U. and Jungermann, K., 2003. Hypoxia-inducible factor-1 and hypoxia response elements mediate the induction of plasminogen activator inhibitor-1 gene expression by insulin in primary rat hepatocytes. Blood 101, 907-914.

Kim, F.J., Manel, N., Garrido, E.N., Valle, C., Sitbon, M. and Battini, J.L., 2004. HTLV-1 and -2 envelope SU subdomains and critical determinants in receptor binding. Retrovirology 1, 41.

Kim, H.H., Lee, S.E., Chung, W.J., Choi, Y., Kwack, K., Kim, S.W., Kim, M.S., Park, H. and Lee, Z.H., 2002. Stabilization of hypoxia-inducible factor-1alpha is involved in the hypoxic stimuli-induced expression of vascular endothelial growth factor in osteoblastic cells. Cytokine 17, 14-27.

Kitamura, T., Tange, T., Terasawa, T., Chiba, S., Kuwaki, T., Miyagawa, K., Piao, Y.F., Miyazono, K., Urabe, A. and Takaku, F., 1989. Establishment and characterization of a unique human cell line that proliferates dependently on GM-CSF, IL-3, or erythropoietin. Journal of Cellular Physiology 140, 323-334.

Klimova, T. and Chandel, N.S., 2008. Mitochondrial complex III regulates hypoxic activation of HIF. Cell Death and Differentiation 15, 660-666.

Koh, M.Y., Spivak-Kroizman, T., Venturini, S., Welsh, S., Williams, R.R., Kirkpatrick, D.L. and Powis, G., 2008. Molecular mechanisms for the activity of PX-478, an antitumor inhibitor of the hypoxia-inducible factor-1alpha. Mol Cancer Ther 7, 90-100.

Kong, Y., Zhou, S., Kihm, A.J., Katein, A.M., Yu, X., Gell, D.A., Mackay, J.P., Adachi, K., Foster-Brown, L., Louden, C.S., Gow, A.J. and Weiss, M.J., 2004. Loss of alpha-hemoglobin-stabilizing protein impairs erythropoiesis and exacerbates beta-thalassemia. Journal of Clinical Investigation 114, 1457-1466.

Koury, M.J., Sawyer, S.T. and Brandt, S.J., 2002. New insights into erythropoiesis. Current Opinion in Hematology 9, 93-100.

Lang, F., Gulbins, E., Lerche, H., Huber, S.M., Kempe, D.S. and Foller, M., 2008. Eryptosis, a window to systemic disease. Cellular Physiology and Biochemistry 22, 373-380.

Lang, F., Lang, K.S., Lang, P.A., Huber, S.M. and Wieder, T., 2006. Mechanisms and significance of eryptosis. Antioxid Redox Signal 8, 1183-1192.

Lang, K.S., Duranton, C., Poehlmann, H., Myssina, S., Bauer, C., Lang, F., Wieder, T. and Huber, S.M., 2003. Cation channels trigger apoptotic death of erythrocytes. Cell Death and Differentiation 10, 249-256.

Lang, K.S., Lang, P.A., Bauer, C., Duranton, C., Wieder, T., Huber, S.M. and Lang, F., 2005. Mechanisms of suicidal erythrocyte death. Cellular Physiology and Biochemistry 15, 195-202.

Le, T., Bhushan V., Vasan N., 2010. First Aid for the USMLE Step 1. 20th Anniversary Edition, USA, 124.

Lee, J.M., Chan, K., Kan, Y.W. and Johnson, J.A., 2004. Targeted disruption of Nrf2 causes regenerative immune-mediated hemolytic anemia. Proceedings of the National Academy of Sciences of the United States of America 101, 9751-9756.

Leopold, J.A., Cap, A., Scribner, A.W., Stanton, R.C. and Loscalzo, J., 2001. Glucose-6-phosphate dehydrogenase deficiency promotes endothelial oxidant stress and decreases endothelial nitric oxide bioavailability. FASEB Journal 15, 1771-1773.

Li, T., Xu, G., Wu, L. and Sun, C., 2007. Pharmacological studies on the sedative and hypnotic effect of salidroside from the Chinese medicinal plant Rhodiola sachalinensis. Phytomedicine 14, 601-604.

Lopez, S., Stuhl, L., Fichelson, S., Dubart-Kupperschmitt, A., St Arnaud, R., Galindo, J.R., Murati, A., Berda, N., Dubreuil, P. and Gomez, S., 2005. NACA is a positive regulator of human erythroid-cell differentiation. Journal of Cell Science 118, 1595-1605.

Lui, J.C. and Kong, S.K., 2006. Erythropoietin activates caspase-3 and downregulates CAD during erythroid differentiation in TF-1 cells - a protection mechanism against DNA fragmentation. FEBS Letters 580, 1965-1970.

Lui, J.C. and Kong, S.K., 2007. Heat shock protein 70 inhibits the nuclear import of apoptosis-inducing factor to avoid DNA fragmentation in TF-1 cells during erythropoiesis. FEBS Letters 581, 109-117.

Lui, J.C., Wong, J.W., Suen, Y.K., Kwok, T.T., Fung, K.P. and Kong, S.K., 2007. Cordycepin induced eryptosis in mouse erythrocytes through a Ca2+-dependent pathway without caspase-3 activation. Archives of Toxicology 81, 859-865.

Lundberg, J.O., Gladwin, M.T., Ahluwalia, A., Benjamin, N., Bryan, N.S., Butler, A., Cabrales, P., Fago, A., Feelisch, M., Ford, P.C., Freeman, B.A., Frenneaux, M., Friedman, J., Kelm, M., Kevil, C.G., Kim-Shapiro, D.B., Kozlov, A.V., Lancaster, J.R., Jr., Lefer, D.J., McColl, K., McCurry, K., Patel, R.P., Petersson, J., Rassaf, T., Reutov, V.P., Richter-Addo, G.B., Schechter, A., Shiva, S., Tsuchiya, K., van Faassen, E.E., Webb, A.J., Zuckerbraun, B.S., Zweier, J.L. and Weitzberg, E., 2009. Nitrate and nitrite in biology, nutrition and therapeutics. Nat Chem Biol 5, 865-869.

Ma, C., Tang, J., Wang, H., Tao, G., Gu, X. and Hu, L., 2009. Preparative purification

of salidroside from Rhodiola rosea by two-step adsorption chromatography on resins. Journal of Separation Science 32, 185-191.

Manel, N., Battini, J.L. and Sitbon, M., 2005a. Human T cell leukemia virus envelope binding and virus entry are mediated by distinct domains of the glucose transporter GLUT1. Journal of Biological Chemistry 280, 29025-29029.

Manel, N., Battini, J.L., Taylor, N. and Sitbon, M., 2005b. HTLV-1 tropism and envelope receptor. Oncogene 24, 6016-6025.

Manel, N., Kim, F.J., Kinet, S., Taylor, N., Sitbon, M. and Battini, J.L., 2003a. The ubiquitous glucose transporter GLUT-1 is a receptor for HTLV. Cell 115, 449-459.

Manel, N., Kinet, S., Battini, J.L., Kim, F.J., Taylor, N. and Sitbon, M., 2003b. The HTLV receptor is an early T-cell activation marker whose expression requires de novo protein synthesis. Blood 101, 1913-1918.

Manganelli, G., Fico, A., Martini, G. and Filosa, S., Discussion on pharmacogenetic interaction in G6PD deficiency and methods to identify potential hemolytic drugs. Cardiovasc Hematol Disord Drug Targets 10, 143-150.

Mansfield, K.D., Guzy, R.D., Pan, Y., Young, R.M., Cash, T.P., Schumacker, P.T. and Simon, M.C., 2005. Mitochondrial dysfunction resulting from loss of cytochrome c impairs cellular oxygen sensing and hypoxic HIF-alpha activation. Cell Metab 1, 393-399.

Maraldi, T., Fiorentini, D., Prata, C., Landi, L. and Hakim, G., 2004. Stem cell factor and H2O2 induce GLUT1 translocation in M07e cells. BioFactors 20, 97-108.

Mason, P.J., 1996. New insights into G6PD deficiency. British Journal of Haematology 94, 585-591.

Matarrese, P., Straface, E., Pietraforte, D., Gambardella, L., Vona, R., Maccaglia, A., Minetti, M. and Malorni, W., 2005. Peroxynitrite induces senescence and apoptosis of red blood cells through the activation of aspartyl and cysteinyl proteases. FASEB Journal 19, 416-418.

Mogyorosi, A. and Ziyadeh, F.N., 1999. GLUT1 and TGF-beta: the link between hyperglycaemia and diabetic nephropathy. Nephrology, Dialysis, Transplantation 14, 2827-2829.

Montel-Hagen, A., Kinet, S., Manel, N., Mongellaz, C., Prohaska, R., Battini, J.L., Delaunay, J., Sitbon, M. and Taylor, N., 2008. Erythrocyte Glut1 triggers dehydroascorbic acid uptake in mammals unable to synthesize vitamin C. Cell 132, 1039-1048.

Mueckler, M., 1994. Facilitative glucose transporters. European Journal of Biochemistry 219, 713-725.

Mueckler, M., Caruso, C., Baldwin, S.A., Panico, M., Blench, I., Morris, H.R., Allard,

W.J., Lienhard, G.E. and Lodish, H.F., 1985. Sequence and structure of a human glucose transporter. Science 229, 941-945.

Nagao, M., Ebert, B.L., Ratcliffe, P.J. and Pugh, C.W., 1996. Drosophila melanogaster SL2 cells contain a hypoxically inducible DNA binding complex which recognises mammalian HIF-binding sites. FEBS Letters 387, 161-166.

Nagy, K., Pasti, G., Bene, L. and Nagy, I., 1995. Involvement of Fenton reaction products in differentiation induction of K562 human leukemia cells. Leukemia Research 19, 203-212.

Nakahata, T. and Okumura, N., 1994. Cell surface antigen expression in human erythroid progenitors: erythroid and megakaryocytic markers. Leukemia and Lymphoma 13, 401-409.

Neumann, C.A., Krause, D.S., Carman, C.V., Das, S., Dubey, D.P., Abraham, J.L., Bronson, R.T., Fujiwara, Y., Orkin, S.H. and Van Etten, R.A., 2003. Essential role for the peroxiredoxin Prdx1 in erythrocyte antioxidant defence and tumour suppression. Nature 424, 561-565.

Ninfali, P., Cuppini, C., Rapa, S., Baronciani, L. and Cuppini, R., 1991. Glucose-6-phosphate dehydrogenase activity in dorsal root ganglia of vitamin E-deficient rats. Annals of Nutrition and Metabolism 35, 174-180.

Oda, T., Hirota, K., Nishi, K., Takabuchi, S., Oda, S., Yamada, H., Arai, T., Fukuda, K., Kita, T., Adachi, T., Semenza, G.L. and Nohara, R., 2006. Activation of hypoxia-inducible factor 1 during macrophage differentiation. American Journal of Physiology Cell Physiology 291, C104-113.

Ouiddir, A., Planes, C., Fernandes, I., VanHesse, A. and Clerici, C., 1999. Hypoxia upregulates activity and expression of the glucose transporter GLUT1 in alveolar epithelial cells. American Journal of Respiratory Cell and Molecular Biology 21, 710-718.

Owusu-Ansah, E. and Banerjee, U., 2009. Reactive oxygen species prime Drosophila haematopoietic progenitors for differentiation. Nature 461, 537-541.

Ozmen, I., Kufrevioglu, O.I. and Gul, M., 2005. Effects of some antibiotics on activity of glucose-6-phosphate dehydrogenase from human erythrocytes in vitro and effect of isepamicin sulfate on activities of antioxidant enzymes in rat erythrocytes. Drug and Chemical Toxicology 28, 433-445.

Paglialunga, F., Fico, A., Iaccarino, I., Notaro, R., Luzzatto, L., Martini, G. and Filosa, S., 2004. G6PD is indispensable for erythropoiesis after the embryonic-adult hemoglobin switch. Blood 104, 3148-3152.

Palayoor, S.T., Mitchell, J.B., Cerna, D., Degraff, W., John-Aryankalayil, M. and Coleman, C.N., 2008. PX-478, an inhibitor of hypoxia-inducible factor-1alpha, enhances radiosensitivity of prostate carcinoma cells. International Journal of Cancer 123, 2430-2437.

Palis J. and Segel G.B., 1998. Developmental biology of erythropoiesis. Blood Rev 12 (2), 106-14.

Pamela C. Champe, Lippincott's Illustrated Reviews: Biochemistry, 3rd edition, 149-151

Pandolfi, P.P., Sonati, F., Rivi, R., Mason, P., Grosveld, F. and Luzzatto, L., 1995. Targeted disruption of the housekeeping gene encoding glucose 6-phosphate dehydrogenase (G6PD): G6PD is dispensable for pentose synthesis but essential for defense against oxidative stress. EMBO Journal 14, 5209-5215.

Panossian, A. and Wikman, G., 2009. Evidence-based efficacy of adaptogens in fatigue, and molecular mechanisms related to their stress-protective activity. Curr Clin Pharmacol 4, 198-219.

Panossian, A., Wikman, G. and Sarris, J., 2010. Rosenroot (Rhodiola rosea): traditional use, chemical composition, pharmacology and clinical efficacy. Phytomedicine 17, 481-493.

Perfumi, M. and Mattioli, L., 2007. Adaptogenic and central nervous system effects of single doses of 3% rosavin and 1% salidroside Rhodiola rosea L. extract in mice. Phytotherapy Research 21, 37-43.

Pouyssegur, J. and Mechta-Grigoriou, F., 2006. Redox regulation of the hypoxia-inducible factor. Biological Chemistry 387, 1337-1346.

Prata, C., Maraldi, T., Zambonin, L., Fiorentini, D., Hakim, G. and Landi, L., 2004. ROS production and Glut1 activity in two human megakaryocytic cell lines. BioFactors 20, 223-233.

Qian, E.W., Ge, D.T. and Kong, S.K., 2011. Salidroside promotes erythropoiesis and protects erythroblasts against oxidative stress by up-regulating glutathione peroxidase and thioredoxin. Journal of Ethnopharmacology 133, 308-314.

Ribeil, J.A., Zermati, Y., Vandekerckhove, J., Dussiot, M., Kersual, J. and Hermine, O., 2005. [Erythropoiesis: a paradigm for the role of caspases in cell death and differentiation]. J Soc Biol 199, 219-231.

Ribeil, J.A., Zermati, Y., Vandekerckhove, J., Cathelin, S., Kersual, J., Dussiot, M., Coulon, S., Moura, I.C., Zeuner, A., Kirkegaard-Sorensen, T., Varet, B., Solary, E., Garrido, C. and Hermine, O., 2007. Hsp70 regulates erythropoiesis by preventing caspase-3-mediated cleavage of GATA-1. Nature 445, 102-105.

Richard, D.E., Berra, E. and Pouyssegur, J., 2000. Nonhypoxic pathway mediates the induction of hypoxia-inducible factor 1alpha in vascular smooth muscle cells. Journal of Biological Chemistry 275, 26765-26771.

Rong, Y., Doctrow, S.R., Tocco, G., Baudry, M., 1999. EUK-134, a synthetic superoxide dismutase and catalase mimetic, prevents oxidative stress and attenuates kainate-induced neuropathology. Proc Natl Acad Sci U S A 96,

9897-9902.

Savourey, G., Launay, J.C., Besnard, Y., Guinet, A., Bourrilhon, C., Cabane, D., Martin, S., Caravel, J.P., Pequignot, J.M. and Cottet-Emard, J.M., 2004. Control of erythropoiesis after high altitude acclimatization. European Journal of Applied Physiology and Occupational Physiology 93, 47-56.

Sauer, H., Wartenberg, M. and Hescheler, J., 2001. Reactive oxygen species as intracellular messengers during cell growth and differentiation. Cellular Physiology and Biochemistry 11, 173-186.

Scheepers, A., Joost, H.G. and Schurmann, A., 2004. The glucose transporter families SGLT and GLUT: molecular basis of normal and aberrant function. JPEN. Journal of Parenteral and Enteral Nutrition 28, 364-371.

Schofield, C.J. and Ratcliffe, P.J., 2004. Oxygen sensing by HIF hydroxylases. Nat Rev Mol Cell Biol 5, 343-354.

Schofield, C.J. and Zhang, Z., 1999. Structural and mechanistic studies on 2-oxoglutarate-dependent oxygenases and related enzymes. Current Opinion in Structural Biology 9, 722-731.

Schriner, S.E., Abrahamyan, A., Avanessian, A., Bussel, I., Maler, S., Gazarian, M., Holmbeck, M.A. and Jafari, M., 2009. Decreased mitochondrial superoxide levels and enhanced protection against paraquat in Drosophila melanogaster supplemented with Rhodiola rosea. Free Radical Research 43, 836-843.

Schweers, R.L., Zhang, J., Randall, M.S., Loyd, M.R., Li, W., Dorsey, F.C., Kundu, M., Opferman, J.T., Cleveland, J.L., Miller, J.L. and Ney, P.A., 2007. NIX is required for programmed mitochondrial clearance during reticulocyte maturation. Proceedings of the National Academy of Sciences of the United States of America 104, 19500-19505.

Seidner, G., Alvarez, M.G., Yeh, J.I., O'Driscoll, K.R., Klepper, J., Stump, T.S., Wang, D., Spinner, N.B., Birnbaum, M.J. and De Vivo, D.C., 1998. GLUT-1 deficiency syndrome caused by haploinsufficiency of the blood-brain barrier hexose carrier. Nature Genetics 18, 188-191.

Semenza, G.L. and Wang, G.L., 1992. A nuclear factor induced by hypoxia via de novo protein synthesis binds to the human erythropoietin gene enhancer at a site required for transcriptional activation. Molecular and Cellular Biology 12, 5447-5454.

Shatrov, V.A., Sumbayev, V.V., Zhou, J. and Brune, B., 2003. Oxidized low-density lipoprotein (oxLDL) triggers hypoxia-inducible factor-1alpha (HIF-1alpha) accumulation via redox-dependent mechanisms. Blood 101, 4847-4849.

Sherwood, L., Klandorf, H. and Yancey, P., 2005. Animal Physiology, Brooks/Cole, Cengage Learning.

Shevtsov, V.A., Zholus, B.I., Shervarly, V.I., Vol'skij, V.B., Korovin, Y.P., Khristich, M.P., Roslyakova, N.A. and Wikman, G., 2003. A randomized trial of two different doses of a SHR-5 Rhodiola rosea extract versus placebo and control of capacity for mental work. Phytomedicine 10, 95-105.

Skopinska-Rozewska, E., Malinowski, M., Wasiutynski, A., Sommer, E., Furmanowa, M., Mazurkiewicz, M. and Siwicki, A.K., 2008. The influence of Rhodiola quadrifida 50% hydro-alcoholic extract and salidroside on tumor-induced angiogenesis in mice. Polish Journal of Veterinary Sciences 11, 97-104.

Smith, T.G., Robbins, P.A. and Ratcliffe, P.J., 2008. The human side of hypoxia-inducible factor. British Journal of Haematology 141, 325-334.

Socolovsky, M., 2007. Molecular insights into stress erythropoiesis. Current Opinion in Hematology 14, 215-224.

Sopjani, M., Föller, M., Haendeler, J., Gotz, F. and Lang, F., 2009. Silver ion-induced suicidal erythrocyte death. Journal of Applied Toxicology 29, 531-536.

Spasov, A.A., Wikman, G.K., Mandrikov, V.B., Mironova, I.A. and Neumoin, V.V., 2000. A double-blind, placebo-controlled pilot study of the stimulating and adaptogenic effect of Rhodiola rosea SHR-5 extract on the fatigue of students caused by stress during an examination period with a repeated low-dose regimen. Phytomedicine 7, 85-89.

Stetler-Stevenson, M. and Braylan, R.C., 2001. Flow cytometric analysis of lymphomas and lymphoproliferative disorders. Seminars in Hematology 38, 111-123.

Sundaresan, M., Yu, Z.X., Ferrans, V.J., Irani, K. and Finkel, T., 1995. Requirement for generation of H2O2 for platelet-derived growth factor signal transduction. Science 270, 296-299.

Swainson, L., Kinet, S., Manel, N., Battini, J.L., Sitbon, M. and Taylor, N., 2005. Glucose transporter 1 expression identifies a population of cycling CD4+ CD8+ human thymocytes with high CXCR4-induced chemotaxis. Proceedings of the National Academy of Sciences of the United States of America 102, 12867-12872.

Tacchini, L., Dansi, P., Matteucci, E. and Desiderio, M.A., 2001. Hepatocyte growth factor signalling stimulates hypoxia inducible factor-1 (HIF-1) activity in HepG2 hepatoma cells. Carcinogenesis 22, 1363-1371.

Tho, L.L., Lee, W.H. and Candlish, J.K., 1988. Erythrocytic enzymes decomposing reactive oxygen species and glucose 6-phosphate dehydrogenase deficiency. Singapore Medical Journal 29, 60-62.

Treins, C., Giorgetti-Peraldi, S., Murdaca, J., Semenza, G.L. and Van Obberghen, E., 2002. Insulin stimulates hypoxia-inducible factor 1 through a phosphatidylinositol 3-kinase/target of rapamycin-dependent signaling

pathway. Journal of Biological Chemistry 277, 27975-27981.

Uchida, M., Watanabe, T., Kunitama, M., Mori, M., Kikuchi, S., Yoshida, K., Kirito, K., Nagai, T., Ozawa, K. and Komatsu, N., 2004. Erythropoietin overcomes imatinib-induced apoptosis and induces erythroid differentiation in TF-1/bcr-abl cells. Stem Cells 22, 609-616.

Veal, E.A., Day, A.M. and Morgan, B.A., 2007. Hydrogen peroxide sensing and signaling. Molecular Cell 26, 1-14.

Vermes, I., Haanen, C., Steffens-Nakken, H. and Reutelingsperger, C., 1995. A novel assay for apoptosis. Flow cytometric detection of phosphatidylserine expression on early apoptotic cells using fluorescein labelled Annexin V. Journal of Immunological Methods 184, 39-51.

Wang, G.L., Jiang, B.H., Rue, E.A. and Semenza, G.L., 1995. Hypoxia-inducible factor 1 is a basic-helix-loop-helix-PAS heterodimer regulated by cellular O2 tension. Proceedings of the National Academy of Sciences of the United States of America 92, 5510-5514.

Wang, H., Ding, Y., Zhou, J., Sun, X. and Wang, S., 2009. The in vitro and in vivo antiviral effects of salidroside from Rhodiola rosea L. against coxsackievirus B3. Phytomedicine 16, 146-155.

Wenger, R.H., 2002. Cellular adaptation to hypoxia: O2-sensing protein hydroxylases, hypoxia-inducible transcription factors, and O2-regulated gene expression. FASEB Journal 16, 1151-1162.

Westra, J., Brouwer, E., van Roosmalen, I.A., Doornbos-van der Meer, B., van Leeuwen, M.A., Posthumus, M.D. and Kallenberg, C.G., 2010. Expression and regulation of HIF-1alpha in macrophages under inflammatory conditions; significant reduction of VEGF by CaMKII inhibitor. BMC Musculoskelet Disord 11, 61.

Winterbourn, C.C., 1990. Oxidative reactions of hemoglobin. Methods in Enzymology 186, 265-272.

Wu, T., Zhou, H., Jin, Z., Bi, S., Yang, X., Yi, D. and Liu, W., 2009. Cardioprotection of salidroside from ischemia/reperfusion injury by increasing N-acetylglucosamine linkage to cellular proteins. European Journal of Pharmacology 613, 93-99.

Wu, Y.L., Piao, D.M., Han, X.H. and Nan, J.X., 2008. Protective effects of salidroside against acetaminophen-induced toxicity in mice. Biological and Pharmaceutical Bulletin 31, 1523-1529.

Xu, Y., Osborne, B.W. and Stanton, R.C., 2005. Diabetes causes inhibition of glucose-6-phosphate dehydrogenase via activation of PKA, which contributes to oxidative stress in rat kidney cortex. Am J Physiol Renal Physiol 289, F1040-1047.

Xu, Y., Zhang, Z., Hu, J., Stillman, I.E., Leopold, J.A., Handy, D.E., Loscalzo, J. and Stanton, R.C., 2010. Glucose-6-phosphate dehydrogenase-deficient mice have increased renal oxidative stress and increased albuminuria. FASEB Journal 24, 609-616.

Ye, Y.C., Chen, Q.M., Jin, K.P., Zhou, S.X., Chai, F.L. and Hai, P., 1993. [Effect of salidroside on cultured myocardial cells anoxia/reoxygenation injuries]. Zhongguo Yao Li Xue Bao 14, 424-426.

Yu, F., White, S.B., Zhao, Q. and Lee, F.S., 2001. HIF-1alpha binding to VHL is regulated by stimulus-sensitive proline hydroxylation. Proceedings of the National Academy of Sciences of the United States of America 98, 9630-9635.

Yu, P., Hu, C., Meehan, E.J. and Chen, L., 2007. X-ray crystal structure and antioxidant activity of salidroside, a phenylethanoid glycoside. Chemistry & Biodiversity 4, 508-513.

Yu, S., Liu, M., Gu, X. and Ding, F., 2008. Neuroprotective effects of salidroside in the PC12 cell model exposed to hypoglycemia and serum limitation. Cellular and Molecular Neurobiology 28, 1067-1078.

Yu, S., Shen, Y., Liu, J. and Ding, F., 2010. Involvement of ERK1/2 pathway in neuroprotection by salidroside against hydrogen peroxide-induced apoptotic cell death. Journal of Molecular Neuroscience 40, 321-331.

Zeng, Y., Wagner, E.J. and Cullen, B.R., 2002. Both natural and designed micro RNAs can inhibit the expression of cognate mRNAs when expressed in human cells. Molecular Cell 9, 1327-1333.

Zhang, J., Liu, A., Hou, R., Jia, X., Jiang, W. and Chen, J., 2009. Salidroside protects cardiomyocyte against hypoxia-induced death: a HIF-1alpha-activated and VEGF-mediated pathway. European Journal of Pharmacology 607, 6-14.

Zhang, L., Yu, H., Sun, Y., Lin, X., Chen, B., Tan, C., Cao, G. and Wang, Z., 2007. Protective effects of salidroside on hydrogen peroxide-induced apoptosis in SH-SY5Y human neuroblastoma cells. European Journal of Pharmacology 564, 18-25.

Zhang, M.Y., Sun, S.C., Bell, L. and Miller, B.A., 1998. NF-kappaB transcription factors are involved in normal erythropoiesis. Blood 91, 4136-4144.

Zhang, Z., Liew, C.W., Handy, D.E., Zhang, Y., Leopold, J.A., Hu, J., Guo, L., Kulkarni, R.N., Loscalzo, J. and Stanton, R.C., 2010. High glucose inhibits glucose-6-phosphate dehydrogenase, leading to increased oxidative stress and beta-cell apoptosis. FASEB Journal 24, 1497-1505.

Zhong, H., Xin, H., Wu, L.X. and Zhu, Y.Z., 2010. Salidroside attenuates apoptosis in ischemic cardiomyocytes: a mechanism through a mitochondria-dependent pathway. J Pharmacol Sci 114, 399-408.

Zhu, J., Wan, X., Zhu, Y., Ma, X., Zheng, Y. and Zhang, T., 2010. Evaluation of salidroside in vitro and in vivo genotoxicity. Drug and Chemical Toxicology 33, 220-226.

Zintzaras, E. and Stefanidis, I., 2005. Association between the GLUT1 gene polymorphism and the risk of diabetic nephropathy: a meta-analysis. Journal of Human Genetics 50, 84-91.